

# Triggerable Patches for Medical Applications

Sofia Sirolli,\* Daniele Guarnera, Leonardo Ricotti,\* and Andrea Cafarelli

Medical patches have garnered increasing attention in recent decades for several diagnostic and therapeutic applications. Advancements in material science, manufacturing technologies, and bioengineering have significantly widened their functionalities, rendering them highly versatile platforms for wearable and implantable applications. Of particular interest are triggerable patches designed for drug delivery and tissue regeneration purposes, whose action can be controlled by an external signal. Stimuli-responsive patches are particularly appealing as they may enable a high level of temporal and spatial control over the therapy, allowing high therapeutic precision and the possibility to adjust the treatment according to specific clinical and personal needs. This review aims to provide a comprehensive overview of the existing extensive literature on triggerable patches, emphasizing their potential for diverse applications and highlighting the strengths and weaknesses of different triggering stimuli. Additionally, the current open challenges related to the design and use of efficient triggerable patches, such as tuning their mechanical and adhesive properties, ensuring an acceptable trade-off between smartness and biocompatibility, endowing them with portability and autonomy, accurately controlling their responsiveness to the triggering stimulus and maximizing their therapeutic efficacy, are reviewed.

are significantly larger than the third one; iii) is ready in its final form at the moment of deposition on the tissue, namely it is previously synthesized and only afterward put in contact with the tissue; and iv) guarantees a therapeutic or diagnostic function, with respect to such a tissue.

Medical patches have a millennial history: archaeological remains demonstrate that ancient Egyptians already employed rudimentary plasters to bandage injured skin, as the first kind of wound dressing.<sup>[2]</sup> Starting from these very first forms of traditional patches used throughout the centuries mainly for the treatment of wounds, nowadays, patches are emerging as promising platforms with multiple therapeutic functions used in different anatomical areas; this is due to the advances in material science and microfabrication technologies that have improved their performance.<sup>[3]</sup> Nowadays, medical patches are used not only as traditional protective coverings for an injured site, but they also constitute effective and safe medical treatments for

## 1. Introduction

According to the Cambridge Dictionary, a patch is defined as a small piece of material sewn or stuck over something to cover it.<sup>[1]</sup> However, in the case of medical applications, this definition could be narrowed as follows: a medical patch is a material that i) can be laid over the surface of a tissue, adapting to the tissue's shape or curvature, but maintaining its own structure and integrity; ii) is featured by a bidimensional geometry, as two of its dimensions

injured tissues and organs, as well as reliable monitoring tools for acquiring physiological and pathophysiological signals from the human body.<sup>[2,4,5]</sup>

Despite a recent remarkable expansion of the application domain of medical patches in the last decades, wound healing still remains an elective application. Application areas include the skin, as in the case of infected wounds or diabetic ulcers,<sup>[6]</sup> and the walls of internal organs, for example following surgery. The current gold standard methods for closure of primary incisions in clinical settings are sutures and staples, which may cause additional trauma to the surrounding tissue and complications, such as inflammation, infection, and leakage of liquid and air, especially in fragile organs, such as the lungs, liver, and spleen.<sup>[3,7]</sup> In these cases, patches represent an alternative solution to seal and repair an injured visceral tissue without causing further trauma, having the double function of protecting the lesion from further harm and promoting reconstruction of the damaged tissue in a more harmonic manner.<sup>[8]</sup> However, the use of patches for tissue regeneration is not strictly limited to wound closure (Figure 1a). For example, cardiac tissue repair following myocardial infarction is a challenge that may benefit from the use of patches:<sup>[9,10]</sup> these systems could help in restoring functional contractile tissue, thereby avoiding the insurgence of post-infarction complications.<sup>[11]</sup> Furthermore, patches for tissue reconstruction have also been investigated for muscles and tendons

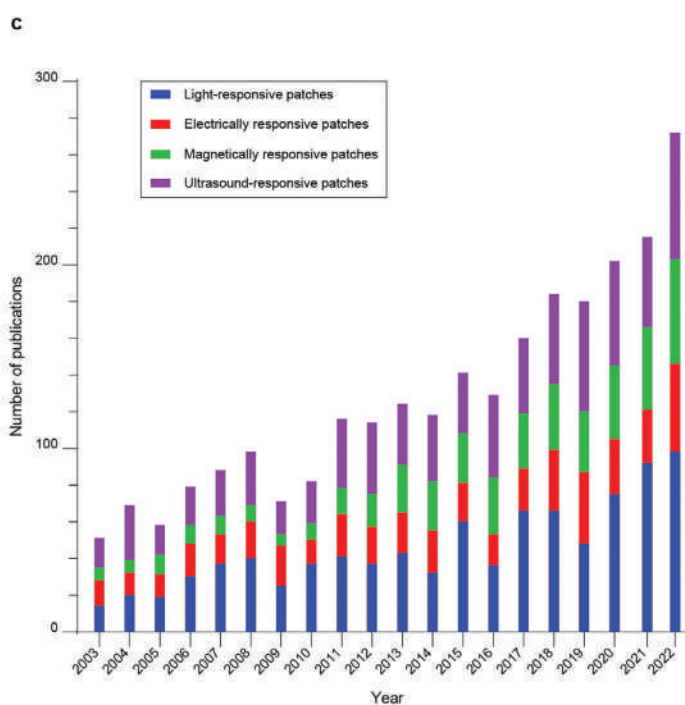
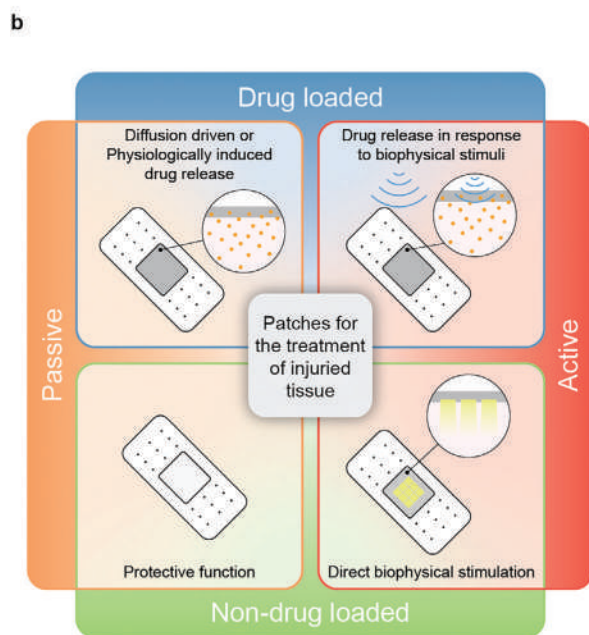
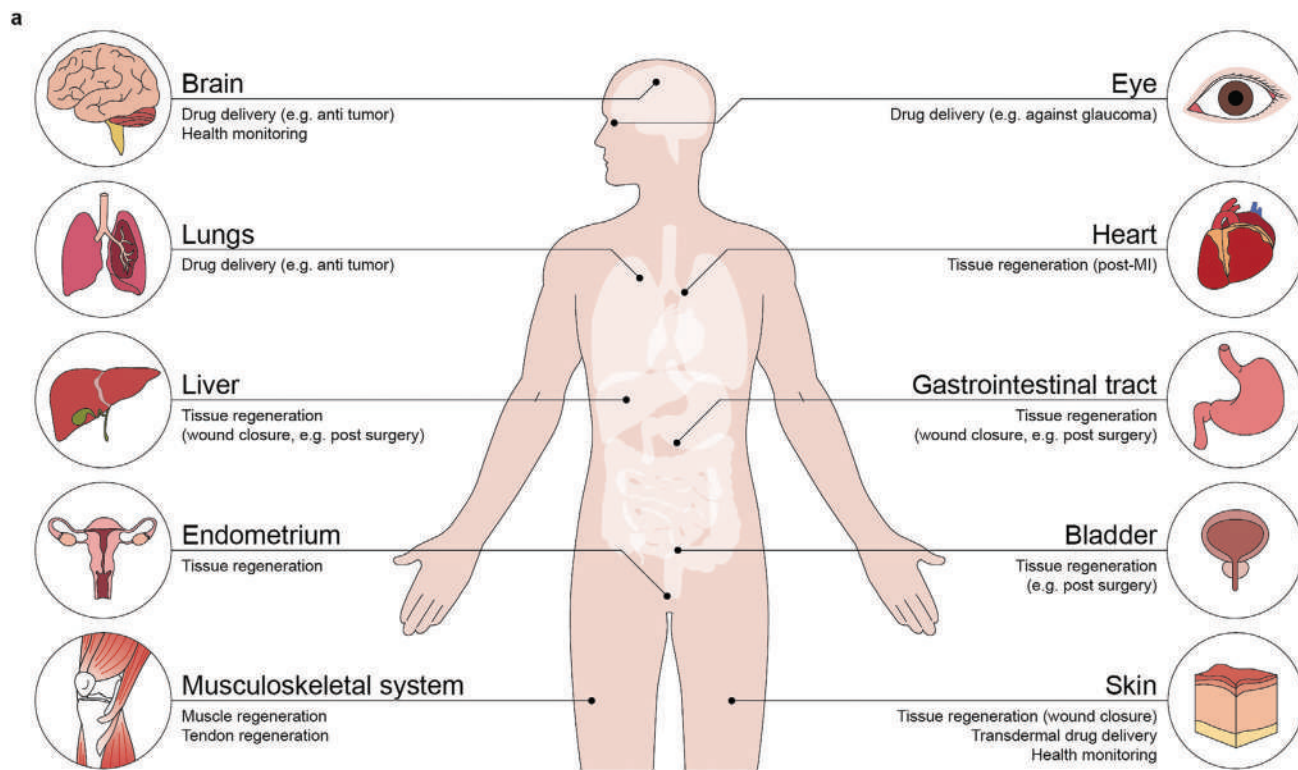
S. Sirolli, D. Guarnera, L. Ricotti, A. Cafarelli  
 The BioRobotics Institute  
 Scuola Superiore Sant'Anna  
 Piazza Martiri della Libertà 33, Pisa 56127, Italy  
 E-mail: [Sofia.Sirolli@santannapisa.it](mailto:Sofia.Sirolli@santannapisa.it); [Leonardo.Ricotti@santannapisa.it](mailto:Leonardo.Ricotti@santannapisa.it)

S. Sirolli, D. Guarnera, L. Ricotti, A. Cafarelli  
 Department of Excellence in Robotics & AI  
 Scuola Superiore Sant'Anna  
 Piazza Martiri della Libertà 33, Pisa 56127, Italy

 The ORCID identification number(s) for the author(s) of this article can be found under <https://doi.org/10.1002/adma.202310110>

© 2024 The Author(s). Advanced Materials published by Wiley-VCH GmbH. This is an open access article under the terms of the [Creative Commons Attribution](https://creativecommons.org/licenses/by/4.0/) License, which permits use, distribution and reproduction in any medium, provided the original work is properly cited.

DOI: 10.1002/adma.202310110



and to treat abnormalities and injuries in organs, such as the bladder and endometrium.<sup>[12–15]</sup>

Another flourishing application field for medical patches is drug delivery. Many patches currently on the market are loaded with specific agents for transdermal drug delivery; thus, overcoming the limitations of systemic drug administration routes, such as intravenous or oral ones. Therefore, transdermal drug delivery allows a local and targeted delivery, achieving: i) higher concentrations of the drug at the target site and consequent minimization of side effects in the other tissues; ii) a sustained and stable delivery over time; iii) an enhancement of the drug bioavailability, since it does not require a transition in the bloodstream or through the gastrointestinal tract; and iv) an improvement of patient compliance.<sup>[16–18]</sup> Transdermal patches are currently used for the sustained release of therapeutics for the treatment of chronic conditions, such as diabetes, and also for the delivery of a variety of other therapeutics, including dermatological drugs against psoriasis or atopic dermatitis and vaccines.<sup>[19,20]</sup> However, the drug delivery potential of patches is not only limited to transdermal applications: it can also be extended to implantable solutions for in situ delivery of therapeutic agents. In recent bioengineering literature, different organs and body areas have been targeted for this purpose, including i) the eyes, whose disorders are challenging to treat through conventional methods due to poor drug permeability and the eye's softness and sensitivity, which make patient compliance very low;<sup>[18,21]</sup> ii) the lungs, especially for cancer treatment, which is extremely difficult to treat with the current clinical approaches;<sup>[22]</sup> and iii) the brain, whose treatment using conventional procedures is heavily hampered by the blood-brain barrier.<sup>[23]</sup>

According to their degree of complexity and ability to interact with the surrounding environment, patches can be classified into two main categories: passive ones, which do not allow external control over their action, and active ones, which can be controlled through an external trigger (Figure 1b).

Majority of existing patches, especially the ones already available on the market, fall into the former category. Within the domain of passive patches, however, there are different levels of complexity, and a further classification can be performed, distinguishing between drug-loaded patches and patches without any drugs. The latter ones are the simplest and most commonly employed for non-specific applications: they can be plasters, gauzes, or foams, which have the function of merely protecting the injured site from further harm.<sup>[24]</sup> However, they can occasionally have an intrinsic ability to enhance the healing process in a lesioned tissue, due to the favorable properties of the materials employed. For example, patches based on decellularized extracellu-

lar matrix are now attracting attention due to their natural bioactivity: they are already commercially available for implantation on cardiac infarcted tissues (CorMatrix) and have been demonstrated to not only provide the infarcted tissue with mechanical support but also to enhance ventricular wall remodeling and even promote neovascularization.<sup>[25]</sup>

Instead, drug-loaded patches incorporate a drug or another therapeutic agent for the topical treatment of a specific disorder or disease, and they can release it passively through diffusion across the patch material. Several patches in this category are already on the market. The FDA approval of the anti-vertigo scopolamine patch (TransdermScop) for the treatment of motion sickness dates back to 1979.<sup>[26]</sup> However, drug-loaded passive patches are still the object of intense studies, as they represent exciting candidates for long-term therapies pursued in a minimally invasive fashion. For example, a biodegradable three-dimensional (3D)-printed cardiac patch has been recently proposed for the treatment of myocardial infarction: the patch is loaded with two drugs that are released with a sustained profile over five months as the polymer material degrades, providing an improved solution for long-term therapy.<sup>[27]</sup>

The abovementioned passive mechanism is the most common delivery method when a predesigned dosage of drugs or other therapeutic molecules is integrated within a patch. Although this approach is simple, and in most cases, easily transferable to clinics, it has a significant drawback of not addressing the complex dynamic nature of many physiological processes of the human body, which would benefit from a higher flexibility and controllability of the process. Semi-passive approaches have been introduced to release therapeutic molecules, depending on endogenous signals, such as pH, temperature, reactive oxygen species (ROS) concentration, or glucose level.<sup>[24]</sup> In this case, responsive materials are employed within the structure of the patch in order to adjust the release rate based on the varying environmental conditions in the treated area.<sup>[2]</sup> Such patches are undoubtedly advanced, but still, the lack of external control over their release profile limits their flexibility of use.

Active patches allow an on-demand treatment by externally triggering their action through the use of biophysical stimuli, such as light, electric or magnetic fields, or ultrasound (US). Additionally, in the active category, the discrimination between non- and drug-loaded patches can be applied. In the case of drug-loaded patches, their load can be released on-demand, in response to an external trigger, exploiting stimuli-responsive materials that change their structure in a controllable way, thereby enabling a precise temporal control of the release profiles.<sup>[28]</sup> Instead, the active non-loaded patches presently represent a less

**Figure 1.** a) Patches can be employed for the treatment of numerous organs and body areas: the skin is the most targeted organ, but other common organs include the heart, musculoskeletal system, gastrointestinal tract, eye, brain, lungs, bladder, endometrium, and liver. b) Classification of the existing medical patches, according to their functionalities and their ability to interact with the surrounding environment: patches can be active or passive, according to whether they carry out their action in response to an external trigger or not, and in both of these cases they can be loaded with drugs or enable their function without relying on any drug. c) The number of publications in the last two decades concerning externally triggerable patches. Source: Scopus. Keywords used for paper search: (TITLE-ABS-KEY (patch AND (medical OR treatment OR release) AND (light OR photo)) AND NOT TITLE-ABS-KEY (antenna OR soil OR vegetation OR macule OR "patch clamp" OR "patch test" OR pigmented)); (TITLE-ABS-KEY (patch AND (medical OR treatment OR release) AND electric) AND NOT TITLE-ABS-KEY (antenna OR soil OR vegetation OR macule OR "patch clamp" OR "patch test" OR pigmented)); (TITLE-ABS-KEY (patch AND (medical OR treatment OR release) AND magnetic) AND NOT TITLE-ABS-KEY (antenna OR soil OR vegetation OR macule OR "patch clamp" OR "patch test" OR pigmented OR "magnetic resonance imaging")); (TITLE-ABS-KEY (patch AND (medical OR treatment OR release) AND (ultrasound OR ultrasonic)) AND NOT TITLE-ABS-KEY (antenna OR soil OR vegetation OR macule OR "patch clamp" OR "patch test" OR pigmented)).

investigated category whose response to an external trigger is exploited to directly stimulate the target tissue. In this scenario, the therapeutic effect is not enabled by a drug, but rather by a physical input.

Patches can also be distinguished between acellular and cell-laden ones. The latter relies on the therapeutic action and regenerative capabilities of the cells embedded on board, although the former exploits the properties of specific appropriate materials and potentially the effect of a physical stimulus to trigger the self-regenerative mechanisms of the body.<sup>[29]</sup> In this review, the focus will be exclusively on acellular active patches, as they show the most intriguing potential for a multitude of applications.<sup>[29]</sup> In fact, the possibility to externally control their action opens avenues for tailored treatment of specific pathological conditions, adapting to single patients' features. Active patches, due to their high controllability degree, allow mimicking the pulsatile and context-dependent release of endogenous molecules. Furthermore, they can minimize the insurgence of tolerance to drugs, which may occur when a drug is continuously present in the body.<sup>[30]</sup>

In this paper, a comprehensive overview of the state of the art of acellular triggerable patches is provided, mainly focusing on the stimulus-responsive aspect. In fact, multiple reviews can be found in the literature concerning patches, but their focus is mainly limited to a specific application or medical problem.<sup>[2,18,29]</sup> In contrast, other review papers focus on the most advanced and promising biomaterials for certain innovative medical applications,<sup>[3,31]</sup> or on the effects of biophysical energies on tissues and human health in general.<sup>[32–34]</sup> Some works even stand at the intersection of these fields, describing how physical stimuli can interact with biomaterials, such as polymers or hydrogels.<sup>[35–37]</sup> However, to the best of our knowledge, no papers have reviewed the specific interaction of biophysical energies with patches, with a strong focus on their active and on-demand feature rather than on their medical application. This study aims to offer such a perspective in the field of triggerable patches, which has seen a great evolution in the last decades (Figure 1c) and holds high potential for even more exciting developments in the future.

The following sections give an overview of the existing active patches, classifying them according to the triggering stimulus they respond to and investigating the interaction mechanisms between the physical energy used and a patch. The focus is on all patches whose responsive character lies in their constituent materials. Therefore, health monitoring patches are set aside, as the core of their function is instead the integration of electronic components, which makes them more complex. We also reviewed the most important challenges that should be addressed for the design of an effective patch, either directly related or unrelated to its stimulus-responsive character. Finally, conclusions were drawn, also offering a glimpse of future perspectives in this study field.

## 2. Triggerable Patches

Active patches offer a high level of control over their action compared to passive ones, owing to their responsiveness to an external triggering signal. Due to this feature, active patches are often defined as triggerable (this is the definition that will be used in the text). In this chapter, the four main biophysical energies that

can be used to trigger the on-demand action of patches are reviewed, with a focus on the possible interaction mechanisms of such stimuli with smart materials and how they have been exploited to design responsive medical patches.

### 2.1. Photostimulation

Electromagnetic radiation is a form of energy based on a stream of photons having different energy levels (corresponding to different wavelengths). The term light most commonly refers to the visible spectrum, ranging between 380–780 nm; however, it is also usually associated with ultraviolet (UV) and infrared (IR) ranges (10–400 nm and 780 nm to 1 mm, respectively).<sup>[38,39]</sup>

Since the beginning of the 20<sup>th</sup> century, it has been found that light can be used to trigger beneficial effects on human health.<sup>[40]</sup> Currently, it is widely used for different therapeutic purposes, exploiting its 3D spatial resolution, non-invasiveness, and minimal side effects.<sup>[41,42]</sup>

Photobiomodulation (PBM), or low-level light therapy, is an example of such applications. It relies on light at low power (up to 500 mW) in the visible and near-IR spectrum to modulate biological activities. In fact, photon absorption by photoreceptor molecules in the tissues (such as cytochrome-c oxidase) and intracellular water converts light into biological signals that can modulate specific signaling pathways, thereby producing biochemical products, such as ROS, adenosine triphosphate, Ca<sup>2+</sup>, and nitric oxide (NO). Evidence of PBM efficacy can be found in the field of cancer treatment, wound healing, neuromodulation, inflammation reduction, as well as in the treatment of ophthalmic disorders, dermatological conditions, tendinopathies, and nerve injuries. PBM is also thought to have a beneficial effect on tissue healing, thereby promoting cell proliferation and differentiation.<sup>[43,44]</sup>

The action of light stimulation varies significantly with wavelength. In fact, irradiation in the UV range (10–400 nm) is much more cytotoxic than longer wavelengths, and represents a possible hazard to healthy tissues, as it may cause damage and photodestruction of active molecules, e.g., producing genotoxicity, which limits the *in vivo* employment of this kind of radiation.<sup>[45]</sup> Furthermore, UV light is unable to penetrate deeply into tissues due to its high absorption loss by endogenous chromophores (such as oxy- and deoxy-hemoglobin, lipids, and water); therefore, it is considered only suitable for superficial treatments involving the skin and mucosa.<sup>[46]</sup> Instead, near-infrared (NIR) light (650–900 nm) is considered safer for tissues and it also possesses a higher penetration ability (up to 3 mm in the muscle and brain and >4.5 mm in less light-attenuating tissues, such as the breast), as hemoglobin and water have their lowest absorption coefficient in the region between 650–900 nm.<sup>[47–49]</sup> Therefore, NIR light is promising, especially for treatments involving deeper tissues and internal organs, even though its penetration never exceeds a few centimeters.

Besides the direct application on the above-mentioned tissues, light can be also used in combination with photo-responsive materials for therapeutic purposes, such as triggering drug release from properly designed responsive carriers. Light-responsiveness may rely on a variety of different interaction mechanisms, such as photo-induced cleavage of bonds,



photo-isomerization and reversible photo-crosslinking.<sup>[46]</sup> In bond photolysis, photocleavable covalent bonds can be broken with a sufficient dose of wavelength-matched irradiation, forcing molecular dissociation; this phenomenon can be exploited to break the links between a therapeutic agent and its carrier or to dissociate a light-sensitive polymer, whose structure relaxes, thereby releasing a physically encapsulated drug. Among photocleavable molecules, nitrobenzyl and coumarin derivatives are worth mentioning.<sup>[45]</sup> In photo-mediated isomerization, photoexcitation can induce the reversible isomerization of selected organic compounds, such as azobenzenes and spiropyrans (both responsive to UV light), by providing the required energy to switch from one stereoisomer to the other.<sup>[45]</sup> This reversible isomerization can serve as a building block for the creation of smart drug delivery systems by exploiting the non-identical chemical affinities of different isomers. This mechanism can be used to directly unbind and release a drug, or alternatively, to modify the structure of a supramolecular construct, where one of the components may change its relative affinity, causing a decrease in the cross-linking density and consequent release of the encapsulated drug.<sup>[50]</sup>

Furthermore, irradiation of tissues with light can also give rise to secondary thermal effects, as in photothermal therapy (PTT), which uses photothermal agents and converts light energy into heat. Conductive materials, such as carbon nanostructures or metal nanomaterials, are exploited for their ability to absorb incident photons in a specific wavelength window and convert their energy by local heating via plasmonic mechanisms.<sup>[45,46]</sup> For a single spherical nanoparticle (NP), the temperature distribution within it and its surroundings can be obtained through the following Equation (1):

$$\rho c_p \frac{\partial T}{\partial t} = k \nabla^2 T + Q \quad (1)$$

where  $Q$  is the local heat intensity due to the light dissipation from the NP, which can be obtained by solving the Maxwell equations;  $\rho$ ,  $c_p$ ,  $T$ , and  $k$  represent the density, specific heat, temperature, and thermal conductivity of the NP, respectively, and  $t$  is time.<sup>[51]</sup> Therefore, the temperature rise ( $t \rightarrow \infty$ ) outside the NP is described by Equation (2):

$$\Delta T(r) = \frac{Q}{4\pi k_0 r} \quad (2)$$

with  $k_0$  being the thermal conductivity of the matrix medium.<sup>[41]</sup>

According to the intensity of the stimulus, the localized heat increase can either kill diseased cells in the case of a strong hyperthermia, or operate a beneficial modulation action on tissues in the case of a mild one.

The secondary thermal effects due to irradiation can also be exploited for light-triggered drug delivery from temperature-responsive materials. For example, thermo-responsive polymers can switch their structure from a shrunk to a swollen structure (or vice versa) in response to a change in temperature, according to their critical solution temperature, which can be tuned through chemical modifications.<sup>[46]</sup> A heat-induced contraction of the polymer network can correspond to a decrease in the free volume in the hydrogel, which results, in turn, in an increase in hydrostatic pressure inside the gel and squeezing action and con-

sequent ejection of the drug-containing fluid. It is also possible to engineer thermo-degradable polymers; for example, by cross-linking their chains via thermo-degradable linkers. Such hydrogels can gradually degrade and therefore release the entrapped cargo when the temperature rises above a specific critical threshold, allowing a tunable on-demand drug release.<sup>[52]</sup> Moreover, temperature changes can also alter the chemical affinity between materials: hence, the possibility to exploit photothermal effects to unbind a compound from its carrier by reducing their relative affinity and trigger drug release.<sup>[53]</sup> Finally, light can also interact with photosensitizers in what is called photodynamic therapy. Photosensitizers are materials that can be excited by wavelength-specific light irradiation, and can transfer their energy to molecular oxygen, thereby generating cytotoxic ROS, such as singlet oxygen.<sup>[54]</sup> Therefore, this therapy is mostly employed for tumor ablation, as ROS can oxidize key cellular macromolecules leading to cell death, but it has also been exploited for killing bacteria in chronic wounds, or to trigger drug release from ROS-sensitive systems.<sup>[55]</sup> The most commonly used photosensitizers are usually porphyrin-based; however, several others exist and are already approved for clinical use.<sup>[54]</sup>

Light stimulation systems have also been used in patches, both for drug delivery and direct tissue stimulation purposes (see **Table 1**). In some cases, the sources of the stimulus are integrated on-board.

For example, Lee et al. developed a skin-adhesive patch for the treatment of wounds through PBM.<sup>[56]</sup> In their study, a hyaluronic acid (HA)-gelatin nanofibrous fabric with catechol moieties (D-HA/Gel) was integrated with multiple light-emitting diode (LED) arrays (**Figure 2a**). The NIR light (630 nm) selected for this purpose proved to penetrate the dressing layer of the patch and reach the skin with an acceptable decrease ( $\approx 30\%$ ) in power density. In vitro and in vivo tests were performed to investigate the synergistic effect of light exposure and dressing presence. Results demonstrated that this synergistic effect boosted the proliferation of fibroblasts cultured on the nanofibrous membrane, up to 500% with respect to the control, and accelerated the wound healing process in rats. Similarly, a wearable PBM patch for skin treatment was developed by Jeon et al., which integrated an organic LED (OLED) on the device surface as a stimulation source.<sup>[57]</sup> OLEDs were used due to their minimal thickness and high flexibility compared to the more traditional LEDs and lasers. Results on human fibroblasts showed no cytotoxic effects throughout the entire wavelength range (600–700 nm). Furthermore, the patch promoted fibroblast proliferation ( $>58\%$  of control) and migration ( $>46\%$  of control) at different stimulation wavelengths.

Li et al. developed a light-activated antibacterial patch based on photothermal pathogen inactivation.<sup>[58]</sup> A flexible polyimide film was modified by integrating an array of gold nanoholes, consisting of a gold layer patterned with regularly spaced holes. This specific surface has the ability to generate heat when irradiated with NIR light due to a plasmonic effect, and it was then post-coated with a reduced graphene oxide (rGO) layer, which increased the light absorption efficiency, thereby avoiding skin inflammation and burning. The advantage of the proposed dressing, compared to classical methods for the thermal treatment of wounds, was the spatial localization of the effect that limited the side effects on the intact skin. In vivo tests performed on mice with

**Table 1.** Light-responsive patches and their operating principles.

Reference	Target organ	Stimulation parameters	Patch material	Action	Results
Lee et al. (2022) <sup>[56]</sup>	Skin	f = 630 nm (NIR) I = N.A.	D-HA/Gel	Photoirradiation (PBM) and bioactive dressing action	In vitro: enhancement of proliferation of murine fibroblasts. In vivo: acceleration of wound closure.
Jeon et al. (2018) <sup>[57]</sup>	Skin	f = 600–700 nm (red) I = 5–10 mW cm <sup>-2</sup>	PET	Photoirradiation (PBM)	In vitro: enhancement of proliferation and migration of fibroblasts.
Li et al. (2017) <sup>[58]</sup>	Skin	f = 980 nm (NIR) I = 0–5 W cm <sup>-2</sup>	Polyimide with rGO-coated Au NHs	Photothermal effect due to the gold nanoholes	In vivo: improvement in healing, without tissue necrosis due to an antibacterial action.
Yu et al. (2022) <sup>[59]</sup>	Skin	f = 808 nm (NIR) I = 1 W cm <sup>-2</sup>	PVA + PDA NPs	Drug release due to light-induced microneedles degradation + mild photothermal effect due to the PDA NPs	In vitro: mass reduction of biofilms for both gram-positive and negative bacteria. In vivo: bactericidal and anti-inflammatory action, acceleration of wound healing.
Pang et al. (2020) <sup>[60]</sup>	Skin	f = 365 nm (UV) I = 110 mW cm <sup>-2</sup>	Azide-PEG5000-acrylate	Drug release due to the photocleavage of the linker used to graft it into the hydrogel	In vivo: antibacterial effect on infected wounds.
Kim et al. (2015) <sup>[61]</sup>	Skin	f in the Vis (blue) range I = 47.5–474 mW cm <sup>-2</sup>	PNIPAM-co-VP + MNPs	Drug release from a temperature-responsive hydrogel due to the photothermal action of MNPs	In vitro: pulsatile drug release using an on-off stimulation pattern.
Teodorescu et al. (2017) <sup>[53]</sup>	Skin	f = 980 nm (NIR) I = 1–10 W cm <sup>-2</sup>	Polyimide + rGO	Drug release due to the photothermal effect of rGO	In vitro: enhanced release upon NIR irradiation, proportional to the laser power density.
Wu et al. (2022) <sup>[62]</sup>	Skin	f = 808 nm (NIR) I = N.A.	HA + MXene	Drug release due to the hydrogel dissolution, induced by the photothermal effect of MXene	In vitro: enhanced release upon NIR irradiation. In vivo: anti-inflammatory effects against psoriasis.

Au NHs, gold nanoholes; D-HA/Gel, dopamine-modified hyaluronic acid/gelatin; MNPs, magnetite nanoparticles; NIR, near-infrared; NP, nanoparticle; PBM, photobiomodulation; PET, polyethylene terephthalate; PVA, polyvinyl alcohol; PDA, polydopamine; PEG, polyethylene glycol; PNIPAM-co-VP, poly(N-isopropylacrylamide-co-vinyl-2-pyrrolidinone); rGO, reduced graphene oxide; UV, ultraviolet.

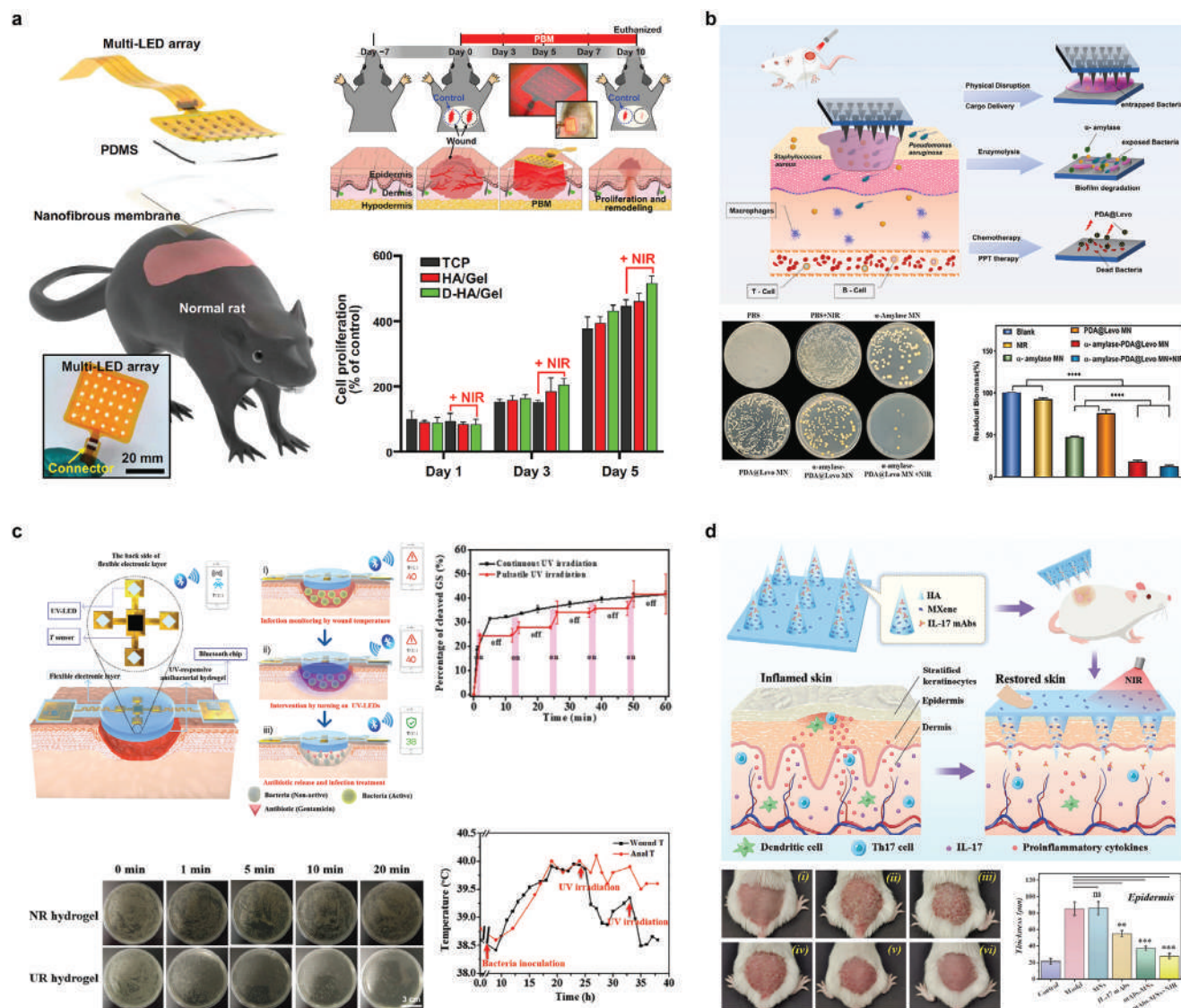


**Figure 2.** Light-triggered patches with tissue stimulation and drug delivery capabilities. a) Illustration of a multi-layered device composed of a flexible multi-LED array and D-HA/Gel nanofibrous membrane and of its operating principle: the combined use of NIR irradiation and of the dressing favors cell proliferation and wound healing. Reproduced under terms of the Creative Commons CC-BY-NC License.<sup>[56]</sup> Copyright 2022, The Authors, published by AAAS. b) Illustration of the mechanism for the treatment of biofilms with dissolving microneedles in infected wounds through the combined action of enzymolysis, photothermal therapy, and chemotherapy: the application of this patch reduced biofilms to 12% and 31% for gram-positive and gram-negative bacteria. Reproduced with permission.<sup>[59]</sup> Copyright 2022, Elsevier. c) Depiction of the structure and operating principle of a smart electronics-integrated wound dressing, consisting of a PDMS-encapsulated flexible electronic layer and an antibiotic-loaded UV-responsive antibacterial hydrogel; drug release can be modulated through photoactivation, resulting in an efficient antibacterial action and effectively lowering the wound temperature in vivo. Reproduced under terms of the Creative Commons CC-BY License.<sup>[60]</sup> Copyright 2020, The Authors, published by Wiley-VCH. d) Depiction of an antibody-loaded photothermal responsive MN patch for psoriasis treatment: through hyperthermia and antibody delivery it produced a decrease in epidermal thickness and reduced erythema and presence of scales. Reproduced with permission.<sup>[62]</sup> Copyright 2022, Wiley-VCH.

subcutaneous skin infections demonstrated improved healing of the treated areas, without the insurgence of tissue necrosis, by using 980 nm continuous wave laser stimulation, with a power properly adjusted to maintain surface temperature at around 50 °C. After 72 h of treatment, infected wounds showed only traces of bacterial infiltration, with granulation tissue abundantly formed beneath the muscular layer, suggesting active wound healing. In the study by Yu et al., PTT was used in combination

with drug delivery to obtain an antibacterial effect on biofilms.<sup>[59]</sup> The authors designed a dissolving microneedle patch encapsulating  $\alpha$ -amylase and levofloxacin-loaded polydopamine (PDA@Levo) NPs: the microneedles destroyed the physical barrier of the biofilm and released  $\alpha$ -amylase to enzymatically degrade the proteins featured by such a compact barrier, thereby making the bacteria susceptible to antimicrobial therapies. The PDA@Levo NPs were combined with antibiotics; the generated

mild hyperthermia acted in synergy with them, killing bacteria without the need of excessively high and potentially dangerous temperatures (Figure 2b). Maximum efficacy was demonstrated at 808 nm, as it caused microneedle dissolution, resulting in the release of the load, acceleration of the levofloxacin release from the NPs, and induction of the photothermal action of PDA. The combined use of enzymolysis, antibiotics, and PTT effectively removed the bio-films both in vitro and in vivo, reducing them to 12% and 31% for gram-positive and gram-negative bacteria, respectively. Additionally, this solution reduced inflammation and facilitated healing in infected full-thickness wounds, which resulted in complete closure at day 11, compared with untreated wounds that still showed an area of 32% with respect to the original size.

Different light-responsive mechanisms have also been exploited for drug delivery. For example, Pang et al. used UV irradiation (365 nm) to control the delivery of gentamicin through photocleavage.<sup>[60]</sup> In their study, a multi-layered wound dressing with monitoring and therapeutic capabilities was developed, consisting of a UV-responsive drug-loaded antibacterial hydrogel, and equipped with flexible electronics, a temperature sensor, and UV LEDs. Gentamicin was covalently grafted into the hydrogel through a UV-cleavable linker; its release was triggered by the activation of an LED array integrated into the patch. In vivo tests demonstrated the ability of this system to monitor the wound temperature in real-time, communicate wirelessly with an external device by Bluetooth, and deliver treatment on-demand. Indeed, when the wound temperature rose above the safe limit of 40 °C, UV irradiation was activated, lowering the infection level through the delivered antibiotic treatment, as suggested by the fact that the local temperature decreased to 38.9 °C for 6 h (Figure 2c).

Kim et al.<sup>[61]</sup> exploited the photothermal effect: a transdermal patch was developed by integrating hybrid hydrogel beads that showed a reversible visible light-induced volume change. They consisted of a drug-loaded temperature-responsive poly(N-isopropylacrylamide) (PNIPAM)-based hydrogel and magnetite NPs that acted as a photothermal conversion agent. The NPs could heat up upon blue light irradiation, causing the on-demand release of the encapsulated dexamethasone. In vitro tests confirmed a rapid and localized release only during the irradiation time by locally controlling the volume change of the hydrogel beads: only the beads in the irradiated area contracted, with a reversible volume decrease of 72%, although the diameter change in non-irradiated areas was negligible. Similarly, Teodorescu et al. developed a transdermal drug delivery system exploiting the NIR-induced photothermal mechanism.<sup>[53]</sup> In this study, rGO was used as the photoconversion agent by exploiting its extremely rapid light-to-heat conversion capability under low-power NIR irradiation. rGO nanosheets were impregnated with ondansetron and incorporated in a flexible polyimide-based patch. Under irradiation at 980 nm, rGO caused an increase in temperature due to the photothermal effect, resulting in a decrease in the affinity between rGO sheets and ondansetron, with a consequent enhancement of drug release up to three times with respect to non-stimulated conditions. In contrast, Wu et al. used MXene, an emerging two-dimensional biodegradable niobium carbide material with excellent light-to-heat conversion properties, as the photoconversion agent for photothermally triggered trans-

dermal drug delivery applications.<sup>[62]</sup> They developed an HA microneedle patch encapsulating MXene and the monoclonal antibody IL-17 for psoriasis treatment. Owing to the high photothermal conversion efficiency of the MXene additive, the patch could rapidly melt and release the encapsulated IL-17 antibody into the dermis under NIR light irradiation, achieving an effective anti-inflammatory effect around the psoriasis lesions, as confirmed by in vivo experiments on mice. The treatment produced a reduction in epidermal thickness of 60–70% with respect to an untreated psoriasis model, which is a symptom of alleviated psoriatic skin inflammation, and decreased the presence of erythema and scales (Figure 2d).

## 2.2. Electrical Stimulation (ES)

Electric field (EF) is defined as the force per unit charge that a charge or a system of charges exerts at a given point; in other words, it represents the physical effect of a charged particle on the surrounding space, which can result in an attractive or repulsive interaction if another charged particle enters such a space.<sup>[63,64]</sup> In most common applications, an EF is generated by applying a voltage difference to conducting electrodes.<sup>[65]</sup>

The use of ES for medical purposes has a long history, starting from ancient Greece and Rome, where it was extensively used to treat pain and improve blood circulation. Nowadays, ES is employed through different stimulation types, such as direct current, alternating current, high-voltage pulsed current, or low-intensity direct current, and used for a plethora of clinical applications, such as fracture repair, pain management, neurostimulation, and wound healing.<sup>[66]</sup> In fact, ES plays a crucial role in the human body: neural and muscle tissues are regularly stimulated through biological electrical signals, but more in general, any human cell can be depicted as an electrical unit, being its biological function regulated by numerous electrochemical processes, such as the direct current exchange of ions in the plasma membrane.<sup>[66]</sup> Therefore, it is not surprising that an EF can trigger a broad variety of intracellular effects, which can be exploited for therapeutic purposes.

There are several applications of ES described in medical literature to accelerate wound healing. Clinical evidence has shown that ES reduces inflammation and infections and increases bacteria eradication. Additionally, EF delivered at a wound site has been reported to guide the migration and proliferation of epithelial cells and fibroblasts, mimicking what happens with endogenous EFs, which play a key role in natural wound repair, guiding the migration of fibroblasts and keratinocytes and downplaying inflammation.<sup>[67–69]</sup>

Furthermore, ES could be beneficial in the regeneration and remodeling of other excitable tissues, such as nerves, myocardium, bones, and muscles.<sup>[70]</sup> For this reason, approaches involving conductive biomaterials with the ability to promote the transmission of endogenous bioelectricity or provide external ES to cells and tissues are of great interest. Some strategies have been envisioned for improving the synchronous beating capability of regenerated cardiac tissue,<sup>[71]</sup> or for healing skeletal muscle defects by promoting myoblasts proliferation and differentiation.<sup>[72]</sup> ES could also find application in reversing the atrophy process of denervated skeletal muscles by transmitting



electrical signals and forcing them to contract.<sup>[73]</sup> For example, functional ES is a technique used to restore movement in patients with central nervous system lesions, stimulating the neuromuscular junctions through electrodes that may be implanted or more commonly placed on the skin surface.<sup>[74]</sup>

An EF can also be used in combination with components featuring a high resistance to produce a temperature increase. For example, the amount of Joule heat ( $P$ ) generated by a single metal NP under an oscillating EF can be directly estimated by the following Equation (3):

$$P = \sigma(\omega) a d E^2 \quad (3)$$

where  $\sigma$  is the Drude model conductivity of the metal at the angular frequency  $\omega$ ,  $E$  is the magnitude of the EF,  $a$  is the cross-sectional area of the NP, and  $d$  is its diameter. Assuming efficient heat transfer from a multitude of NPs to the surrounding medium, the volumetric-induced heating rate is given by Equation (4):

$$\frac{dT}{dt} = \left[ \frac{\sigma(\omega) a d |E|^2}{v c_w} \right] \quad (4)$$

where  $v$  is the volume of the medium and  $c_w$  is its heat capacity.<sup>[75]</sup>

Hyperthermia is in fact attracting a growing interest in clinical practice due to its ability to increase blood flow, relieve pain, and reduce joint stiffness. Even though electrically induced hyperthermia is not widely investigated, it could be a valid alternative to other strategies, such as PTT.<sup>[76]</sup>

In combination with electrically-responsive biomaterials, EFs can also be employed as a trigger for on-demand drug delivery. EF is highly tunable in terms of the applied voltage or current amplitude, frequency, waveform shape, duty cycle, and electrode configuration, thereby allowing pulsatile release profiles or other complex release patterns.<sup>[48,77,78]</sup> However, the use of electro-responsive systems for drug administration in clinical settings is mostly hindered by the need for an external power supply, which is often bulky, and by the limited tissue penetration capability of EFs, which in most cases requires the use of implantable electronics or invasive electrodes.<sup>[70,79]</sup>

Nevertheless, the use of EFs as a trigger for externally controlled drug delivery in combination with electro-responsive materials still remains appealing and it is widely investigated. The main mechanisms responsible for drug release from electro-responsive polymers are: electrophoresis, forced convection of the drug out of the gel, alteration of the redox chemistry of the delivery vehicle, and release of the drug upon erosion of electro-erodible polymers.<sup>[77]</sup> In most cases, electrically triggered drug delivery is the result of the interplay between two or more of these phenomena, depending on the type of responsive material, charge of the drug molecules, and the interaction between the matrix and the drug.

Polyelectrolytes are the most widely used class of polymers that exhibit electrosensitive behaviors, namely the ability to undergo mechanical deformation when an EF is applied. Upon ES, polyelectrolytes undergo a deswelling, which results in forced ejection of their water content along with the drug molecules entrapped in their pores.<sup>[79]</sup> This anisotropic contraction mechanism is also often associated with the electro-osmotic flow of

charged solutes and mobile counter-ions migrating towards the cathode or anode, thereby dragging water and drug molecules with them.<sup>[80]</sup>

In other cases, conductive systems are used as electro-responsive drug delivery vehicles. For example, conductive polymers (CPs), such as polypyrrole (PPy), show EF-induced changes in their net charge due to their redox chemistry, which results in the release of encapsulated drugs due to a decrease in their affinity with the polymer chains, especially when the drug molecules are themselves charged.<sup>[79]</sup> In other cases, drugs entrapped in the pores of a CP can be released by an electrically driven increase in the pore size, since the expansion and contraction of CPs depend on their oxidation state, resulting in a physical ejection of the drug out of the system.<sup>[81]</sup> However, the conductivity of a bio-material system may be derived not only from a CP matrix but also from conductive fillers, such as carbon nanotubes, graphene, and metal NPs. In this case, the conductivity ( $\rho$ ) of the composite can be estimated through the following Equation (5) for the resistivity<sup>[82]</sup>:

$$\rho = \frac{\rho_m \rho_f}{(1 - V_f) \rho_f + V_f \omega_g \rho_m} \quad (5)$$

where  $\rho_m$  is the resistivity of the non-conducting matrix,  $\rho_f$  is the resistivity of the conductor,  $V_f$  is the volume fraction of the conductive phase, and  $\omega_g$  is the weight fraction of the conductive phase in an infinite cluster (a function of the number of contacts per particle and probability of contact).

These materials have been studied as electrically responsive components for drug delivery purposes, being able to release a range of bioactive molecules, including anti-inflammatory and chemotherapeutic agents upon ES.<sup>[81]</sup>

Finally, EFs may also be used to drive the scission of supramolecular block copolymers by controlling their assembly and disassembly behavior through the reversible association and dissociation of the polymer components, which results in control of the drug release rate according to the applied voltage.<sup>[83]</sup>

Many of the ES systems described above have also been investigated in patch applications (see Table 2).

For example, Wang et al. developed a flexible electrode in the form of a patch for ES of wounds.<sup>[69]</sup> A conductive hydrogel, made by a methacrylated alginate matrix incorporating silver nanowires, which show good conductivity, biocompatibility, and intrinsic antibacterial properties, has been used in this regard (Figure 3a). In vitro tests performed on fibroblasts showed an enhancement of cellular migration and improvement in cell alignment. The efficacy of the patch was also assessed in vivo on an infected full-thickness wound model by exploiting a pulsed EF stimulation (6 V, 10 Hz, and 1 ms of pulse duration) through a portable pulse width modulator. Results showed a significant reduction of the wound area, an angiogenesis enhancement, and lower inflammation and infection levels when ES was delivered through the patch, ultimately resulting in total wound closure in seven days instead of 20 days for control. In another work, Wang et al. exploited ES and a responsive patch to deliver hyperthermia therapy for targeting superficial tumors and joint injuries.<sup>[76]</sup> This hyperthermia patch was endowed with excellent electrothermal characteristics due to

**Table 2.** Electro-responsive patches and their working mechanisms.

Reference	Target organ	Stimulation parameters	Patch material	Action	Results
Wang et al. (2022) <sup>[69]</sup>	Skin	V = 6 V	MAA + AgNWs	Combined effect of ES and antibacterial dressing	In vitro: enhancement of migration and alignment of fibroblasts; antibacterial efficacy. In vivo: acceleration of wound closure with reduction of inflammation and infection.
Wang et al. (2022) <sup>[76]</sup>	Skin	V = 0.7 V	PVP-PVA + AgNFs	Hyperthermia due to the electrothermal action of AgNFs	In vivo: size reduction of subcutaneous tumors.
Lee et al. (2016) <sup>[84]</sup>	Skin	V = 0.1–0.4 V	PDMS	Chemical stimulation through NO release due to the reduction of a precursor	In vitro: pulsatile release in response to a pulsed EF; effective bactericidal action.
Xu et al. (2021) <sup>[85]</sup>	Skin	V = 0.5 V	PPy	Drug release due to PPy redox switching	In vitro: electrically enhanced drug release; antibacterial efficiency. In vivo: acceleration of wound healing.
Liu et al. (2012) <sup>[86]</sup>	Skin	V = 2–15 V	PVA + rGO	Drug release due to a decrease in affinity between the drug and the conductive filler	In vitro: enhancement of release upon ES; stepwise release profile obtained with a pulsed on-off EF.
Sung et al. (2018) <sup>[87]</sup>	Brain	V = 1–1.4 V	Epoxy + gold membrane	Drug release due to the electrochemical dissolution of the gold membrane sealing the drug reservoirs	In vivo: effective local release of an anti-epileptic drug upon application of a voltage.
Tamayol et al. (2017) <sup>[88]</sup>	Skin	V = 8–18 V	PGS-PCL + PEGylated-chitosan nanocarriers	Drug release from a thermo-responsive polymer due to the presence of an electroresistive heater	In vitro: controlled release in response to a stimulation pattern.
Mostafafalu et al. (2017) <sup>[89]</sup>	Skin	V = 2.5 V	PNIPAM/PEGDA	Drug release from a thermo-responsive polymer due to the presence of an electroresistive heater	In vitro: antibacterial efficacy and angiogenesis enhancement. In vivo: promotion of wound healing.
Son et al. (2014) <sup>[90]</sup>	Skin	V = N.A.	Polyimide + silica NPs	Drug release due to the thermal cleavage of the link between drug molecules and carrier	In vitro: enhanced drug release upon ES.

MAA, methacrylated alginate; AgNWs, silver nanowires; ES, electrical stimulation; PVP, polyvinyl pyrrolidone; PVA, poly(vinyl alcohol); AgNFs, silver nanofibers; PDMS, polydimethylsiloxane; NO, nitric oxide; EF, electric field; PPy, polypyrrole; rGO, reduced graphene oxide; PGS-PCL, poly(glycerol sebacate)-poly( $\epsilon$ -caprolactone); PEG, poly(ethylene glycol); PNIPAM, poly(N-isopropylacrylamide); PEGDA, poly(ethylene glycol) diacrylate; NP, nanoparticle.

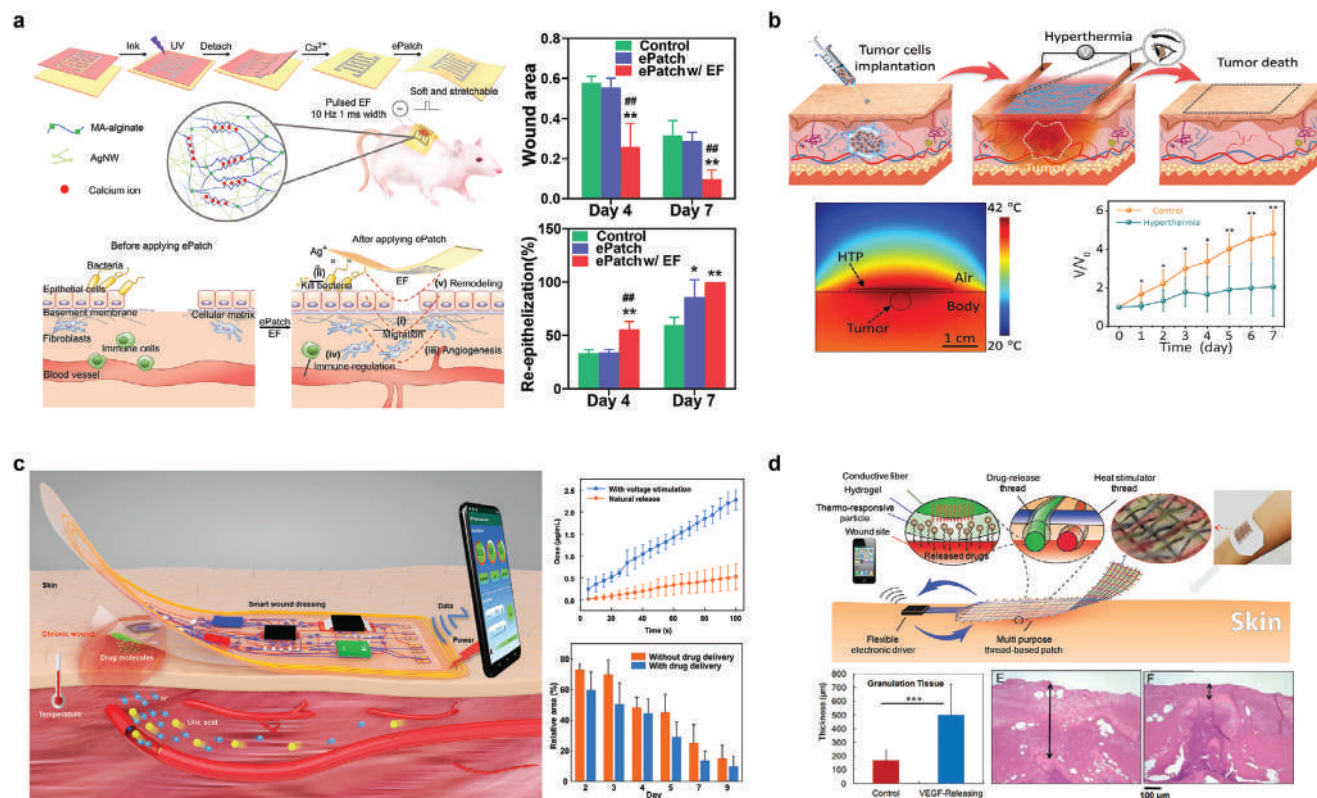


**Figure 3.** Electrically triggered patches with tissue stimulation and drug delivery capabilities. a) Schematic illustration of the electrical patch fabrication and structure and illustration of its biological activity; the application of the electrically stimulated patch in rats significantly reduced the wound area and increased re-epithelialization. Reproduced with permission.<sup>[69]</sup> Copyright 2022, Elsevier. b) Schematic illustration of the thin, soft, transparent, and high-performance hyperthermia patch based on silver nanofibers network for subcutaneous tumor apoptosis: in seven days, the localized temperature increase inhibited tumor growth by two folds with respect to a control. Reproduced with permission.<sup>[76]</sup> Copyright 2022, Wiley-VCH. c) Schematic illustration of the electrically-controlled antibacterial patch, where a wireless near-field communication module stimulates a conductive polypyrrole membrane, modulating the release of the encapsulated cefazolin antibiotics; this is due to the redox properties of polypyrrole, and the stimulated release was five times higher with respect to natural release, which resulted in a faster wound healing in vivo. Reproduced with permission.<sup>[85]</sup> Copyright 2021, Wiley-VCH. d) Schematic illustration of a multipurpose thread-based patch for transdermal drug delivery in which a hydrogel layer carrying thermo-responsive particles is coated on a flexible thread-based heater; the system was used in vivo for the treatment of wounds, which showed a significant increase in granulation tissue deposition in the wound bed. Reproduced with permission.<sup>[89]</sup> Copyright 2017, Wiley-VCH.

unidirectional silver nanofibers, which acted as independent conducting paths with the ability to induce a temperature increase by the Joule heating effect. The hyperthermia patch effectively treated subcutaneous tumors in nude mice, where tumor growth was suppressed two-fold with respect to control after mild-thermic (42 °C) treatment operated at an ultra-low voltage (0.7 V), which induced cell apoptosis (Figure 3b). Additionally, ES was exploited to chemically stimulate tissues through NO release for wound healing applications in Lee et al.'s work.<sup>[84]</sup> In fact, NO is endogenously produced, and it plays a dual role as a key agent in signaling for cell stimulation, angiogenesis promotion, and re-epithelialization and as a cytotoxic antimicrobial agent; its exogenous delivery could therefore promote the healing of chronic wounds. A polydimethylsiloxane (PDMS) patch, equipped with gold electrodes and a reservoir filled with nitrite and copper(II)-tri(2-pyridylmethyl)amine (CuTPMA) complex, was developed for this purpose: upon ES, electrochemical reduction of nitrite ions happens due to CuTPMA mediation, thereby producing NO, which is then released in the tissue. In vitro tests showed continuous NO release up to 4 days, resulting in an excellent

antimicrobial effect on both gram-positive and gram-negative bacteria.

However, the majority of electro-responsive patches focus on the application of EF for drug delivery purposes. For example, Xu et al.<sup>[85]</sup> developed a smart wound dressing with closed-loop monitoring and on-demand drug delivery abilities for wound treatment. It consisted of a PPy membrane encapsulating cefazolin antibiotics as anionic dopants that could be electrically controlled by an integrated wireless near-field communication module to modulate the release of its load. When a negative voltage stimulation was applied, the PPy film switched from an oxidized to a reduced state, and the drug molecules dissociated from the polymer backbone, moving out of the patch under electrical and diffusional forces. The release kinetics in the case of electrically controlled stimulation was significantly faster than the natural release, with a delivered dose five times higher than the passive release (Figure 3c). Furthermore, the efficacy of the patch was also tested in vivo, resulting in an enhancement of wound healing, with reduced scabbing, abundant capillary regeneration under the skin, and increased granulation tissue deposition on the

wound bed, which was almost three times thicker than that in a control group. In another work by Liu et al., a patch for drug delivery was made electrically responsive by introducing rGO nanosheets as a filler.<sup>[86]</sup> The system consisted of a poly(vinyl alcohol) (PVA) membrane incorporating rGO nanosheets and loaded with lidocaine hydrochloride, which is linked to rGO through intermolecular interactions. The application of ES on this hydrogel system enhanced the release of lidocaine, as the applied EF changed the charge of rGO nanosheets, causing the dissociation of its interactions with drug molecules. This phenomenon was thought to contribute to drug release in synergy with electroosmosis and electrophoresis. The amount of drug released from the hydrogel increased with the applied voltage, up to three times, while passive release in the absence of stimulation was remarkably low due to the dispersion of rGO nanosheets in the polymer matrix; this formed a 3D physical barrier hindering the diffusion of lidocaine molecules. Temporal control over the release could be achieved by providing an on-off voltage, which triggered a stepwise delivery profile; the higher the graphene concentration in the composite, the more distinct and precise in following the stimulation pulses.

In contrast, Sung et al. reported a flexible drug delivery microdevice for controlled local administration of therapeutics in the brain.<sup>[87]</sup> Their patch consisted of a flexible polyethylene terephthalate substrate, which allowed implantation on the curved surface of the cerebral cortex, and an epoxy multi-reservoir array loaded with a drug and covered by a gold sealing membrane also acting as an electrode. This device can be triggered by an EF through a wireless power transfer system employing near-field communication technology, and upon receiving a constant bias, the gold sealing membrane dissolves via an electrochemical reaction in human body fluid, freeing the drug in the reservoir and allowing its delivery. The performance of the patch was tested in vivo for the treatment of epilepsy and prevention of seizure activity using an anti-epileptic drug: it was implanted in the subdural space, filled with cerebrospinal fluid, and upon external powering, a specific drug (muscimol) was successfully administered in the targeted brain area.

Electrically induced hyperthermia has also been investigated for drug delivery purposes from patches, in combination with thermo-responsive polymers. For example, an electroresistive heater was exploited to trigger drug release from a thermo-responsive polymer in a study by Tamayol et al.<sup>[88]</sup> A bioresorbable heater, made of various metals, including silver, gold, zinc, and magnesium, was directly patterned on top of a poly(glycerol sebacate)-poly(caprolactone) (PGS-PCL) patch containing PEGylated-chitosan-based drug nanocarriers. A microcontroller was used to tune the voltage delivered to the heater, and upon stimulation by the heating unit, the thermo-responsive NPs released the encapsulated antibiotics due to the sol-gel transition that PEGylated chitosan undergoes at a critical temperature of  $\approx 37$  °C. Good control was achieved on this system, with a drug release rate that was proportional to the applied voltage. Furthermore, the drug release stopped when the ES was turned off, owing to a decrease in the patch temperature, thereby allowing drug delivery with a desired temporal profile. In a study by Mostafalu et al., a very similar concept was explored with the aim of achieving an on-demand release of different drugs with controlled and independent temporal profiles.<sup>[89]</sup> A wound

dressing was fabricated by weaving composite fibers, each consisting of a core electrical heater covered by a layer of hydrogel containing PNIPAM/poly(ethylene glycol) diacrylate thermo-responsive drug carriers (Figure 3d). The fibers were loaded with either antibiotic drugs or vascular endothelial growth factor (VEGF); they could be individually triggered by a wireless microcontroller, working as independent functional units to allow the on-demand release of a specific drug. The effectiveness of the patch in eliminating bacterial infection and inducing angiogenesis was tested in vitro; additionally, in vivo experiments were performed to test the efficacy of VEGF release, producing a higher than three-fold increase in granulation tissue and matrix deposition in the wound bed, compared to a control. Son et al.'s study also focused on electrically induced thermal effect for transdermal drug delivery, exploiting silica NPs as the thermo-responsive component.<sup>[90]</sup> An electroresistive heater raised the temperature of a polyimide patch incorporating drug-loaded mesoporous silica NPs, causing the degradation of the physical bonding between the NPs and drugs, thereby accelerating drug release and skin penetration. The system was then enriched with strain sensors for the measurement of movement disorders, such as tremors, and a memory device with the ability to feed recorded data to a circuit controlling the heater.

### 2.3. Magnetic Stimulation

Magnetic field (MF) represents the physical effect generated by a permanent magnet, a moving charge, or a changing EF in a surrounding space, which can result in an interaction with a moving charged particle entering the field space.<sup>[63]</sup> In practical applications, MFs are created using permanent magnets, or more frequently, electromagnets, i.e., wire coils or loops carrying a current.<sup>[91]</sup>

For centuries, natural magnetic materials have been used for therapeutic purposes; today, magnetotherapy is a clinically accepted treatment for various pathological conditions. Clinical data suggest that exogenous magnetic and electromagnetic fields can have remarkable effects on numerous biological processes. For example, over the past several decades, both static and alternating MFs have been successfully applied to treat therapeutically resistant pathologies of the musculoskeletal system, such as bone fractures, pseudo-arthroses, soft tissue edema, chronic tendinitis, and pain. However, a number of clinical studies and in vivo animal experiments also suggest that magnetic and electromagnetic stimulation can accelerate other kinds of healing processes, such as wound healing, nerve repair and regeneration, and immune and endocrine-related functions.<sup>[91]</sup> In fact, it has been shown that electromagnetic fields can beneficially affect cell proliferation and differentiation, expression of growth factors, and biochemical signaling.<sup>[34]</sup>

The attractiveness of magnetic therapy mainly comes from its non-invasiveness and ease of application to any target site. In fact, when delivering electromagnetic fields to the human body, especially in a relatively low-frequency range (<100 kHz), the electric and MF components behave differently: the EF generates an electric current mostly along the application surface, while the MF penetrates deeply into tissues, as the human body is mainly transparent to it.<sup>[91,92]</sup> Therefore, magnetotherapy represents



an attractive method of treating deep tissues. However, despite some definite advantages, clinical applications of magnetic and electromagnetic fields must be performed cautiously due to possible adverse effects, especially on DNA and cell replication; therefore, it is essential to further investigate the underlying mechanisms of MF- and electromagnetic field-induced effects on human health.<sup>[34]</sup>

In clinical practice, MFs in the kHz to MHz range have also been investigated for heat generation in combination with magnetic materials, which respond to an externally applied oscillating MF by causing a localized temperature increase.<sup>[93]</sup> The transformation of radio-frequency magnetic energy into heat by magnetic NPs (MNPs) has been attributed to Néel and Brown relaxation mechanisms occurring in single-domain superparamagnetic materials related to the inner fluctuation of the magnetic moment and rotation of the whole particle, respectively.<sup>[94]</sup> To characterize the heating of MNPs under alternating MF (AMF) exposure, their specific absorption rate (SAR) can be computed as heat generation per mass of NPs or iron content of NPs according to Equation (6):

$$SAR = \frac{m_s c_p}{m_{np}} \left( \frac{\Delta T}{\Delta t} \right) \quad (6)$$

where  $m_s$  is the mass of the particle suspension,  $m_{np}$  is either the mass of NPs or the mass of iron in the NPs,  $c_p$  is the heat capacity of the suspension, and  $(\Delta T/\Delta t)$  is the initial slope of the temperature rise versus time curve for NP heating. The power generated in response to an applied AMF, resulting in thermal energy, is described by the Rosensweig equation (Equation 7):<sup>[93]</sup>

$$P = \pi \mu_0 \chi_0 H^2 f \frac{2\pi f \tau}{1 + (2\pi f \tau)^2} \quad (7)$$

where  $\chi_0$  is the magnetic susceptibility of the particles,  $H$  is the MF strength,  $f$  is the frequency of the MF, and  $\tau$  is the relaxation time of the particles.

Moderate magnetic hyperthermia can be effectively employed for local stimulation of regenerative processes, including repair of damaged tissues and modulation of immune reactions, which benefit from thermal treatments.<sup>[34]</sup> In majority of cases, superparamagnetic iron oxide nanoparticles (SPIONs) are utilized as transducing material due to their excellent magnetic properties and biocompatibility. Additionally, several other inorganic magnetic materials, such as gold and silver NPs, are currently used in magnetically induced hyperthermia therapies.<sup>[79,95]</sup>

Furthermore, MFs are also largely employed to externally trigger drug release from magnetically responsive delivery systems, thereby incorporating magnetic materials generally in the form of NPs. Drug release can be magnetically triggered using either static or alternating MFs, exploiting different mechanisms. The application of a static MF can be used to mechanically deform or move parts of a composite delivery system, for example, to trigger a compression of the carrier and therefore cause the drug to be squeezed out of it. In contrast, AMFs can induce mainly two different effects according to the driving frequency: low-frequency AMFs can locally shear the material adjacent to the MNPs, creating damage in the carrier that leads to enhanced drug release; alternatively, the application of a high frequency (tens to hun-

dreds of MHz) AMF results in the local generation of heat that can induce drug release via thermal triggering when coupled to thermo-responsive materials.<sup>[48,79]</sup>

The idea of using magnetic stimulation to activate drug release dates back to the 1970s, when a study was conducted on adriamycin-loaded magnetic microspheres for tumor targeting;<sup>[96]</sup> since then, MFs have represented the most common method for external activation of injectable drug carriers, such as NPs, micro and nanocapsules, polymersomes, and liposomes.<sup>[79,97]</sup> Regarding macroscopic delivery systems, like scaffolds and patches, magnetic triggering has been much less investigated with respect to other triggering methods, such as light and electric stimulation. However, some studies focus on macroscopic magnetic delivery systems based on magnetic polymer composites, which consist of a combination of hydrogels or polymer films and MNPs;<sup>[98,99]</sup> they have been demonstrated to activate a reversible on-off drug release upon application and removal of an external MF (see Table 3).<sup>[100]</sup>

For example, Lee et al. developed a flexible magnetically responsive patch with the ability to provide in situ a prolonged drug delivery to brain tumors.<sup>[23]</sup> This device included a magnesium-based bioresorbable heater, which could be activated wirelessly through a radiofrequency MF (220 Hz, 360 A), and a polylactic acid (PLA) layer acting as a drug reservoir, which encapsulates doxorubicin. Upon external application of the AMF through a coil, eddy currents, and Joule heating were generated in the heater, causing mild hyperthermia that enhanced drug diffusion from the reservoir and drug penetration, which is about three times with respect to the natural diffusion of doxorubicin (Figure 4a). The application of the patch in a mouse model confirmed an improved survival rate due to an actual tumor growth suppression, with a tumor volume reduction of more than 10 times with respect to untreated tumors. Exploiting an analogous mechanism, a biodegradable flexible device for breast cancer treatment was proposed by Li et al.<sup>[101]</sup> It consisted of a zinc energy receipt coil, which can be powered by an external AMF, MgO insulating layer, and zinc heater, which converts the energy received by the coil to heat, all encapsulated in a drug-loaded poly(lactic acid-trimethyl carbonate) layer. When the patch was excited by an external AMF, its temperature increased, depending on the input power, allowing magnetothermal treatment of cancer and boosting the release of the preloaded drug due to enhanced diffusion. In vitro experiments on breast cancer cells (MCF-7) showed that the combined effects of controlled drug release and hyperthermia induced a reduction of tumor cell viability of 75% with respect to controls.

Lee et al. presented a mucoadhesive patch for controlled drug release and hyperthermia treatment to the gastrointestinal tract.<sup>[102]</sup> Their device consisted of a PVA patch with a chitosan-catechol layer loaded with doxorubicin and MNPs, which are responsible for the temperature rise upon the application of an external AMF. In vitro tests on HT-29 tumor cells confirmed the therapeutic efficacy of the proposed patch: the AMF-induced hyperthermia alone reduced cell viability from 90% to 37%, and the synergistic effects of hyperthermia and magnetically enhanced drug release resulted in an apoptosis of 25% for the loaded patch under AMF application. Similarly, a magnetic nanofibrous patch for controlled topical delivery of anti-psoriatic drugs was developed by Andrýsková et al.<sup>[103]</sup> PCL nanofibers with embedded

**Table 3.** Magnetically responsive patches and their working mechanisms.

Reference	Target organ	Stimulation parameters	Patch material	Action	Results
Lee et al. (2019) <sup>[23]</sup>	Brain	I = 360 A f = 220 Hz	PLA	Drug release due to a temperature increase induced by a magnetic heater	In vitro: enhanced drug release upon MF application. In vivo: tumor size reduction.
Li et al. (2021) <sup>[101]</sup>	Breast	I = N.A. f = 315 kHz	PLA + zinc heater	Hyperthermia treatment + drug release due to a temperature increase induced by a magnetic heater	In vitro: reduced tumor cells viability due to the synergistic effects of magnetic hyperthermia and enhanced drug release.
Lee et al. (2022) <sup>[102]</sup>	Gastrointestinal tract	I = 320 A f = 272 kHz	PVA-chitosan + MNPs	Magnetic hyperthermia generated by MNPs + drug release due to the temperature increase	In vitro: enhanced drug release upon MF application; reduced tumor cells viability upon treatment with the patch under MF.
Andrišková et al. (2021) <sup>[103]</sup>	Skin	I = 64 mA f = 3.5 MHz	PCL + MNPs	Drug release due to the hyperthermic effect of MNPs	In vitro: enhanced drug release upon MF application.
Hoare et al. (2011) <sup>[100]</sup>	-	B = 0–20 mT f = 220–260 kHz	PNIPAM + SPIONs	Drug release due to an increased permeability of the thermo-responsive membrane induced by magnetic hyperthermia	In vitro: pulsatile release in response to an on-off MF.
Gonçalves et al. (2021) <sup>[104]</sup>	-	H = 24 kA/m f = 418.5 kHz	PVP + PNIPAM-chitosan-SPIONs particles	Magnetic hyperthermia generated by SPIONs	In vitro: temperature increase upon application of a MF.

PLA, polylactic acid; MF, magnetic field; PVA, poly(vinyl alcohol); PCL, polycaprolactone; MNPs, magnetic nanoparticles; PNIPAM, poly(N-isopropylacrylamide); SPIONs, superparamagnetic iron oxide nanoparticles; PVP, poly(vinyl pyrrolidone).

MNPs were electrospun to form a smart hyperthermia patch, in which the heat generated by the MNPs in response to an AMF induced drug release from PCL, when its melting temperature was reached. The magnetically triggered release of tazarotene and its permeation through a skin sample were demonstrated in vitro: the release increased up to 60% after 24 h under the effect of an AMF compared to a passive release of just 5% in the absence of the field. Hoare et al. described another device for drug delivery, exploiting magnetic hyperthermia as well, but with a different mechanism.<sup>[100]</sup> This device consisted of a composite membrane containing both PNIPAM-based temperature-sensitive polymer NPs and magnetically activated SPIONs, which covered a reservoir filled with the drug solution. The SPIONs behave as local heat sources activated by an oscillating MF; in response to the thermal trigger, the PNIPAM NPs underwent a phase transition and collapsed, generating an increase in the total free volume inside the membrane and enhancing the transport of the drug molecules from the reservoir and across the membrane. The study showed that it was possible to precisely control drug dosing by tuning the duration, frequency, or power of the pulsed MF applied, and that a repeatable on-off switching of the drug flux could be achieved. In fact, the drug release rate was shown to be a function of the temperature, with a drug flux ratio through the membrane between the on and off states of approximately eight (Figure 4b).

Gonçalves et al. proposed a magnetic patch for hyperthermia treatment of tumors.<sup>[104]</sup> Hybrid microgels, consisting of PNIPAM, chitosan, and iron oxide NPs, were incorporated in poly(vinyl pyrrolidone) (PVP) fibers through colloidal electrospinning, forming a cross-linked membrane. Results of magnetic hyperthermia assays demonstrated that incorporating SPIONs into microgels and PVP membranes did not significantly affect their heating ability. The membranes were shown to produce a temperature variation adequate for cancer treatment through magnetic hyperthermia, with a tumor cell viability reduction of 10% with respect to controls.

#### 2.4. US Stimulation

Ultrasound is a mechanical wave with frequencies >20 kHz (that is the upper limit of the human hearing range). US waves, unlike the electromagnetic ones, cannot travel in vacuum, but necessarily need a medium to be propagated. US propagation in a quiescent and isotropic medium can be described by the following second-order equation (Equation 8):

$$\nabla^2 P_{US} - \frac{1}{c_0^2} \frac{\partial^2 P_{US}}{\partial t^2} = 0 \quad (8)$$

where  $P_{US}$  is the acoustic pressure and  $c_0$  represents the speed of the wave in the medium.<sup>[33,105]</sup>

In clinical practice, US is widely employed and accepted as an imaging modality for diagnostic purposes due to its ease of use, low cost, and non-invasiveness.<sup>[48]</sup> However, besides this well-known use, US is recently emerging as a therapeutic tool to induce beneficial bioeffects within the human body for a wide range of applications.<sup>[105]</sup> The attractiveness of this kind of biophysical energy for therapeutic purposes lies primarily in its highly effective penetration in most tissues in the human body, specifically

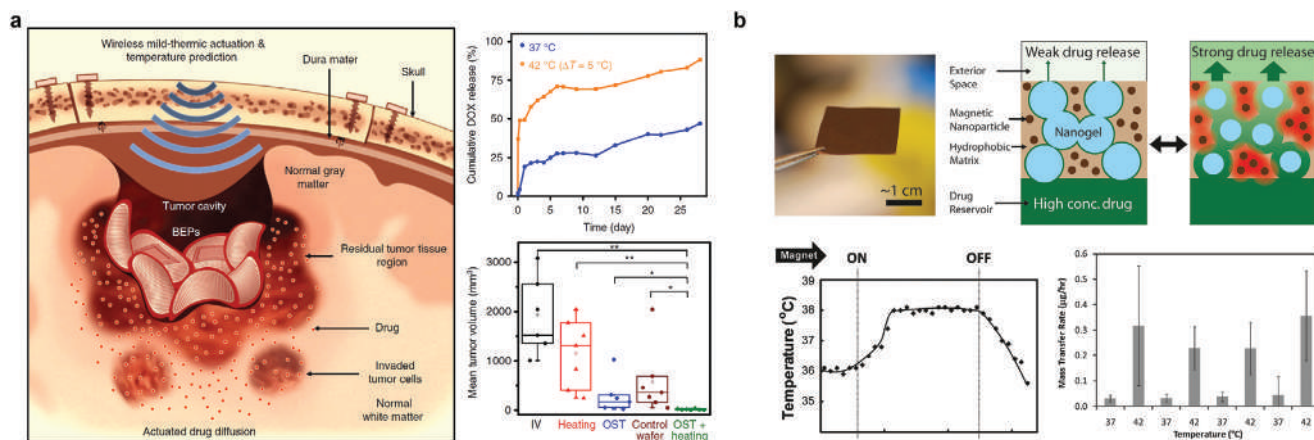


**Figure 4.** Magnetically triggered patches with drug delivery capabilities. a) Schematic illustration of the localized drug delivery in deep glioblastoma tissues through the bioresorbable patch with magnetic mild-thermic actuation; a temperature increase enhanced the release of doxorubicin, producing a dramatic decrease of tumor volume with respect to control. Reproduced under terms of the Creative Commons CC-BY License.<sup>[23]</sup> Copyright 2019, The Authors, published by Springer Nature. b) Photograph and schematic illustration of the working mechanism of a membrane containing ferromagnetic nanoparticles and nanogels: through magnetic actuation, a temperature increase can be obtained, resulting in an enhancement of drug release with respect to the off states. Reproduced with permission.<sup>[100]</sup> Copyright 2011, American Chemical Society.

in soft tissues<sup>[79]</sup> Therefore, US allows safe and non-invasive targeting of most deep tissues.<sup>[46,106]</sup> Furthermore, US also allows a good spatial resolution within the body due to its high focusing capability and controllability.<sup>[107]</sup>

In general, depending on the stimulation parameters and the nature of the tissue, therapeutic US is used to induce thermal or mechanical effects in a target area.<sup>[105]</sup>

The main mechanical effects induced by US are acoustic cavitation, radiation force, and microstreaming. The former involves the formation, oscillation, and possible collapse of gas bubbles, called cavitation nuclei, within tissues or fluids; the probability of inducing such an effect is described by the mechanical index (MI), which is defined as follows by Equation 9:

$$MI = \frac{P_{nP}}{\sqrt{f}} \quad (9)$$

where  $P_{nP}$  is the negative peak pressure and  $f$  is the frequency of the US wave.<sup>[105]</sup> Radiation force is derived from a pressure gradient across the surface of the bubble and it results in bubble translation in the direction of the sound field.<sup>[108]</sup> Microstreaming refers to flow induction in fluids through US due to the production of shear forces near the surface of the oscillating gas bubbles.<sup>[106]</sup>

The thermal effect of US, also known as the hyperthermia effect, is due to the fact that when US passes through tissues, the friction and absorption by the medium convert part of the ultrasonic energy into localized heat.<sup>[46,106]</sup> The absorbed US energy, described in terms of the rate of heat deposition per unit volume ( $\dot{Q}$ ), is given by the following Equation (10):

$$\dot{Q} = \mu I \quad (10)$$

It depends on the absorption coefficient ( $\mu$ ) of the medium and acoustic intensity ( $I$ ) of the wave.<sup>[105]</sup>

US at high intensities, namely high-intensity focused US, is used for destructive applications, such as cancer treatment and surgery. It can induce high thermal effects, typically associated with temperatures  $>56$  °C, which lead to tissue necrosis.<sup>[105]</sup> Furthermore, it is also associated with lethal mechanical effects at high MI, like inertial cavitation, where the high acoustic pressure causes rapid collapse of microbubbles (MBs), producing irreversible mechanical damage to tissues, such as cell membrane rupture.<sup>[106]</sup>

In contrast, low-intensity US ( $20\text{--}1000$  mW cm<sup>-2</sup>) is exploited in non-destructive applications for tissue modification and/or repair, for example, in physiotherapy, regenerative medicine, and targeted drug delivery.<sup>[33,105]</sup> For example, low-intensity pulsed US (LIPUS), consisting of on/off cycles of US waves, induces non-lethal mechanical effects at low MI, such as mild microstreaming and stable cavitation. In this case, bubbles periodically oscillate around their equilibrium radius without collapsing and lead to mild localized stress on cell membranes, thereby increasing the exchange of nutrients and promoting drug delivery and absorption.<sup>[106]</sup> Low-intensity continuous US (LICUS) can also induce mild hyperthermia besides the mechanical effects just mentioned, resulting in a low thermal rise in tissues, typically lower than 43 °C.<sup>[105]</sup> Thus, LIPUS and LICUS have been investigated as potential therapeutic means for a wide variety of conditions. For example, their effectiveness is accepted in promoting fracture healing, osteoporosis, and osteoarthritis, but they have also been proved to accelerate regeneration and healing of soft tissues, such as cartilage, ligaments, and tendons; furthermore, US has been investigated for chronic wound healing purposes. Its regenerative efficacy is thought to be derived from its effects on molecular and cellular pathways, which result in increased cell proliferation, differentiation, and migration, and in the promotion of neovascularization.<sup>[106,109,110]</sup> Additionally, US stimulation has been suggested to modulate inflammation and infections and to be effective in pain management and neuromodulation.<sup>[33,111,112]</sup>

Finally, US can also be employed in combination with piezoelectric materials in order to generate localized EFs, combining the therapeutic advantages of ES with the non-invasiveness and penetration ability of US. Piezoelectric materials, owing to the non-centrosymmetry of their crystal structure, can either generate electric dipole moments in response to the application of mechanical stress (direct piezoelectric effect) or produce mechanical strain under the application of an EF (inverse piezoelectric effect).<sup>[113]</sup> Therefore, ultrasonic stimulation of piezoelectric nanostructures constitutes an appealing paradigm, enabling the induction of electrical cues within the body in a localized, wireless, and minimally invasive fashion.<sup>[105,114]</sup>

US has also been explored as a biophysical trigger for non-invasive targeted drug delivery from US-responsive carriers, such as MBs. MBs consist of a gas core, such as perfluorocarbons (PFC), nitrogen, or air, surrounded by an outer shell of lipids, polymers, or proteins,<sup>[46]</sup> and they are characterized by their ability to undergo compression and expansion in response to the pressure created by US. The release of their payload can therefore be triggered through the mechanical action of US: by cavitation, if oscillation at the MB's resonance frequency causes the vaporization of its gas core, or by microstreaming, if the ultrasonic oscillation of the MBs generates shear-field streamlines in surrounding fluids, promoting drug release from the MBs.<sup>[48]</sup> Alternatively, US-induced heating can be used to trigger drug delivery from thermo-responsive vehicles.<sup>[79]</sup>

Similar to MF, US is significantly investigated to trigger drug release from intravenously-administered vehicles, such as microemulsions, polymer micelles, liposomes, and microcapsules, thereby exploiting both thermal and mechanical effects.<sup>[107,115,116]</sup> Some studies also reported the use of US stimulation to trigger drug delivery from acoustically-responsive scaffolds, incorporating drug-loaded sonosensitive particles, such as emulsions or MBs,<sup>[117,118]</sup> or from thermosensitive hydrogels.<sup>[119]</sup> However, to date, attempts to exploit US to control drug release from a patch are quite limited (see **Table 4**).

One of the first attempts in this regard was made by Kost et al., who synthesized a drug-loaded polymer patch with the ability to degrade on demand in response to US exposure.<sup>[120]</sup> The authors tested several bioerodible polymers, including polyglycolides and polylactides, which rapidly responded to an ultrasonic trigger, thereby increasing their release rate due to US-induced cavitation effects. In fact, the shock waves created during cavitation induced the rupture of polymer chains and increased the penetration of water species into the polymer, thereby promoting its hydrolytic degradation. Under US stimulation, an increase of up to five-fold in the degradation rate of the polymers was achieved, accompanied by an increase in the release rate of the incorporated molecules of up to 20-fold. The drug-loaded disks were also subcutaneously implanted in rats, thereby also confirming the effectiveness of this approach *in vivo*. More recently, a wearable transdermal patch for US-enhanced delivery of lidocaine was developed by Soto et al.<sup>[121]</sup> This patch consisted of a flexible drug reservoir containing hundreds of micropores loaded with lidocaine and PFC emulsion. US waves could trigger the vaporization of the emulsions through acoustic droplet vaporization (ADV) phenomena, resulting in enhanced lidocaine release. Furthermore, the highly localized stress force produced by ADV also concurred to enhance skin permeability by more than two times with re-

spect to passive diffusion, reversibly breaching the dermal barrier and effectively enabling the therapeutic payload to pass faster through the skin, as shown by *ex vivo* drug release tests on pig skin samples (**Figure 5a**). Huang et al. developed a drug delivery system in which US was employed both as a drug release trigger and a means to improve penetration.<sup>[122]</sup> They designed and fabricated a US-responsive transdermal patch by embedding drug-loaded polyethylene glycol/poly(lactic-co-glycolic acid) (PEG-PLGA) microcapsules into a PEG hydrogel patch. *In vitro* release experiments validated the US-responsive behavior of the patch, showing a stepwise release curve under intermittent US stimulation and an enhancement in drug release of up to five-fold under continuous US with respect to passive release. *Ex vivo* and *in vivo* tests also demonstrated quick permeation of the drug released by the patch through the skin and into subcutaneous tissues due to the sonophoretic effect of US, which caused a temporary disruption of the lipid bilayer structures in the stratum corneum.

US has also been investigated in association with piezoelectric patches for both externally controlled drug delivery and patch-mediated tissue stimulation. For example, Vannozzi et al. developed a piezoelectric vascular nanopatch loaded with an anti-restenotic drug with tunable drug release kinetics for the local treatment of restenosis (**Figure 5b**).<sup>[123]</sup> Their study reported the fabrication of a polyelectrolyte layer-by-layer nanofilm, in the middle of which the drug was embedded, deposited on a PLA-supporting membrane incorporating barium titanate NPs, which endowed the film with piezoelectric properties. *In vitro* tests demonstrated enhanced drug release from the films upon US triggering, with a 1.5-fold increase after 4 h, and a consequent effective inhibition of smooth muscle cell proliferation, suggesting the possibility to prevent restenosis phenomena. Such enhanced drug release was attributed to mechanical deformations of polyelectrolytes, induced by US waves *per se*, and electrical effects generated by US interactions with barium titanate NPs, which generated local electrical potentials.

Gazvoda et al. developed a piezoelectric biodegradable film composed of poly-L-lactide (PLLA) for antimicrobial applications.<sup>[124]</sup> Owing to the use of a piezoelectric polymer, with high biocompatibility and biodegradability, the application of US stimulation caused mechanical deformation of the patch, thereby generating a surface charge modification that affected the presence of bacteria. The film was shown to have an antibacterial effect on both gram-positive and gram-negative bacteria *in vitro* and *in vivo*, as piezostimulation damaged the bacterial membrane, without having any harmful effects on the membranes of human cells, such as the red blood cells (**Figure 5c**). Similarly, Shi et al. reported another piezoelectric patch consisting of a piezoelectric copolymer, poly(vinylidene fluoride-tri-fluoroethylene), incorporating a piezoelectric filler of barium titanate (BaTiO<sub>3</sub>) NPs.<sup>[125]</sup> The ability of these membranes to induce localized electrical stimuli under US therapy was tested, also implanting them at different depths in porcine tissue to assess the effective penetration of US in tissues. It resulted that, even if the output voltage decreased with increasing implantation depth, the membranes generated significant voltages of >8 V even at depths of 4.5 cm, confirming their remote activation. Furthermore, *in vivo* tests demonstrated that US stimulation of these piezoelectric membranes could



**Table 4.** Ultrasound-responsive patches and their working mechanisms.

Reference	Target organ	Stimulation parameters	Patch material	Action	Results
Kost et al. (1989) <sup>[120]</sup>	Skin	f = 20–75 kHz I = 5 W cm <sup>-2</sup>	Polyglycolides and polylactides	Drug release due to mechanically induced polymer degradation	In vitro: pulsed release in response to an on/off US stimulation. In vivo: enhanced drug release upon external triggering.
Soto et al. (2018) <sup>[121]</sup>	Skin	f = 2.25 MHz I = N.A.	PVP + PFC	Drug release and skin permeation enhancement due to ADV-induced cavitation	In vitro: faster drug release upon US stimulation. Ex vivo: enhanced drug penetration through a skin sample.
Huang et al. (2019) <sup>[122]</sup>	Skin	f = N.A. I = 2 W cm <sup>-2</sup>	PEG + PEG-PLGA microcapsules	Drug release and skin permeation enhancement due to mechanical effects of US	In vitro: drug release enhancement under US stimulation. Ex vivo: enhanced drug penetration through skin upon US stimulation.
Vannozzi et al. (2016) <sup>[123]</sup>	Arteries	f = 40 kHz P = 9 W cm <sup>-2</sup>	PLA + BaTiO <sub>3</sub> NPs / HA-PLLA	Acceleration of drug release due to mechanical and piezoelectric effects due to the presence of BaTiO <sub>3</sub> NPs	In vitro: burst release in response to US triggering.
Gazvoda et al. (2022) <sup>[124]</sup>	Skin	f = 37 kHz; I = N.A.	PLLA	Piezoelectric stimulation mediated by a piezoelectric polymer	In vitro: effective bactericidal action.
Shi et al. (2022) <sup>[125]</sup>	Skin	f = 1 MHz I = 0.5–2.5 W cm <sup>-2</sup>	P(VDF-TrFE) + BaTiO <sub>3</sub> NPs	Piezoelectric stimulation mediated by a piezoelectric composite	In vitro: enhanced fibroblast proliferation and migration. In vivo: acceleration of wound healing.
Lyu et al. (2021) <sup>[126]</sup>	Skin	f = 2.2 MHz I = 10–40 mW cm <sup>-2</sup>	PZT-4 + PDMS	Generation of US due to a piezoelectric transducer	In vitro: activation of a key protein for wound healing. In vivo: acceleration of wound closure.

US, ultrasound; PVP, polyvinylpyrrolidone; PFC, perfluorocarbon; ADV, acoustic droplet vaporization; PEG, poly(ethylene glycol); PLGA, poly(lactic-co-glycolic acid); PLA, poly(lactic acid); NP, nanoparticle; HA, hyaluronic acid; PLLA, poly(L-lactic acid); P(VDF-TrFE), poly(vinylidene fluoride-tri-fluoroethylene); PZT, lead zirconate titanate; PDMS, polydimethylsiloxane.

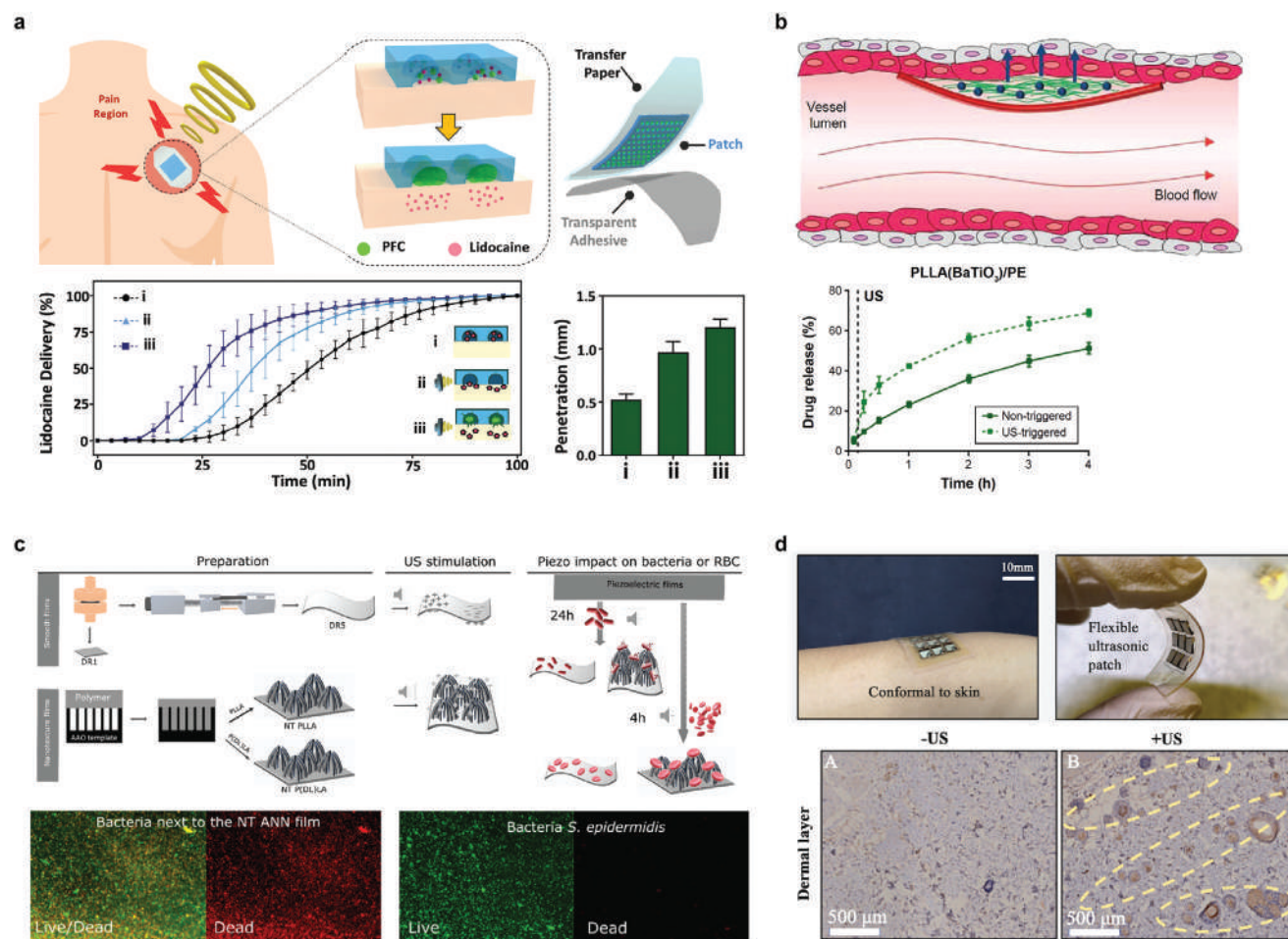


**Figure 5.** Ultrasound-triggered patches with tissue stimulation and drug delivery capabilities. a) Schematic illustration of the layered patch and its operational principle of ADV delivery; the application of ultrasound waves increased drug release and penetration through the skin more than two-fold. Reproduced with permission.<sup>[121]</sup> Copyright 2018, Wiley-VCH. b) Illustration of a piezoelectric nanofilm for the treatment of restenosis: its drug delivery performances are shown to be enhanced under US stimulation with respect to non-stimulated conditions. Reproduced with permission.<sup>[123]</sup> Copyright 2016, Dove Medical Press Ltd. c) Schematic illustration of the preparation of piezoelectric polymer films and their expected response to ultrasound stimuli: they display an efficient antibacterial effect, without causing damage to the red blood cells. Reproduced under terms of the Creative Commons CC-BY-NC License.<sup>[124]</sup> Copyright 2022, The Authors, published by Royal Society of Chemistry. d) Photograph of the skin-conformable ultrasonic patch, which accelerates wound healing, as shown by a higher production of the marker protein, Rac1. Reproduced with permission.<sup>[126]</sup> Copyright 2021, Wiley-VCH.

facilitate the proliferation and migration of fibroblasts, with a migration rate of 92.6% after 24 h; in vivo, they accelerated wound closure rate in mice, favoring complete re-epithelialization without scabbing.

Furthermore, a patch that directly stimulates tissues through US was developed by Lyu et al., who fabricated a US transducer, shaping it in the form of a patch, with the ability to focus the generated sound beams according to its bending radius and adapt itself properly to the skin surface due to its flexibility, unlike conventional US transducers.<sup>[126]</sup> The device was made of piezoelectric ceramic units, linearly arranged and integrated into a PDMS flexible circuit substrate, which ensured US generation upon external supply of an electric stimulus (Figure 5d). Immunohistochemical tests indicated that the generated US accelerated wound closure, shortening healing time by approximately 40% through the activation of Rac1 protein in both dermal and epidermal lay-

ers, which plays an important role in new tissue formation and wound healing.

## 2.5. Comparison between Stimuli

As reported in the above sections, light, ES, MFs and US have all been investigated to control triggerable patches for different applications.

Light and ES are mainly used for applications on superficial tissues, such as wound healing and transdermal and subcutaneous drug delivery, due to their very limited ability to penetrate human tissues. The only way to exploit this kind of biophysical energies to target internal organs is to employ invasive stimulation tools, such as optical fibers or needle electrodes bringing the stimulus directly to the target site, or to design implantable

devices integrating the source of the stimulus. For both light and EF, stimulation systems are currently flexible and highly miniaturized, which makes them easy to incorporate in a patch; therefore, the latter option is not unfeasible at the state of the art. However, to date, these two stimuli are mostly employed for external applications.

EF is widely used, since it is quite safe, as something naturally occurring in numerous processes in the human body, obviously within intensity limits. Furthermore, it is particularly suitable for closed-loop systems, since monitoring sensors can directly communicate with triggering systems through electrical signals.

Light has the advantage of allowing a very high focus, even with simple and standard equipment (e.g., LED arrays and lasers), permitting good spatial control over the stimulation. However, it poses some concerns in terms of cytotoxicity, especially for UV light. Even if NIR light is considered safer and has a slightly higher penetration ability, UV is much more frequently employed in triggerable systems, mainly because majority of photosensitive materials and molecules are responsive to UV light, which carries a higher energy per photon. However, it would be possible to address this issue due to specific materials, such as upconversion NPs, which can convert NIR light into UV or visible light, enabling UV-triggered technologies to be activated with NIR light.<sup>[46,79]</sup>

US and magnetic stimulation are most suited for internal applications, since they penetrate easily through most human tissues. US propagation is only hindered by the hard tissues, such as bones. This makes US hardly usable for targeting organs such as the lungs, which are right behind the ribs, or the brain, which is protected by the skull. In contrast, MF is mostly unaltered by all tissues and can propagate in every body area with almost no attenuation. However, it must be considered that magnetic stimulation, unlike US, is not suitable for targeting very small organs or body parts, as MFs do not have a high focusing ability, but usually invest relatively large regions.

From this summary, it shows that due to its physical nature, each stimulus is more suited for some applications on specific target organs than others. Therefore, having in mind a specific clinical application, it is always recommended to perform a feasibility study in order to understand whether a chosen stimulus can be suitable for the said target. For example, this can be made through appropriate simulation tools, which allow consideration of parameters, such as the penetration ability of the stimulus in the specific anatomic environment of the target, and its focusing capability, which puts constraints on the spatial resolution of the stimulation.

In **Table 5**, we report some parameters that could guide the process of selecting the most fitting biophysical trigger for a specific application. The penetration ability of each stimulus is reported along with the focus that can be achieved with different kinds of stimulation equipment available. “Standard” equipment refers to stimulation devices that are commonly employed for triggering patches, while “advanced” equipment refers to devices that are not currently employed in combination with patch systems, but have been used for therapeutic stimulation and offer some improvements with respect to the standard. Furthermore, safety ranges are reported for the intensity of each stimulus, according to the literature on biophysical stimulation. Finally, we report the most common applications, which can be found in the state of

the art, considering patches that are triggered by a specific stimulus, but do not integrate the stimulus source on board.

### 3. Crucial and Desirable Patch Features: Currently Available Technologies and Open Challenges

Besides endowing patches with the desired functional features to carry out the meant therapeutic action, there are other essential aspects that must be carefully taken into consideration during the design process in view of a medical application (**Figure 6**). Clinical patches must fulfill at least a few general requirements, such as proper mechanical and adhesive properties, biocompatibility, and in some cases, biodegradability. Addressing these issues is still challenging in general, and even more so for active patches, for which the tuning of these aspects should not interfere with their functionality. Furthermore, there are other collateral aspects (such as modeling, control, portability, sensing, delivery procedures, and selection of a suitable therapy for the specific clinical target), which are not as fundamental as the previous ones, but could be of great help in guiding future study efforts, thereby improving current performances and facilitating clinical translation. In the following, all these open challenges, both related to general patches and strictly concerning active patches, are discussed in detail.

#### 3.1. Tailoring Mechanical Properties

Tuning the mechanical properties of a patch is a crucial aspect. In fact, as any patch must conform to the organ surface on which it is applied to, it is of paramount importance that its mechanical properties reflect, or at least are compatible with the mechanical properties of the target tissue. A possible mismatch in mechanical behaviors may cause unwanted stresses on either the patch or the tissue, which could result in patch detachment, damage, or undesired bioeffects.<sup>[145]</sup> For example, wearable patches are required to conform and adhere to the skin, which is a highly dynamic surface, and are expected to have high flexibility to tolerate skin stretching and straining, especially in correspondence of joints, such as knees or elbows, where strain can reach up to 50%, and to maintain their characteristics while supporting physiological loads. Furthermore, being exposed to the external environment, they should also be tough enough to withstand compression and stretching.<sup>[146]</sup> However, for other target organs, the mechanical requirements could be very different. For example, for cardiac applications, toughness and elastic modulus are important parameters to allow the patch correctly withstand the heart beating. In addition to patches having an elastic modulus in the range of the human myocardium (between 20 and 500 kPa), patches and scaffolds with higher Young's moduli (between 7–20 MPa) have also been proven to be suitable for cardiac applications, as they help retain the mechanical strength of the organ until complete regeneration of heart tissue; however, it is important to always maintain a right balance between stiffness and flexibility to support repeated stretch cycles, without constraining the contractions and relaxation of cardiac muscle.<sup>[145,147,148]</sup> In visceral wound healing applications, the degree of elasticity is crucial, as patches need to bear the traction force of the organ

**Table 5.** Summary of performance parameters of the four biophysical stimuli presented and their most common applications. LED = light-emitting diode; OLED = organic light-emitting diode; DC = direct current; NFC = near-field communication; EF = electric field; RF = radiofrequency; PEMF = pulsed electromagnetic field; TMS = transcranial magnetic stimulation; MRI = magnetic resonance imaging.

	Safety	Penetration (order of magnitude)	Equipment (stimulus source)	Applications with patches (to date)
<b>Photo-stimulation</b>	Laser <5 W cm <sup>-2</sup> [127]	μm-mm	<b>Standard</b> Laser, LED, OLED	<b>External:</b> wound healing, dermatological diseases (skin)
			<b>Advanced</b> Two-photon excitation	
<b>Electrical stimulation</b>	<100 mA cm <sup>-2</sup> [130]–140 mV mm <sup>-1</sup> [131]	μm-mm	<b>Standard</b> Portable voltage supplier, DC power supply, NFC equipment, mini-batteries, EF wireless generators	<b>External:</b> wound healing, subcutaneous tumors (skin)
			<b>Advanced</b> High-density electrodes arrays	
<b>Magnetic stimulation</b>	<3.0 T (5–30 minutes)[133]	cm	<b>Standard</b> RF generators, solenoids (different models), permanent magnets, PEMFs	<b>External:</b> skin <b>Internal:</b> brain, breast, gastrointestinal tract
			<b>Advanced</b> Navigated TMS, MRI, OctoMAG	

(Continued)



Table 5. (Continued)

	Safety	Penetration (order of magnitude)	Equipment (stimulus source)	Applications with patches (to date)
<b>US stimulation</b>	<3000 mW cm <sup>-2</sup> [135]	cm (in soft tissues)	<p><b>Standard</b></p> <p>Piezoceramic transducers</p> <p><b>Advanced</b></p> <p>Capacitive/piezoelectric micromachined ultrasonic transducers (CMUT/PMUT)</p>	<p><b>External:</b> wound healing</p> <p><b>Internal:</b> arteries, antibacterial effects on tissues</p>
			<p><b>Focus</b> mm</p> <p><b>Bulkiness</b> cm</p> <p><b>Cost</b> 1–10 k\$</p> <p><b>Focus</b> mm</p> <p><b>Bulkiness</b> 100 μm</p> <p><b>Cost</b> 100–1000 \$</p>	

walls while limiting their deformation to keep the wound edges close at any moment.<sup>[7]</sup>

Furthermore, patch stiffness is also a crucial factor in determining the foreign body response, which is a recurrent phenomenon that risks impairing the functionality of implantable devices.<sup>[149]</sup> The stiffness of the implant influences the behavior of a wide variety of cells involved in the fibrotic reaction: fibroblasts and macrophages have been shown to adhere more substantially to the surface of stiffer materials,<sup>[150]</sup> which also favor the polarization of macrophages toward a pro-inflammatory phenotype. Similarly, neutrophil activation can also be modulated through stiffness: their migration speed was found to decrease on stiff (100 kPa) polyacrylamide hydrogels compared to softer (5 kPa) ones.<sup>[151]</sup>

In the literature, several solutions are proposed to tune the desired mechanical properties of patches, according to the specific application. A common strategy consists of integrating the bulk structure with additive materials, chosen specifically for their mechanical properties, besides the “functional” ones selected for their intelligent behavior. For example, the introduction of low molecular weight plasticizers, which can be interposed between polymer strands, has been shown to improve patch flexibility and toughness. In the study by Pushp et al., glycerol or propylene glycol reduced tensile strength and Young’s modulus of PVA–PVP patches, allowing it to fall in the required mechanical range for cardiac patches, and also increased the percentage elongation at break by nearly two times.<sup>[147]</sup> In another study, to limit the deformation of a suture-free adhesive patch for visceral wounds, a strengthening layer of PLLA was added to the patch structure: this addition produced a 50% increase in the tensile strength of the patch with respect to the bare matrix and increased the elastic modulus up to 84 MPa.<sup>[7]</sup>

To increase the toughness of a matrix (besides the employment of interpenetrating double networks) formed by the interlocking of two different polymer chains, it is also possible to modulate the crosslinking density of chains.<sup>[146]</sup> For example, the mechanical properties of PGS are directly associated with the cross-linking degree and are easily tunable by altering curing time: cross-linking of ester bonds in the PGS backbone forms a 3D network of random thermoset coils, which has a rubber-like elastic behavior, and an increase in cross-linking makes it ideal for targeting soft tissues in dynamic environments, such as the cardiac tissue.<sup>[10]</sup> Additionally, Yekrang et al. used cross-linking modulation to obtain a significant increase in tensile strength and Young’s modulus of pure chitosan/PVA patches, which exhibited low mechanical stability (Figure 7a).<sup>[152]</sup> Similarly, PVP microneedle patches were prepared using gamma-ray crosslinking technique, which can induce a cross-linking reaction without chemical additives and allows simultaneous sterilization to compensate for their mechanical properties while maintaining biocompatibility (Figure 7b).<sup>[136]</sup>

Introducing a filler in the matrix is another common strategy for strengthening, as the mechanical properties of the filler elements, such as graphene sheets, carbon nanotubes, NPs, or fibers, affect the composite mechanical properties. For example, the integration of cellulose nanofibrils in a PGS patch has been proven to produce a three-fold increase in Young’s modulus,<sup>[27]</sup> while the addition of graphene, graphene oxide, or rGO nanosheets to a polymer matrix, such as PVA or chitosan,

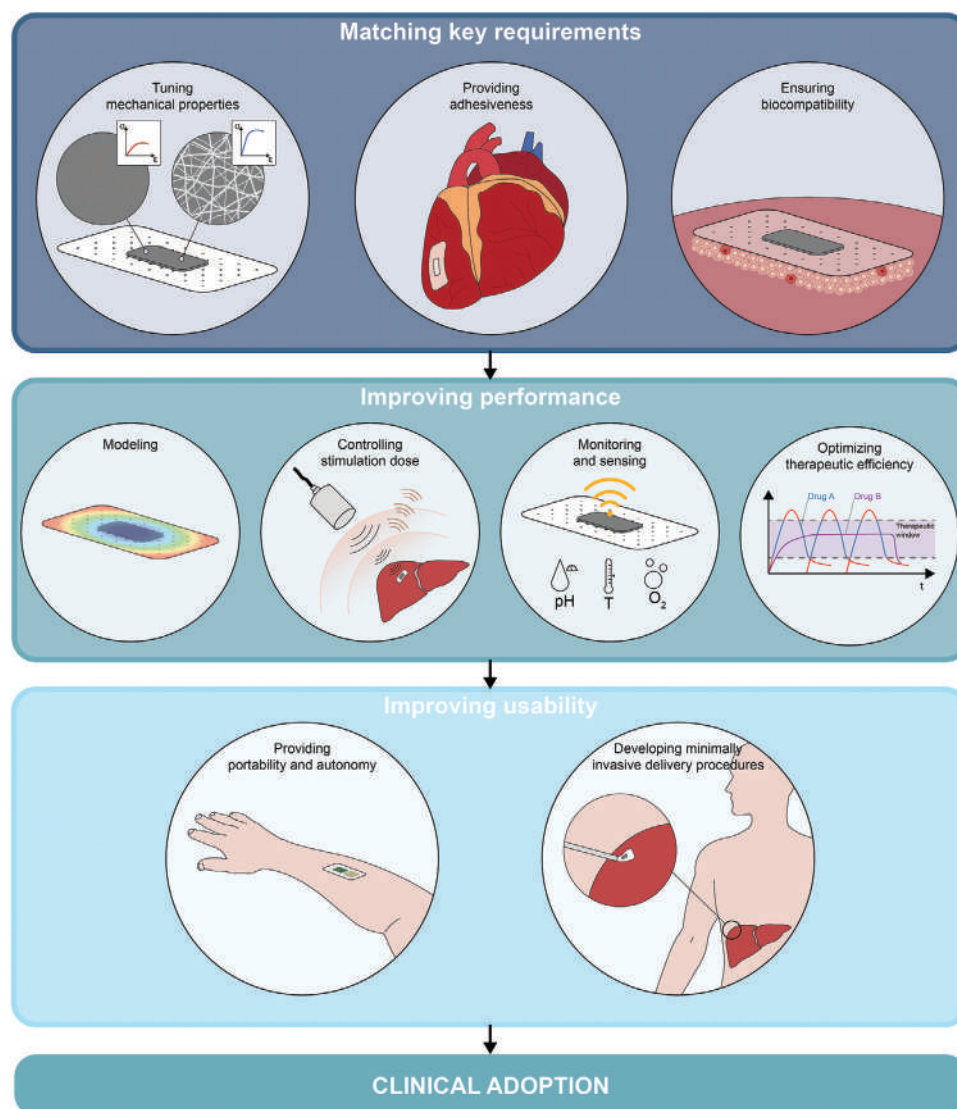


**Figure 6.** Key aspects to be addressed in the pathway towards clinical adoption of active patches. Crucial aspects that must necessarily be addressed in the design of a patch are: mechanical properties tailoring, to match the target tissue ones;<sup>[136]</sup> integration of an adhesion strategy, to efficiently adhere to the target tissue;<sup>[137]</sup> and use of biocompatible materials.<sup>[138]</sup> Moreover, there are further aspects that, albeit not fundamental to applicability, could be of significant help in improving patch performances: modeling of its response, for an easier performance optimization;<sup>[139]</sup> accurate control of the dose of the triggering stimulus that is delivered to the patch to obtain the desired therapeutic response;<sup>[140]</sup> monitoring of the action of the patch;<sup>[141]</sup> careful definition of the clinical needs of the target disease, in order to maximize therapeutic efficiency.<sup>[142]</sup> Finally, some secondary issues are anyway significant for improving patients compliance towards the use of these devices: in particular, the development of technologies to make triggerable patches portable and usable in daily life;<sup>[143]</sup> and the development of minimally invasive procedures to avoid open surgeries for the delivery of implantable patches.<sup>[144]</sup>

has been shown in various studies to improve both tensile strength and elasticity of the nanocomposite in a concentration-dependent manner (Figure 7c,d).<sup>[86,145]</sup> However, in some cases, increasing the concentration of the filler could interfere with other mechanisms within the matrix, such as the ability to form cross-links, which is, in turn, a strengthening mechanism; for example, in some cases, an increase in graphene oxide content has been associated with a decrease of compressive strength.<sup>[136]</sup>

Each of the aforementioned approaches used alone or in combination with other approaches, can be employed for a fine tuning of patch mechanical properties. However, careful consideration must be given when using a combination of strengthen-

ing factors. The beneficial effects of individual tuning strategies are not necessarily synergistic when combined; indeed, they may downplay each other due to an unexpected interplay of different phenomena. Furthermore, it is worth stressing how the mechanical tuning should not interfere with the functionality of a patch. This is especially challenging for smart ones, whose stimulus-responsive character is often based on the use of specific materials or fillers, whose presence and concentration usually also affect the mechanical properties of the structure.

To date, the main challenge from a mechanical point of view is probably the need to closely replicate the mechanical properties of target tissues, which still represents an open challenge for

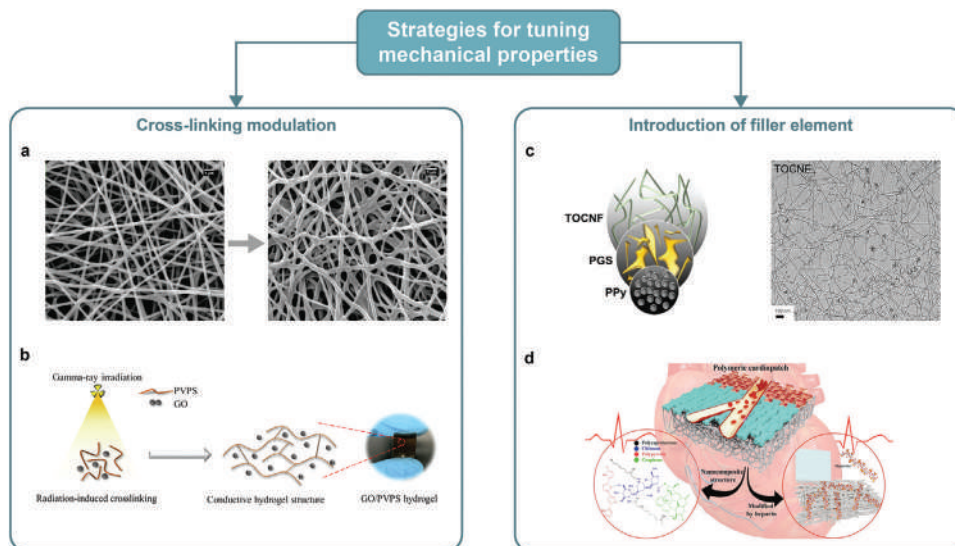


**Figure 7.** Some of the possible strategies to achieve modulation of the mechanical properties of patches. To increase the toughness of a matrix, it is possible to modulate the cross-linking density of the polymer chains, a) through chemical or b) physical mechanisms, such as irradiation. Reproduced with permission.<sup>[136,152]</sup> Copyright a) 2023 and b) 2022, Elsevier. Another possibility for strengthening comprises introducing filler elements in the matrix, such as c) cellulose nanofibrils or d) carbon-based nanomaterials like reduced graphene oxide. Reproduced with permission.<sup>[27,145]</sup> Copyright 2020, c) Wiley-VCH and d) American Chemical Society.

many human body tissues. In this regard, a promising approach that has gained attention in the last decade is the optimization of the micro- and nano-architecture of biomaterials used for scaffolds and patches using additive manufacturing technologies, which allow for an easy modification of multiple structural parameters.<sup>[153]</sup> In particular, 3D printing techniques are emerging as extremely promising in this field. For example, materials with a heterogeneous microstructure obtained through dual-material 3D printing were found to accurately mimic the strain-stiffening behavior of soft tissues, with a mechanical behavior, depending on the design parameters.<sup>[154]</sup> Similarly, precise tuning of tissue-mimicking properties has been recently achieved by exploiting multi-material jetting techniques; for example, changing the relative concentration of the materials employed,<sup>[155]</sup> or investigating different crystal lattice-like microstructure designs.<sup>[156]</sup> Exploring these manufacturing techniques further, along with examining how design parameters and the use of different materials combinations affect the properties of the final products, is an important and timely subject that warrants attention.

Furthermore, it must be considered that the properties of a target tissue may change during the treatment; for example, during the transition from a pathological condition to a healthy one (i.e., during healing). Therefore, the ideal patch should have dynamic properties that change in harmony with the state of the target organ, adapting to the process and facilitating the coupling with the tissue in every phase. This aspect is clearly even more challenging, but there are some interesting perspectives in this regard. For example, techniques such as four-dimensional printing enable the development of structures that can display micro- and nano-scale dynamic patterns, whose features change in time and space in response to an external stimulus and according to selected programs.<sup>[157]</sup> Phototunable materials are currently the most explored category to achieve this goal, since many light-sensitive moieties are already used to functionalize tradi-

tional polymeric materials, endowing them with the ability to be crosslinked in situ in a spatio-temporally controllable manner.<sup>[45]</sup> For example, functionalization of HA with methacrylates has been demonstrated to enable sequential crosslinking, giving the possibility to obtain a partially gelled hydrogel that can be further stiffened in situ at a user-defined time by exposing it to UV light.<sup>[158]</sup> The exploration of innovative photo-responsive materials is an exciting avenue that deserves further investigation. Other stimuli, such as EFs, mechanical stimuli, or endogenous signals are also worth exploring in combination with innovative biomaterial formulations able to respond by changing some of their structural properties, thereby achieving a dynamic control of their stiffness.

### 3.2. Adhesiveness to the Target Tissue

The ability of a patch to adhere to the target tissue for the whole duration of its diagnostic/therapeutic action is a crucial feature for its medical use. For wearable patches, the self-adherence to the skin during everyday activities without the need for additional adhesives and tapes is desirable; in the case of implantable patches, the need for intrinsic adhesive properties is more essential but also more challenging. In fact, the patch integration with internal organ walls is commonly achieved through sutures, but this practice may cause damage to the diseased organs, such as bleeding, further injury, and risk of infection.<sup>[137]</sup> Additionally, many tissue surfaces, such as the intestinal epithelium and mucosa, are wet, slippery, and dynamic, and blood at the interfaces, in general, limits the ability of many materials to adhere.<sup>[146]</sup>

In recent years, some alternatives to surgical stitching have been identified, and various biological glues, such as medical-grade cyanoacrylates or fibrin sealants, are currently available in clinical practice. However, some of them seem to be easily

washed out in dynamic conditions, and therefore cannot be used in some applications, such as inside the cardiac chambers or in major blood vessels. Conversely, stronger glues have been associated with some degree of toxicity and tissue stiffening, which can lead to undesired inflammatory and fibrotic events.<sup>[137,159]</sup> Therefore, the search for new safe and suture-free approaches for the attachment of patches to internal organs is an active and challenging process.

Some polymers, such as chitosan and poly(acrylic acid), have been found to be mucoadhesive, as they are capable of forming electrostatic interactions with the mucosa, which makes them particularly suitable for applications, such as oral, nasal, and vaginal drug delivery.<sup>[146]</sup>

Other strategies are mainly bioinspired, as many sophisticated architectures can be found in numerous living beings with the ability to stick to very different surfaces in diverse environments. Some of these strategies consist of the chemical functionalization of the patch surface through the integration of specific molecules present in the secretions of some animals.<sup>[2]</sup> For example, marine mussels have been widely studied for their ability to bond to any type of organic and inorganic substrate, which relies on their byssal threads' secretion of particular proteins rich in catechol moieties; therefore, molecules containing catechol groups, such as dopamine and the 3,4-dihydroxyphenyl-alanine (DOPA) residue, have been used to functionalize polymers.<sup>[160]</sup> Thus, DOPA-modified PEG hydrogels have been shown to adhere to external liver surfaces for up to one year.<sup>[161]</sup> Dopamine moieties were employed to modify HA in a multi-layered structure, resulting in increased cellular adhesion and proliferation,<sup>[160]</sup> or integrated into polyacrylamide hydrogels, endowing them with the ability to adhere firmly to the curved joints of the hand during the motion of the fingers (Figure 8a).<sup>[162]</sup> Tough adhesives were also inspired by the viscous mucus secreted by slugs, which consists of two main components acting synergistically; similarly, these adhesives have a surface consisting of a positively charged polymer with the ability to form covalent bonds across tissue surfaces and a matrix capable of effectively dissipating energy when the interface is stressed. They showed remarkably high peeling energies ( $\approx 1000 \text{ J m}^{-2}$ ) on different tissues, such as porcine skin, cartilage, heart, arteries, and liver, and displayed high adhesion energies on wet surfaces, independent of blood exposure and compatibly with in vivo dynamic movements.<sup>[163,164]</sup>

Other adhesion strategies rely on physical modifications of the material surface in order to mimic some complex morphological architectures that can be found in nature. For example, gecko lizards and beetles are characterized by nano- and micro-scaled hairy structures (setae) with protruding thin-film tips (spatulas) on their feet, which enable a strong and reversible adhesion to various surfaces due to van der Waals interactions and without leaving any chemical residues.<sup>[17]</sup> Kwak et al. took inspiration from this unique structure to create a skin adhesive patch equipped with micropillars with bulged tips of soft PDMS, with the ability to maximize normal and shear adhesion on rough skin surfaces (Figure 8b, top left);<sup>[165]</sup> in a following work, the same bioinspired adhesive patch was employed to monitor electrocardiography over 48 h at two locations of a volunteer's skin (i.e., chest and wrist), showing no observable side effects, such as redness or allergic responses (Figure 8b, bottom left and right).<sup>[166]</sup> However, these gecko-inspired solutions, although ex-

remely effective on dry surfaces, perform poorly in wet conditions. Adhesives inspired by octopi suckers are more suitable to adhere to blood-wet surfaces, being capable of adhering to slippery, rough, and irregular surfaces, such as the marine intertidal zones.<sup>[167]</sup> Mimicking this functionality, film surfaces have been functionalized with artificial sucker arrays, which can generate negative pressure at the contact point with the target surface: Chen et al. presented a deformable PDMS-coated nanosucker array patterned on a silicon substrate, displaying optimal adhesive capabilities on both micro-rough and flat surfaces in dry and wet environments (e.g., porcine heart; Figure 8c, bottom left and right).<sup>[167]</sup> Similarly, Choi et al. proposed a wearable patch endowed with cephalopod-inspired miniaturized suction cups, which promote adhesion to mice skin while being breathable and comfortable due to a soft interfacial layer on the cups that reduces the strain on the skin (Figure 8c, top left).<sup>[168]</sup> Zhu et al. investigated blue-ringed octopus-inspired suction cups to achieve effective wet adhesion of a silk fibroin patch.<sup>[169]</sup> Such hydrogel cups were designed to remain stable for days on wet tissues, such as oral mucosa, resisting tear tests performed with forces  $>10 \text{ kPa}$ . Their remarkable performance is due to a dual physical and chemical joint bonding ability: their flexible structure can achieve physical adhesion because of air pressure difference, while the modification with tannic acid of their inner walls guarantees a chemical bonding with the tissue surface.

Equipping patches with microneedles is another intriguing strategy for guaranteeing adhesion through mechanical interlocking with the tissue in a minimally invasive way. This strategy has been shown to work suitably on both dry and wet surfaces in both static and dynamic conditions. A cardiac patch, endowed with a conical microneedles array, has been proved to adhere effectively to a beating heart, even not penetrating the tissue due to an increased contact area and roughness (Figure 8d, top left).<sup>[170]</sup> Swelling microneedles have been used in the study by Yang et al., which was inspired by the behavior of needle-like proboscides of an endoparasite.<sup>[171]</sup> The biphasic microneedles consist of a supporting core and water-responsive outer layer capable of penetrating tissue with minimal insertion force and depth and swelling upon skin penetration by absorbing body liquids, which guarantees a stable attachment to intestinal mucous surfaces with minimal damage and easy removal (Figure 8d, bottom left and right). The use of swellable microneedles provides higher adhesion strength and lower invasiveness with respect to conventional practices, such as suture and staple fixation, reducing the risk of site infection; however, it represents a slightly more aggressive adhesion strategy when compared to the ones mentioned above.

Some patches can even become adhesive upon the application of some kind of physical stimulus, which means that they can be triggered to adhere to their target right at the moment of their delivery. For example, poly(glycerol sebacate acrylate), a degradable and biocompatible elastomer that cures in five seconds under UV light, has been used as a light-responsive glue, capable of retaining high adhesive strength also during prolonged contact with blood on a tissue surface, even in dynamic environments (Figure 8e, right).<sup>[159]</sup> Similarly, a light-controlled adhesive patch modified by photosensitive N-(2-aminoethyl)-4-(4-(hydroxymethyl)-2-methoxy-5-nitrosophenoxy) butanamide (NB) groups on the surface proved to be suitable for suture-free wound closure and full-thickness repair of the stomach walls in



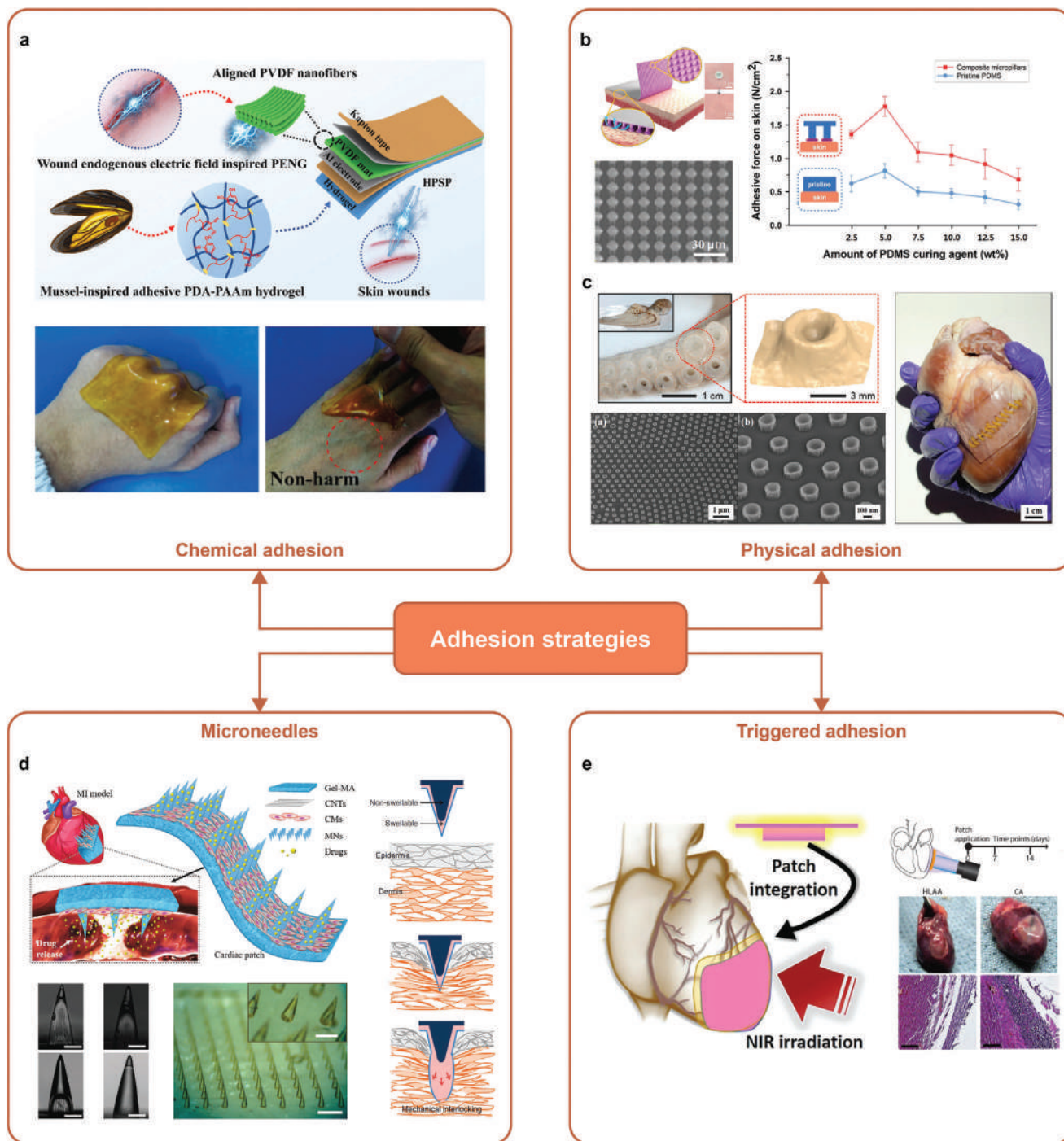


**Figure 8.** Some examples of the adhesive strategies that have been employed to favor the adhesion of medical patches to tissue. a) An in situ bioinspired strategy, based on the chemical modification of the patch surface, incorporating an adhesive layer based on the molecules typical of mussels secretions. Reproduced with permission.<sup>[162]</sup> Copyright 2020, Springer Nature. b) Physical modification of the patch surface to mimic the structures present on gecko feet, or c) the suction cups on octopus tentacles. Reproduced with permission.<sup>[165–168]</sup> Copyright 2011, Wiley-VCH (b, top left); Copyright 2013, Wiley-VCH (b, right and bottom left); Copyright 2017, American Chemical Society (c, right and bottom left); Copyright 2015, Wiley-VCH (c, top left). d) Integration of a microneedle array on the patch surface, to favor interlocking with the tissue. Reproduced with permission.<sup>[170,171]</sup> Copyright 2021, Elsevier (top left); Copyright 2013, Springer Nature (right and bottom left). e) Integration of light-sensitive components on the patch surface to achieve photo-triggered adhesion upon delivery. Reproduced with permission.<sup>[137,159]</sup> Copyright 2022, American Chemical Society (left); Copyright 2014, AAAS (right).

rabbits due to the conversion of o-nitrobenzene groups of NB to o-nitrosobenzaldehyde under UV light irradiation; this can react with the amino groups on the tissue surface.<sup>[7]</sup> Gold nanorods were employed in a cardiac patch to favor sealing to the myocardium under irradiation with a NIR laser, as they can convert absorbed light into thermal energy, which locally changes the structure of the scaffold, engraving it with the heart walls (Figure 8e, left).<sup>[137]</sup>

As highlighted in the previous paragraph, several innovative solutions exist for endowing patches with effective adhesive properties, bypassing more invasive clinical practices, such as suturing. Of course, it is essential to select the most suitable adhesion strategy on the basis of the application, taking into account the nature of the target tissue and type of biological environment the patch is destined to. Furthermore, it is worth highlighting that the choice of the functionalization strategy must also be compatible with the choice of materials and fabrication techniques employed for the functional core of the patch.

A recently emerging trend proposes the use of machine learning algorithms to optimize the topography of bioadhesive surfaces, thereby enhancing adhesive performance. For example, a machine-learning-based approach has been proposed in combination with finite-element-method-based mechanical simulations to automatically optimize the design of 3D fibrillar structures in terms of shear; this resulted in an adhesive surface that outperformed predefined standard fibril designs.<sup>[172]</sup> Additionally, the application of machine learning techniques to the other above-mentioned adhesion strategies based on the physical modification of surfaces is an exciting study topic that may allow considerable adhesion improvement.

Another cutting-edge strategy is synthetic biology. This approach allows to build highly customizable materials, starting from the assembly of elementary building blocks, combining monomers with proteins, nucleic acids, and other natural and artificially designed modules, which can endow the final material with potentially any desired feature.<sup>[173]</sup> Synthetic biology has been exploited to obtain ultra-strong underwater adhesives by rationally assembling different adhesive domain-containing proteins, giving rise to hybrid materials that hierarchically self-assemble into higher-order structures with suitably exposed adhesive domains.<sup>[174,175]</sup> This strategy appears extremely promising for developing materials with tuned properties, particularly in terms of adhesiveness, that are difficult to achieve with conventional materials engineering techniques.

### 3.3. Biocompatibility and Biodegradability

Biocompatibility is clearly an essential requirement for medical patches, which need to be in direct contact with tissues. Consequently, in the development phase of a new patch, extreme attention must be paid to all aspects related to cytotoxicity and other possible adverse reactions of the target cell types. The use of materials, such as collagen, chitosan, fibrin, alginate, gelatin, and other natural polymers is a safe choice for ensuring compliance with biocompatibility requirements. Many polymers of biological origin have been proven to be biocompatible and rich in cell-adhesive chemical moieties, which promote integration with tissues.<sup>[176]</sup> However, some animal-derived biomaterials, such as

collagen, may evoke adverse immune responses, albeit rare. This is due to the fact that collagen may include epitopes extraneous to the human species, which, depending on the donor species, may induce weaker or stronger antigenic reactions.<sup>[177]</sup> Furthermore, most of the natural polymers show poor mechanical properties and do not exhibit significant stimulus-sensitive behaviors. This is why most of the currently developed smart patch systems employ other types of materials in addition to the aforementioned natural polymers, such as synthetic and smart polymers and ceramic, metallic, or carbon-based micro and nanofillers, which can provide the system with the desired functional properties. Unfortunately, toxicity issues still need to be effectively addressed for many of these smart materials; this is one of the reasons hindering the clinical translation of smart therapeutic devices, such as patches, which struggle to fit the biosafety regulatory standards.<sup>[77]</sup> This is even more critical in the presence of nanomaterials, which show entirely different properties with respect to their bulk counterparts and raise concerns about toxicity and biosafety that are often not envisioned by standard protocols.<sup>[105]</sup> Oxide NPs, metal NPs, polymeric NPs, and quantum dots, which are often used due to their outstanding functional properties, have been extensively studied, and many efforts have been conducted to understand their potential toxicity mechanisms on diverse cell lines and mitigate them (for example, by providing them with protective coatings). However, their clinical applications are still in their infancy, owing to biosafety concerns.<sup>[46]</sup> Toxicity strongly depends on physicochemical parameters, such as particle size, shape, surface charge, and chemistry, composition, and stability. Therefore, assessing the biocompatibility of a whole class of materials is a challenge, as these properties may also vary within the same class, depending on the synthesis parameters, starting materials or functionalization. This makes NPs hazard identification not straightforward.<sup>[178]</sup>

Gold is known to be safe and chemically inert, and gold NPs were shown not to elicit immune reactions below the concentration limit of 1% w/v, although some structures based on electroconductive polymers, such as PPy and polyaniline, seem to sometimes induce some level of cytotoxicity in a dose-dependent manner.<sup>[11]</sup> Silica NPs demonstrated a good degree of biocompatibility both *in vitro* and *in vivo*, showing the ability to enter cells without affecting their survival. SPIONs are usually classified as biocompatible, showing no severe toxic effects *in vitro* and *in vivo*, nor immunomodulatory effects on human macrophages. However, other studies found that when murine macrophages were exposed to dextran-coated SPIONs, an increased secretion of pro-inflammatory cytokines occurred.<sup>[178]</sup> Carbon nanotubes have been shown to cause high inflammatory and cell injury effects in the lungs at high concentrations (5 mg kg<sup>-1</sup>), but to date, there are no defined standards on their maximum safe concentration in tissues.<sup>[179]</sup>

The high caution towards these materials is also due to the fact that majority of biocompatibility studies aim to assess very short-term effects, and only rarely consider medium-term effects of nanomaterials. Long-term clinical effects have rarely been investigated, which severely hampers the clinical translation of formulations employing this kind of materials. In this regard, long-term preclinical studies using appropriate large animal models are required to confirm their biocompatibility at a higher level.<sup>[178]</sup>

Furthermore, the onset and severity of toxicity and assessment of safe dosages strongly depend on the mode of administration and the way cells and tissues are exposed to these materials. There is a significant difference between injecting NPs into the bloodstream, allowing them to circulate freely in the body, and implanting a patch structure incorporating a nanofiller. Majority of the biocompatibility studies mentioned above focus on the effects of nanomaterials in direct contact with cells, which represents a riskier scenario compared to cases where the tissue is in direct contact with the patch matrix but not with the filler. In this scenario, potential minor toxicity effects that nanomaterials may have when in direct contact with cells are mitigated by the embedding matrix. Of course, it is essential to ensure that there is no risk of leakages of the filler during the lifetime of the device. A small number of studies have proved the biocompatibility of patch formulations incorporating different types of smart fillers, such as SPIONs,<sup>[95]</sup> rGO,<sup>[86]</sup> silver nanorods,<sup>[180]</sup> PDA NPs,<sup>[59]</sup> and Mxene.<sup>[138]</sup>

That being said, the selection of the stimulus-responsive materials to include in the patch must be not only driven by the application, but should also consider biocompatibility issues, as they are crucial for a potential clinical translation. In contrast, there is an urgent need for updating the current clinical regulatory standards. Furthermore, in the case of active patches triggered by external stimuli, it is also important to ensure that the stimulus dose that is meant to drive the therapeutic response falls within the safety ranges established for clinical use.

Obviously, it would be beneficial to find safer alternatives to some nanomaterials that have raised concerns and controversies regarding cytotoxicity. For example, magnetic particles are among the most discussed smart materials: they are widely employed in magnetic-responsive biomaterials, although they have been sometimes reported to pose safety hazards. In this regard, there have been some attempts to engineer soft, metal-free, intrinsically magnetic polymers, based on stable organic free radicals. These polymers exhibit good paramagnetic properties while showcasing better biocompatibility than traditional magnetic materials.<sup>[181]</sup> Following this trend, it would be interesting to engineer innovative stimuli-responsive materials working at a molecular level through bottom-up techniques.

Beyond biocompatibility, biodegradability is not a compulsory requirement for medical patches, but it could be a desirable feature in particular applications, such as for implantable patches. In fact, in the case of non-permanent implants, the use of patches fabricated with materials that naturally hydrolyze into biocompatible metabolites after a certain lifetime in a biological environment makes the retrieval surgery unnecessary, which would be clinically beneficial for short or medium-term applications.<sup>[23,79]</sup> An ideal implantable patch should therefore maintain its shape and structure to perform its intended function on the target tissue for a given period, and only afterward should start to gradually degrade in the body, to be either naturally excreted or absorbed.<sup>[18,182]</sup>

Generally, degradable devices are made of polymers, such as PCL, PGS, polyglycolic acid, PLA, PLLA, or PLGA, which contain unstable bonds that are easily degraded by water or enzymes.<sup>[18]</sup> Among them, polyesters of lactic and glycolic acids are the most widely studied, mainly because they are already approved by

the FDA as delivery systems for a variety of drugs but also because they offer good customizability in terms of degradation profile through the control of the ratio of their individual constituents.<sup>[176]</sup>

For example, for PGS, a common polymer used for patches, especially for cardiac applications, mechanical and degradation properties can be controlled by tuning the ratio of glycerol and sebacic acid, leading to an easily customizable polymer.<sup>[183]</sup> It is also possible to combine different polymers in a complex patch structure for achieving the desired degradation profile. For example, Pok et al. developed a multi-layered cardiac patch with a core of PCL coated with a chitosan and extra-cellular matrix gel, which was implanted and monitored for eight weeks in a full-thickness post-myocardial infarction rat model, showing a fast degradation of the gel portion at week four, and a much slower successive degradation of the PCL core, whose thickness decreased by 40% after eight weeks.<sup>[184]</sup> Another tunable parameter that can be considered to modulate the degradation profile of a polymer is crystallinity. For example, in order to extend the life of PLLA, its crystallinity can be tuned by reducing the amorphous content, being more susceptible to hydrolysis, while degradation of the crystalline structures is much less significant.<sup>[176]</sup> In contrast, Temiral et al. explored the degradation profile of an alginate patch modified with two different biocompatible nanofillers, cellulose nanocrystals, and cellulose nanofibrils.<sup>[182]</sup> The alginate-nanofibrils composite showed a 30% erosion, in terms of weight loss in the first 2 days, afterward slowing down and reaching only a 50% degradation after 30 days. The alginate-nanocrystals composite showed a much slower initial degradation of 18% in the first two days, and then remained always within the 30% weight loss threshold for a period of 15 days, proving to have a more favorable behavior in terms of stability in the first period of the patch lifetime; afterward, the degradation rate significantly picked up, reaching 90% erosion after 30 days.

As highlighted by this last study, when using naturally degradable polymers, although tunable degradation profiles can be obtained, it is in general challenging to guarantee unaltered mechanical and functional properties for the whole time needed to perform their therapeutic action before starting the degradation process. To solve this issue, it could be useful to employ materials that start to degrade upon a cue, like an external physical stimulus, which offers the advantage of precise spatiotemporal control over degradation. For example, photodegradable hydrogels can be obtained through the integration of photocleavable motifs, such as the nitrobenzyloxycarbonyl group, which can degrade into an aldehyde and carboxylic acid parts upon UV light activation. Johnson et al. investigated the photodegradation of PEG hydrogels that contained nitrobenzyloxycarbonyl linkages, and confirmed the fragmentation of the polymer structures after photoinduced cleavage of the networks.<sup>[185]</sup> Of course, for active patches, triggered degradation strategies should not interfere with the functionality of the patch: the stimulus triggering degradation should be different and have no interference with the one triggering the therapeutic action. Moreover, for patches to be implanted in deep tissues, it is crucial that this stimulus has good tissue penetration ability, in order to induce degradation in the patch through non-invasive procedures.



Finally, it is worth highlighting that in the case of active patches, the biodegradability issue is even more challenging due to smart materials selected for functional purposes, which may not be inherently degradable. To endow a smart patch with biodegradability properties, the selection of proper materials is therefore even more crucial, requiring a trade-off between responsiveness and degradability of all of their components. For example, when employing specific micro or nanofillers, it is necessary to establish that they do not cause cytotoxicity not only when embedded in the patch structure but also when in direct contact with the biological environment, as they are to be released during the patch degradation. This represents a more demanding biocompatibility requirement.<sup>[186]</sup> In fact, NPs can permeate cell membranes, accumulate in certain tissues, and spread along nerve cell synapses, blood vessels, and lymphatic vascular system, thereby giving rise to potential health threats when circulating through the body in direct contact with cells and tissues.<sup>[178]</sup> Therefore, it is important to carefully consider the clearance of these fillers, assessing the time required for the human body to expel them, their biodistribution, potential accumulation in specific tissues during this time, and the effects on the organs involved in their expulsion.

An interesting study field is the development of biodegradable smart nanomaterials. To date, there have been some successful efforts in this direction, but achieving biodegradable materials with the same level of responsiveness as their non-biodegradable counterparts is still challenging. For example, there is some evidence of biodegradable piezoelectric materials, such as ZnO NPs, PLLA, silk, collagen, and amino acids, but their piezoelectric output is still inferior compared to conventional ones, limiting their use.<sup>[186]</sup> A possible route to overcome this bottleneck and increase the stimulus-responsiveness, while guaranteeing degradability, could rely on optimizing the micro and nanostructure of these materials, especially at the atomic level. This is because the responsiveness to biophysical stimuli mainly depends on parameters, such as crystallinity and alignment, which are intimately linked to the atomic structure of materials. In this sense, artificial intelligence (AI) is recently emerging as an extremely powerful tool that may revolutionize the future of material science. Therefore, AI-based algorithms are being employed to help in material design, performance prediction, and synthesis, overcoming the traditional but inefficient trial-and-error methods for studying new materials. Powerful machine learning algorithms can predict specific properties of materials, such as conductivity, piezoelectric coefficients, or magnetic permeability, starting from their atomic structure based on the use of large materials datasets. Several libraries of materials have been developed in the last decade, mainly concerning materials for energy, gas storage, and electronics applications. However, this kind of tool holds great potential for health applications as well.<sup>[187,188]</sup> So far, these algorithms perform well only for perfect crystal structures, which are only a small part of the materials that may be interesting to investigate for biomedical applications. Future development of AI-based tools in combination with the constant increase of computational power can pave the way for more complex algorithms with the ability to take into account more variables and explore a higher number of material types.

### 3.4. Modeling

Mathematical modeling may play an important role in all medical patches-based applications involving drug delivery and biophysical energy transmission. Accurate models could represent a valuable tool during the design phase of a new patch, with the goal of predicting how design parameters affect the patch behavior.<sup>[189]</sup> In particular, in drug delivery systems, modeling can be the driver for elucidating the underlying release mechanisms, both for passive and active mechanisms. A modeling step would facilitate the development of new drug-loaded devices by a systematic, rather than trial-and-error, approach, and could also help in the optimization of the stimulation parameters in the case of active patches.<sup>[190]</sup> Modeling can also be useful for explaining and predicting how the application of an external triggering stimulus can modify materials properties, such as mechanical or morphological, or induce them to convert the applied stimulus into another one.

Passive drug release has been extensively investigated in the past from a modeling viewpoint: a large number of mathematical models have been proposed to describe the release of drugs from inert matrix systems. Among them, it is possible to distinguish between empirical/semi-empirical models and mechanistic ones. The former aims to describe the release profiles without necessarily taking into account the underlying mechanisms, and they are employed to empirically summarize and evaluate experimental data; in contrast, the latter strives to explain the release on the basis of physical and chemical processes that control the release rate, which makes them suitable for predicting release profiles from new formulations.<sup>[189]</sup>

One of the most commonly used semi-empirical models is the Korsmeyer–Peppas power law, reported by Equation 11, where the ratio between the amount of drug released at time  $t$  and the amount of drug released in the equilibrium state ( $M_t/M_\infty$ ) is governed by the release rate constant  $K$  and by the release exponent  $n$ , whose value is related to the diffusion mechanism.<sup>[191,192]</sup>

$$\frac{M_t}{M_\infty} = Kt^n \quad (11)$$

In contrast, the mechanistic model of drug release is described by the well-known Higuchi's law, expressed by the Equation 12:

$$\frac{M_t}{A} = \sqrt{D(2c_0 - c_s)c_s t} \quad (12)$$

where  $M_t$  is the cumulative amount of drug released at time  $t$ ,  $A$  is the surface area of the matrix exposed to the release medium,  $D$  is the drug diffusivity in the matrix, and  $c_0$  and  $c_s$  are the initial drug concentration and drug solubility in the matrix, respectively.<sup>[193,194]</sup>

Some of the existing models are analytical, meaning that by using equations, they relate a response variable (e.g., the amount of released drug) to an independent variable (e.g., time) and to one or more parameters, such as the diffusion coefficient, drug solubility, and initial drug loading. However, many problems of practical interest are too complicated to be solved by analytical methods due to non-linearities or complex geometries; in these



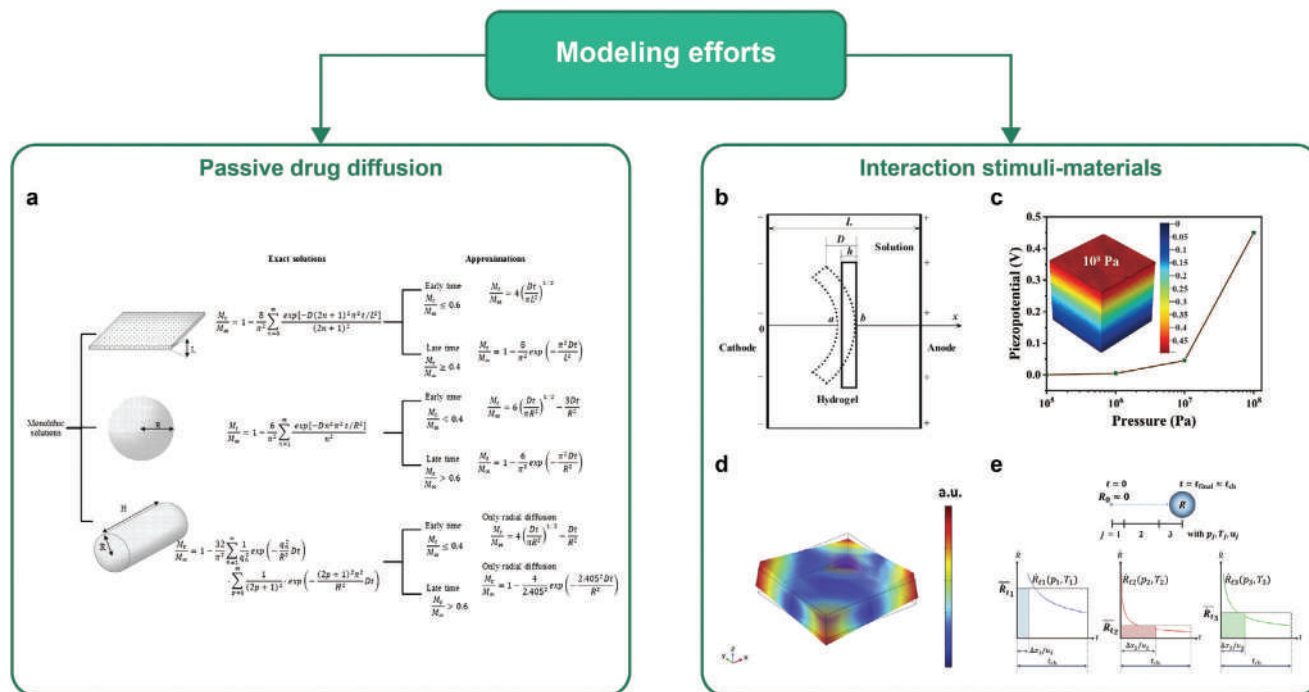


**Figure 9.** Examples of analytical and numerical modeling efforts. a) The passive diffusion of a drug from a matrix has been extensively modeled through variations of the Fick's law, depending on the type and shape of the reservoir. Image reproduced with permission.<sup>[195]</sup> Copyright 2011, Elsevier. Modeling efforts have also been spent to predict the behavior of several smart materials in response to a stimulation: b) the swelling of an electro-responsive hydrogel; image reproduced with permission,<sup>[201]</sup> Copyright 2007, Wiley; c) the voltage generated by a piezoelectric particle upon US stimulation; image reproduced with permission,<sup>[205]</sup> Copyright 2020, Wiley-VCH; d) the deformation of a degradable polymeric capsule in response to a mechanical stimulus; image reproduced with permission,<sup>[139]</sup> Copyright 2020, Elsevier; e) the cavitation dynamics of microbubbles upon the application of a pressure field; image reproduced with permission,<sup>[209]</sup> Copyright 2021, Elsevier.

cases, numerical analyses are needed, such as finite difference methods or finite elements methods (FEM).<sup>[189]</sup>

The existing models describing drug diffusion are in large part derived from the Fick's law, which has already been solved for various geometries and initial and boundary conditions, giving rise to a large number of more or less complex diffusion models (Figure 9a). Many reviews explore them in detail, classifying them on the basis of the type of loaded system (such as reservoir or matrix system), the characteristics of the polymer matrix (homogeneous or porous), and rate-controlling release mechanism (such as diffusion, erosion, and swelling).<sup>[189,190,195]</sup>

Multiple efforts have also been spent to model the behavior of a wide variety of stimulus-responsive materials, with the aim of predicting their response to the application of chemical or physical energy.

The smart features of photo-responsive materials have been mainly investigated through small-scale, particle-based simulation methods.<sup>[196]</sup> For example, Choi et al. performed molecular dynamics (MD) simulations to investigate the isomerization behavior of azobenzene photoswitches and how it affects the stiffness of a polymer composite,<sup>[197]</sup> while Zheng et al. studied the photo-controlled assembly and disassembly of responsive micelles through coarse-grained MD.<sup>[198]</sup> Ghani et al., developed a thermodynamic model based on Hansen solubility parameters, to estimate the work of adhesion between drug and polymer network. This model was used to optimize polymer composition and estimate how its affinity to a loaded drug changed

upon light-triggered alteration of the polymer structure, thereby helping in predicting the measure drug desorption caused by irradiation.<sup>[199]</sup>

A chemo-electromechanical model has been developed by Bassetti et al. (Equation 13) to predict the swelling and deswelling kinetics of hydrogels in response to an EF, based on the Nernst-Planck and Poisson equations, which describe the flux of the  $k$ -th ionic species in a direction ( $x$ ):<sup>[200]</sup>

$$\Gamma_{kx} = \Phi \left[ -\bar{D}_k \frac{\partial c_k}{\partial x} - \bar{\mu}_k z_k c_k \frac{\partial \Psi}{\partial x} \right] + c_k U_x \quad (13)$$

where  $\Phi$  is the gel porosity,  $D_k$  is the effective diffusivity of the  $k$ -th ion inside the hydrogel,  $c_k$ ,  $\mu_k$ , and  $z_k$  are the concentration, ionic mobility, and valence of the  $k$ -th ion, respectively,  $\Psi$  is the electric potential, and  $U_x$  is the fluid velocity in the  $x$ -direction.

A similar model was developed by Luo et al., who found a very good agreement between their simulated results and experimental data extracted from literature,<sup>[201]</sup> although more recently, Boas et al. proposed a numerical model to describe the electrically induced deformation of a fibrous polyelectrolyte membrane in terms of its geometry, porosity, and elastic modulus and of the applied ES (Figure 9b).<sup>[202]</sup>

The interaction of US waves with piezoelectric materials, such as NPs, which generate electrical charges in response to mechanical stimulation, has been modeled as well. For example, an analytical model of the behavior of barium titanate NPs was developed

by Marino et al. (Equation 14), describing the voltage generated at the surface as linearly proportional to the radius of the spherical particle and US wave pressure:<sup>[203]</sup>

$$\varphi_R = -\frac{R(e_{rr} + 2e_{r\theta})}{s\epsilon_{rr}} \left( \frac{p_{US}}{s\gamma + 2\alpha} \right) \quad (14)$$

where  $R$  is the particle radius,  $e_{rr}$  and  $e_{r\theta}$  are the piezoelectric coefficients,  $\epsilon_{rr}$  is the dielectric constant of the NP,  $\alpha$ ,  $\gamma$ , and  $s$  are known expressions, depending on the elastic properties of the NP (the Young modulus and Poisson ratio), and  $p_{US}$  is the maximum pressure associated with the US wave.

With the same aim, FEM simulations have also been recently proposed (Figure 9c).<sup>[204,205]</sup> Sciurti et al. also used the COMSOL Multiphysics FEM simulations to identify the resonant frequencies of PLGA microparticles, in order to maximize their mechanical deformation and degradation, thereby optimizing drug release (Figure 9d).<sup>[139]</sup> Other US-driven phenomena, such as ADV of low-boiling point compounds, such as PFCs, or inertial cavitation of MBs, have been extensively modeled on the base of a variety of physical theories. For example, Lacour first and Ghasemi later have modeled ADV dynamics by means of a three-phase model,<sup>[206,207]</sup> while Aliabouzar et al. reported a model for the same phenomenon based on classical nucleation theory,<sup>[208]</sup> predicting the acoustic pressure needed to trigger the vaporization ( $p_i$ ) by solving Equation (15) for the nucleation rate:

$$J_n = \zeta \exp\left(-\frac{16\pi\sigma^3 f(\Phi)}{3k_B T (p_b - p_i)^2}\right) \quad (15)$$

where  $\zeta$  is a kinetic pre-factor,  $\sigma$  is the liquid–vapor interfacial tension,  $f(\Phi)$  is a geometric factor taking into account the probability of a heterogeneous nucleation,  $k_B$  is the Boltzmann's constant,  $T$  is the temperature, and  $p_b$  is the total pressure inside a critical bubble nucleus.

Inertial cavitation has as well been extensively studied, with a large number of models developed to predict the cavitation pressure threshold as a function of diverse variable parameters, both empirical and analytical, the majority of which were based on the Rayleigh–Plesset's equation (Figure 9e).<sup>[209,210]</sup>

The effect of MF on magnetically responsive materials, such as ferrogels, has been investigated mainly through particle-based models, such as MD and Monte Carlo methods, which allow to predict the structural deformation and amount of volume change and shrinkage under an applied MF.<sup>[211–213]</sup> Analytical and numerical methods have also been employed to model the interaction between AMFs and MNPs; for example, in predicting the power or temperature increase generated by these magnetically responsive particles.<sup>[93,214]</sup>

From the overview provided above, it clearly shows that drug release from carriers and stimulus-responsive behaviors of smart materials have been modeled in multiple ways. However, in spite of the large number of published models, there is a clear lack of models in the literature, aiming to predict the stimulus-triggered drug release behavior of active matrices. To the best of our knowledge, from a modeling and simulation viewpoint, no study has integrated the action of an external stimulus in combination with drug release phenomena. In contrast, nobody has described the

diffusive behavior of a drug within the matrix in a model investigating the stimulus-responsive character of a material. In some experimental studies concerning drug release triggered by external stimuli, efforts have been devoted to fit the measured release data with semi-empirical models, such as Peppas, both in the absence and presence of the triggering stimulus.<sup>[86,123,215,216]</sup> However, this is an analysis of the experimental data performed to try and better understand the mechanisms behind the drug release, but it cannot be considered a step forward towards the prediction of the behavior of new systems.

In addition to these considerations, the in vivo use of smart patches presents further challenges that could be addressed by mathematical modeling. First, prediction of the release behavior from the patch system should be accompanied by modeling of the drug diffusion through the tissues, to optimize the therapeutic efficiency of the active principle. In recent years, modeling of in vitro drug release profiles has been combined with computational fluid dynamics simulations to predict drug transport in living tissues, such as the brain, liver, and bone.<sup>[190]</sup>

### 3.5. Control of Energy Dose

As the therapeutic action performed by active patches is a response to a triggering stimulus, the first crucial step for increasing efficiency and repeatability of the procedure is to have accurate control of the energy actually released at the target site. This means finding a precise quantitative relationship between the exact dose of stimulus the patch is exposed to and the entity of the observed response. A lack of this kind of control also compromises the reliability and possibility of comparing different experiments performed through different setup configurations, both in vitro and in vivo, and this obviously slows down the translation to clinical reality.<sup>[105]</sup>

Therefore, in in vitro studies, it is needed to measure, or at least correctly estimate the stimulus dose the patch materials are exposed to. This might seem trivial, but it can actually be quite challenging. First, it is necessary to make sure that no spurious signals from the environment interfere with the triggering signal, altering the dose actually reaching the target; this generally applies to many biophysical energies, such as light and electromagnetic fields, and it can be avoided by performing the in vitro tests in suitable and controllable environments. Furthermore, it is crucial to calibrate the stimulating device in order to know its exact output in terms of field intensity and distribution, and the exact intensity of the signal in the target area, where the patch under test is placed. For example, in the case of US transducers, it is possible to measure the generated pressure field for a given input electric signal using a calibrated hydrophone;<sup>[217]</sup> for a coil system, the MF distribution can be calculated from the known distribution of currents, or the generated field can be experimentally mapped by scanning the 3D space through an appropriate magnetometer.<sup>[218]</sup> Finally, for stimuli that are not applied in direct contact with the patch, but propagate through free space, there is one more factor to be kept under control. In fact, the setup employed for the stimulation tests must be carefully designed to avoid altering the field measured during calibration. This may apply to MFs, which can be distorted by disturbing elements, but is even more problematic for US fields. This is because US

waves are sensitive to many elements commonly present along the acoustic path in the testing setups, such as water/air interfaces and glass plates and tubes, which results in multiple and uncontrolled reflection, diffraction, and attenuation phenomena that can alter the actual US dose delivered to the target up to 700% with respect to the expected one.<sup>[219]</sup>

In addition to these issues, the *in vivo* translation poses further challenges in terms of control. The optimal stimulus dose found *in vitro* should be translated *in vivo* in the desired target area within the human body, which is not straightforward. The dose reaching the target can be substantially different from the dose applied externally due to the effects of different tissues on the propagation of the stimulus through the body, especially for implantable patches. For example, light stimuli cannot propagate more than a few centimeters due to tissue absorption; therefore, they are not suitable for targeting deep tissues, while US waves can be propagated through most human tissues, generating attenuation and reflection phenomena that must be kept under careful consideration.<sup>[49,79]</sup> The control and metering of the intensity of the external signal required to safely deliver a desired stimulus dose *in vivo*, thereby inducing the desired therapeutic action, is a key challenge that must be addressed in order to successfully move towards clinical translation.<sup>[79]</sup> Currently, although it is rather challenging to directly measure the dose reaching a target in deep human tissues, analytical models and FEM analysis are fundamental tools that could help in predicting the stimulus propagation as a way to tackle this challenge.<sup>[105]</sup> For example, light transport in tissues has been mainly modeled through Monte Carlo simulations, which allow calculation of reflection, transmission, and fluence rates in tissue through a detailed book-keeping of the scattering and absorption experiences of individual photons.<sup>[220,221]</sup> Acoustic propagation of ultrasonic fields through heterogeneous media, such as soft tissues, has been addressed through analytical and numerical techniques.<sup>[222,223]</sup> However, there are still very few studies addressing the issue of stimuli propagation through realistic tissue models, and greater efforts should be attempted in this regard. This kind of modeling can significantly help in correctly tuning the output of the external stimulation devices in order to reach the target inside the body with the desired stimulus dose, which represents a pivotal information for enabling an effective *in vivo* translation.

### 3.6. Portability and Autonomy

The use of triggerable materials within medical patches implies the need for a device able to activate stimulus. Often, such stimulating devices (e.g., electromagnetic coils and US transducers) are bulky, and they need a power supply and require specialized operators to handle them. This implies that the treatments need to be performed in specialized laboratories or hospitals, hindering the diffusion of such devices. It would be highly favorable to miniaturize these stimulating devices, making them portable and available to non-expert users. For example, the enormous advancements in microelectronics have led to the development of portable, patient-friendly, and personalized ES platforms, offering a concrete and promising alternative to bulky clinical equipment.<sup>[70]</sup> The same is now happening for US stimulation, as an important study area in US technologies presently focuses

on producing smaller and smaller transducers, also making them user-friendly. Concrete efforts are ongoing toward the development of thin and flexible transducers in a wearable form.<sup>[126]</sup> Additionally, light sources can be easily integrated into miniaturized portable devices, and several examples of flexible and wearable LED patches already exist.<sup>[56,60]</sup> However, this is more difficult for magnetic stimulation, as the miniaturization of coil systems or permanent magnets is an open challenge: even if efforts in this direction have recently been made, it is still hard to reach the values of MF intensity needed for activating materials inside the body by means of small devices.<sup>[224,225]</sup>

For skin-wearable patches, the integration of the stimulus source in the therapeutic patch itself would be an optimal solution to portability issues, resulting in a single compact device of limited size. This has already been achieved, for example, for electrically-triggered patches, which can easily integrate printed electronic circuits with the ability to trigger the actuation system on the basis of commands received wirelessly by a computer or a smartphone.<sup>[85,143]</sup> In this regard, recent advancements in ultrathin, stretchable, and organic electronics are particularly intriguing, as they move towards creating soft, conformable, and highly flexible electronic circuits for a plethora of health applications.<sup>[226,227]</sup> For other types of stimulation, such as US or MFs, the integration goal is still far from being entirely achieved. For example, flexible patch-like US transducers have been developed, exploiting thin-film structural design strategies and micromachining techniques borrowed from the micro-electro-mechanical-systems (MEMS) field. However, this design approach that makes them flexible also affects their performance by reducing their quality factor and narrowing their bandwidth. One of the main technical challenges for flexible transducers lies in the integration of the damping layer, which normally consists of a thick layer of rigid materials and absorbs the backward US energy; to this aim, an exciting perspective could be the development of new materials endowed with good flexibility and suitable acoustic impedance, even at low thicknesses.<sup>[228]</sup> However, easy-to-use portable devices, small enough to be carried around or kept at home without excessive hindrance, even if not wearable, could be a great improvement to promote the diffusion of such smart devices.

For implantable patches, the issue is even more complicated. First, some stimuli, such as electric and optical stimuli, are characterized by a small penetration ability in human tissues. Therefore, in the case of a deep tissue target, it would not be feasible to provide the stimulation externally through a wearable device, as it could be done for US or magnetic stimulation approaches. In this case, the possible solutions would be to either make the implantable device self-sufficient, with its own stimulus and power source integrated, or to leave exposed ports, even after the implantation surgery, such as long needle electrodes penetrating in the tissue or catheters transporting light to the target.<sup>[48]</sup> The second solution is clearly not ideal in terms of safety and patient compliance, and would significantly hinder clinical translation. The first solution appears to be less prohibitive, but is not ideal as well, since batteries could require replacement, if their operating life is shorter than the meant therapeutic life of the patch. However, recent advancements in electronics miniaturization and wireless technologies are opening the door to the possibility of powering implantable devices from the outside in a

non-invasive manner, especially for electrically-triggered patches.<sup>[48]</sup> However, it is worth highlighting that such patches should anyhow include some on-board electronics to be able to wirelessly communicate with the external world and generate the triggering signal, which would impose stricter requirements from a regulatory point of view. This kind of battery-free systems would represent a significant improvement with respect to the current state of the art.

An emerging and promising study field concerns bioresorbable electronics aimed at creating electronic implants capable of dissolving at controlled rates or triggered times. This can be achieved through engineered chemical or physical processes after a required period of operation, without the need for secondary removal surgeries. The chemistry of constituent materials is currently under investigation, with the aim to balance performance durability during the desired lifetime and suitable degradation rates afterward. To tackle this challenge, two main paths have recently emerged: on the one hand, the development of biodegradable functional materials, such as inorganic (e.g., alkali-earth and transition metals, such as magnesium, molybdenum and zinc, silicon and germanium nanostructures, and MgO thin films) and organic (e.g., PPy, polyaniline, poly[3,4-ethylenedioxythiophene], silk, wax, PLA, PEG, and polyanhydride) compounds, hybrids and composites (e.g., Fe/PCL, Mg/PLA, and PPy/silk fibroin) for semiconductors, and conductors and insulators; on the other hand, the development of encapsulation materials (e.g., layered structures alternating organic films made of PLGA, polyanhydride, or polyurethane, with inorganic layers made of silicon dioxide [SiO<sub>2</sub>], silicon nitride [SiN<sub>x</sub>], or silicon oxynitrides [SiON]) with good water barrier performances to protect the embedded electronics, while also having suitable degradation behavior aligned with desired operational lifetimes of the device.<sup>[229,230]</sup> To date, bioresorbable transistors, inductors, sensors, antennas, and even power supplies have been developed. Notably, biodegradable piezoelectric powering systems and energy harvesters are worth mentioning, as they can generate power for small electronics deeply seated inside the body by harvesting ultrasonic waves.<sup>[231]</sup>

### 3.7. Minimally Invasive Application Procedures

Patches, with respect to hydrogel scaffolds, are more suitable for the treatment of certain anatomical targets, such as the heart or walls of organs like the stomach or intestine. In fact, their 2D shape and highly organized morphological structure can help the integration and regeneration of target tissues by mimicking their native structure and reproducing their functional properties. However, placing a functional patch onto an internal organ usually requires open surgery.<sup>[232]</sup> Although hydrogels are easily injectable due to their gel-like form and shape-changing ability, patches have a fixed shape with an area typically in the range of square centimeters, thereby requiring relatively large incisions for introduction into the body. Furthermore, they often need to be delivered through narrow spaces and adhere to wet surfaces in the presence of blood, which further complicates surgical procedures.<sup>[233]</sup>

The need for invasive surgery for patch implantation mainly limits their applicability in the clinical practice.<sup>[232]</sup> These types

of procedures carry risk with respect to minimally invasive delivery methods, which offer higher success rates with a lower risk of complications and reduced costs due to smaller incision size, shorter duration, and faster patient recovery.<sup>[144]</sup> Therefore, the adoption of minimally invasive surgery in patch delivery is expected to be promising in reducing the risks associated with implantation, thereby improving patients' compliance and acceptance and facilitating clinical translation.<sup>[234]</sup>

In this regard, in the last decade, there have been efforts to design patches with certain properties that enable their application through minimally invasive methods. For example, Fan et al. proposed a cardiac PVA-GO patch that can be placed in the chest through a tiny incision (4 mm) due to its ability to fold for the insertion and then quickly recover its original shape upon irradiation with NIR light for 10 s.<sup>[234]</sup> This NIR-triggered shape memory property is due to the presence of GO, which heats the PVA upon light absorption, causing its relaxation and unfolding of the patch on the heart walls (Figure 10a). In this case, the size of the incision and surgery duration (1 min) are significantly reduced, and the surgical procedure could be performed using microsurgical tools, as the unfolding and placement on the target are essentially autonomous, not requiring complex intervention by the surgeon. However, this method appears to be only applicable to relatively easily accessible targets, such as the chest cavity. Another strategy has been proposed by Montgomery et al. who developed an elastic shape-memory patch that can be delivered through a 1 mm diameter needle, which unfolds spontaneously after injection due to the properties of its microfabricated lattice design (Figure 10b).<sup>[232]</sup> The study reported how the injection did not alter the patch functionalities, as the results from in vivo tests were equivalent to those obtained by delivering the patch through traditional open surgery. Similarly, Mei et al. designed a heart pouch with self-unfolding properties conferred by the shape memory properties of its lattice structure inspired by origami, which has been proven to be deliverable by means of a flexible needle, similar to a catheter in rodent and swine models.<sup>[235]</sup> In both of these studies, the intended target was the heart, but this injection technique is likely to be also exploitable for other internal targets, even the less accessible ones, which could be reached with relative ease through flexible catheters. A bioadhesive origami patch was also developed by Wu et al., and it can be integrated with a variety of minimally invasive tools, such as a balloon catheter or a surgical stapler, offering interesting opportunities for various clinical scenarios (Figure 10c). For example, the use of a catheter could be useful for intraluminal sealing of tube-shaped organs, such as the trachea, esophagus, and blood vessels, while endoscopic staplers can successfully operate linear seals in resections and anastomoses.<sup>[233]</sup> The origami-based fabrication strategies employed in this study allow the patch to remain folded while integrated with the surgical tools, and then transition to a rubbery state upon contact with wet tissues, thereby releasing the plastic deformation and spontaneously unfolding to conform to the tissue surface. Furthermore, Lee et al. proposed an innovative delivery strategy using an ingestible magnetically-driven capsule.<sup>[236]</sup> The capsule, measuring 13 mm, contains three microneedle patches attached to a permanent magnet. The capsule can be guided toward the target through an external electromagnetic field and then release the patches one by one, again through magnetic actuation, so that they can adhere to lesions at various



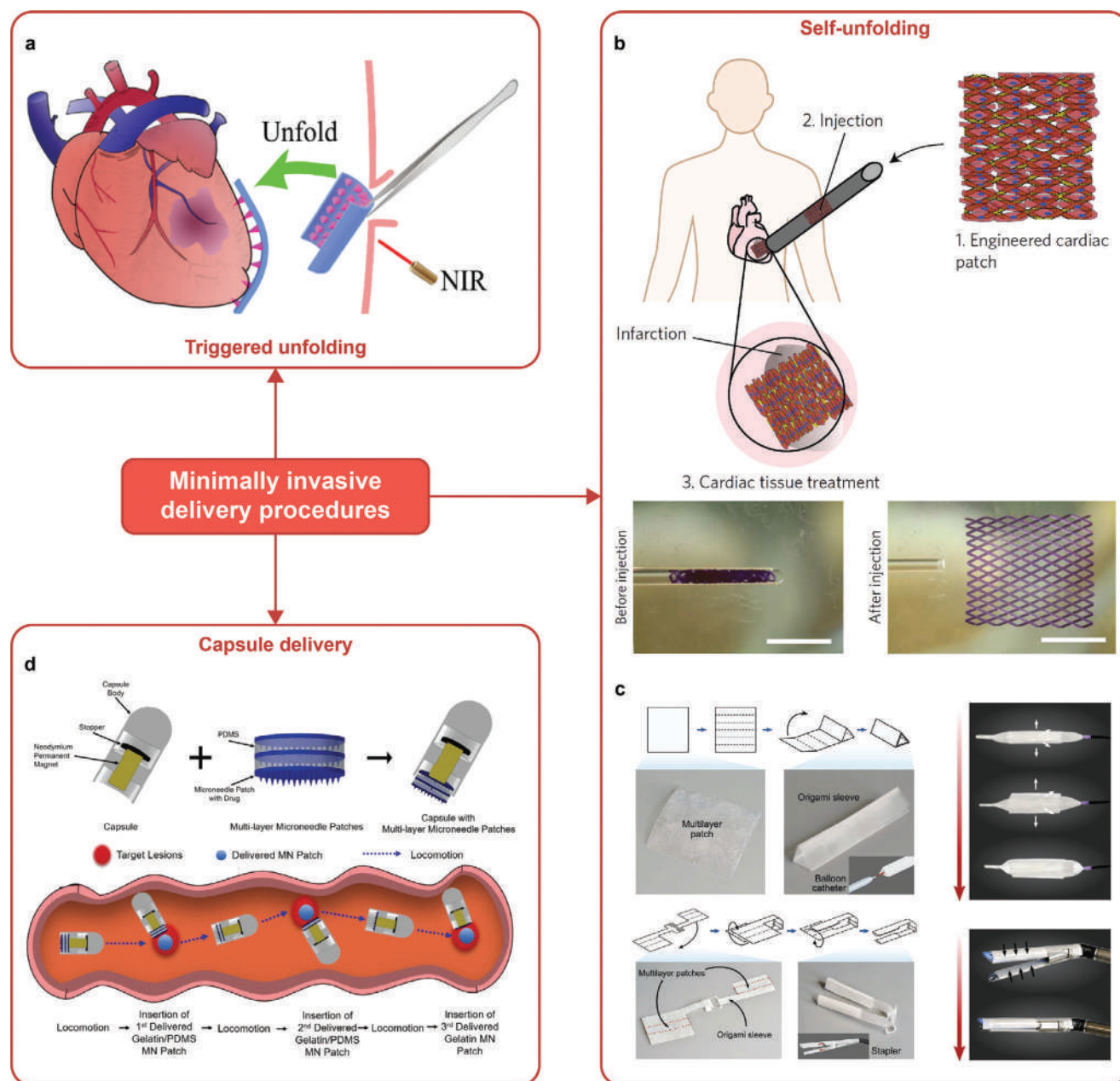


**Figure 10.** Some examples of minimally invasive procedures that have been proposed for the delivery of implantable patches. a) Unfolding upon implantation can be controlled through an external triggering stimulus, such as NIR light. Image reproduced with permission.<sup>[234]</sup> Copyright 2021, American Chemical Society. b) Shape-memory patches with self-unfolding capabilities have been delivered through needles, or c) through balloon catheters and endoscopic staplers. Reproduced with permission.<sup>[232,233]</sup> b) Copyright 2017, Springer Nature; c) Copyright 2021, Wiley-VCH. d) Patches to be implanted in the gastrointestinal tract can also be delivered through an ingestible capsule, which can expel them at the desired locations by magnetic actuation. Reproduced with permission.<sup>[236]</sup> Copyright 2020, Elsevier.

locations (Figure 10d). In this study, the target was the small intestine, which is a scarcely accessible tissue through conventional surgical tools, but this method can be an interesting solution for patch delivery to the entire gastrointestinal tract.

The use of smart materials with the ability to curve, fold, or roll-up in a dynamic and controllable manner has yielded several encouraging and promising results toward achieving minimally invasive delivery of implantable patches. This goal seems

within reach in the coming decades. However, to promote the clinical translation and introduction of these techniques into routine clinical procedures, more extensive in vivo investigations, particularly in large animal models, are necessary to demonstrate their safety, feasibility, and efficacy.<sup>[144]</sup> Additionally, refinement of these techniques is necessary before their translation to clinical practice. For example, identifying the optimal site for patch injection, which is still under investigation in many studies, and

training clinicians to maneuver the delivery instruments in vivo are important aspects to consider.<sup>[235]</sup> At the same time, it is essential to ensure that the functionality of the patches is preserved through these delivery procedures, which should not excessively stress the patch structure or compromise its functional integrity. In this regard, a possible solution to ensure patch integrity during minimally-invasive insertion procedures, at the same time facilitating patch delivery, is to fabricate the patch *ex situ*, without completing its crosslinking/solidification, thus without consolidating its final mechanical properties. This allows easy insertion of the patch in a delivery tool and to release it in the target area, exploiting its flexibility. Once released, the constituent materials can be directly cross-linked in situ to obtain the final patch features. An example of pre-manufactured (not crosslinked) 3D structure was reported by Luo et al. They developed a stent made of shape memory copolymers incorporating catalyst-free cross-linkable functional groups. This structure could undergo significant mechanical deformation during insertion due to the weak bonding strength of each printed layer. Subsequently, the device was strengthened in situ by activating the cross-linking sites via light irradiation.<sup>[237]</sup>

### 3.8. Sensing and Monitoring

When delivering a treatment through a patch, it could be helpful to know in real-time how the treatment is progressing, whether the patch is functioning as expected, and how the target tissue is responding.

This is why wearable patches, particularly those used for transdermal drug delivery or wound healing, are often endowed with sensing capabilities to monitor physiological parameters that provide insights into the patient's health status. For example, temperature, pH, or concentration of specific biomarkers are crucial indicators of inflammation or bacterial infection in a wound site,<sup>[2]</sup> while glucose concentration in blood, the concentration of specific analytes in sweat, or the presence of skin tremors can aid in monitoring particular diseases.<sup>[17]</sup> In the last decade, advancements in printable and flexible microelectronics have led to the development of various miniaturized and wearable electronic and electrochemical sensors for measuring these markers. For example, in a recent study, Sani et al. demonstrated the effectiveness of a wearable bioelectronic system integrating an electrochemical biosensor array, capable of wirelessly and continuously monitoring a panel of wound biomarkers, such as temperature, pH, ammonium, glucose, lactate, and uric acid levels, thereby revealing the infection, metabolic, and inflammatory status of a chronic wound during different healing stages.<sup>[238]</sup> In contrast, Lee et al. developed a wearable device for diabetes monitoring and treatment, equipped not only with glucose, pH, and humidity sensors for monitoring pathological symptoms but also with a temperature sensor to monitor skin temperature during the thermal actuation of the device, serving as a feedback control system to prevent overheating and skin damage.<sup>[141]</sup> Some biological markers can also be detected using sensors that rely on the properties of specific molecules or dyes without integrated electronics, such as colorimetric sensors.<sup>[28]</sup> Mirani et al. incorporated color-changing resin beads doped with a pH-responsive dye into an alginate wound dressing. The color changes of these

beads could be easily detected with a smartphone and custom-made app, which autonomously provided quantitative information about the infection status of the wound through image acquisition and processing.<sup>[239]</sup> In another study, silica NPs modified with cyanine dyes (Cy3, Cy5) were embedded in a hydrogel to act as fluorescent probes for detecting bacterial infection based on the FRET effect between Cy3 and Cy5.<sup>[240]</sup> Besides pH, oxygen levels can also be detected using colorimetric methods, such as employing a reference dye and porphyrin-dendrimer phosphor that fluoresces in oxygen.<sup>[241]</sup>

The information obtained from monitoring the status of the target site could be of particular interest in active patches, which could allow implementing a closed-loop treatment. In fact, communication between a sensing system and an actuation system, which controls the triggering of the patch, would enable modulation and adjustment of the timing and dosage of therapeutic actions based on the specific real-time needs of a patient.<sup>[48]</sup> To date, substantial efforts have been made to integrate various biosensors and therapeutic platforms into skin-conformal multicomponent packaging formats.<sup>[26]</sup> Specifically, numerous studies have successfully investigated feedback-controlled drug delivery. For example, Pang et al. developed a dressing that integrates a temperature sensor capable of detecting wound infection and activating UV-triggered antibiotics release on-demand.<sup>[60]</sup> Similarly, Mostafalu et al. developed an electrically-responsive wound dressing that is automatically activated by an electrochemical pH sensor.<sup>[143]</sup>

However, for implantable patches, the implementation of sensing and monitoring strategies is significantly more complex and less widespread due to difficulties related to accessing internal tissues for information collection and transmission.

Non-invasive imaging techniques, such as US or magnetic resonance could be of significant help for certain purposes. For example, they can be used to assess whether the patch remains in the correct position after a certain time, or whether it adheres properly to the target tissue. This monitoring function can also be achieved by integrating in advance labeling or contrast agents into the patch, which aid in detecting its position or orientation in vivo. For example, MNPs can serve as both magnetic resonance imaging probes and functional components of a patch.<sup>[34,42]</sup>

Some mechanical properties of target tissues or a patch can also be non-invasively monitored, aiding in assessing the progression of the delivered treatment and functionality of the patch over time. Techniques, such as US elastography, enable a non-invasive, non-destructive, quantitative, and real-time assessment of several mechanical parameters of tissues and implanted biomaterials in vivo. US elastography has been employed to evaluate the stiffness and viscoelastic properties of soft tissues, which are key parameters reflecting alterations in cellular and extracellular components, and ultimately, the health status of the tissue.<sup>[242]</sup> Additionally, it is commonly used to evaluate biomaterial degradation in vivo by measuring changes in mechanical parameters. It can also be employed to assess the viability of implanted cells, which is applicable in monitoring the proliferation status in implanted cell-based patches.<sup>[243]</sup>

Currently, non-invasive external observation is the extent to which it is possible to monitor the activity of an implanted patch in vivo. The use of proper sensors, such as the wearable ones described above, to be implanted on the target tissue is still

prohibitive. For the case of implantable solutions, sensors without integrated electronics would be preferable, but reading their output in a non-invasive manner from outside represents a challenging issue. Alternatively, implantable electronic sensors, while raising safety concerns and complicating device design and fabrication due to the need for circuitry and a power source, can more easily communicate with external devices. Wireless communication and powering technologies are rapidly developing and starting to be applied in the field of implantable and ingestible medical devices, which can integrate radiofrequency antennas for wireless transmission of physiological measurements from internal tissues to external control equipment.<sup>[244]</sup> Although such technologies have been integrated into some implants, such as brain implants and ocular and bladder pressure sensors,<sup>[245]</sup> their development is still in an early stage, and their application is limited. Presently, we are still far from the development of closed-loop implantable patches that monitor the status of internal tissues with sufficient precision and time resolution to the on-demand delivery of treatment based on acquired data. However, this is an exciting perspective for future study efforts.

### 3.9. Clinic-Derived Specifications and the Perspective of Multiple Drug Delivery

Driven by the specific treatment needs, when developing a new patch formulation, a crucial step is represented by the choice of the type of active agent to be delivered, release profile to be implemented, or stimulation protocol and parameters, in the case of tissue-stimulating patches.

For the treatment of common and widespread diseases, information regarding best clinical and pharmacological approaches are readily available in the literature. For example, it is well-known that an ideal treatment for diabetes would require a sustained baseline insulin delivery accompanied by pulsatile release at specific times.<sup>[246]</sup> Similarly, for disorders related to the circadian rhythm, a therapy synchronized with the onset of symptoms is required. In this case, a pulsatile drug delivery profile to be triggered on-demand is highly preferable.<sup>[247]</sup> In these cases, the ideal therapeutic approach is relatively well-defined, and efforts can focus on finding technological solutions to achieve practical implementation. However, for less common diseases, especially in the tissue regeneration field, there is limited knowledge regarding the ultimate treatment to be applied. In the last decades, a better understanding of the molecular and biochemical pathways involved in the different regeneration processes has led to the development of novel therapeutic solutions, even though comprehension of the exact role of all the biological mechanisms involved in these complex processes is still incomplete.<sup>[2,248]</sup> Selecting the appropriate growth factor combinations and determining crucial variables, such as effective dosages, timing, and delivery sequences still remain major challenges in tissue engineering. An improper growth factor combination or an unbalanced dosing schedule can activate signaling cascades that lead to undesirable outcomes.<sup>[249,250]</sup> The scarcity of standard therapeutic protocols and practical approaches for tissue regeneration in the literature is a critical issue that hinders the development of innovative and highly-efficient therapeutic devices for tissue regeneration and their practical application.

In general, it is widely recognized that natural tissue regeneration processes rely on a well-controlled cascade of sequential exposures to different growth factors, as each phase of regeneration involves different signaling pathways, biological molecules, and cell types.<sup>[30]</sup> Therefore, achieving a controlled spatiotemporal delivery of multiple and suitable factors can guide tissue regeneration by mimicking the natural processes of the human body.<sup>[45,251]</sup> Several studies have reported enhanced regeneration of various tissues, such as nerves, bones, muscles, and blood vessels, upon temporally organized co-administration of multiple growth factors compared to delivery of single factors. Chen et al. investigated the efficacy of sequential release of VEGF and platelet-derived growth factor (PDGF) on angiogenesis. They found that VEGF plays a role in initiating the formation of new vessels, while PDGF promotes their stabilization and maturation.<sup>[251]</sup> Thus, sequential exposure to VEGF followed by PDGF induced the growth of mature and well-developed vessels, while exposure to VEGF alone resulted in more numerous but smaller and immature vessels. Similarly, Kempen et al. proposed a strategy for bone regeneration based on the burst delivery of VEGF followed by sustained delivery of bone morphogenetic protein (BMP-2). This approach aims to re-establish vascularity before inducing bone formation through BMP-2, and it has shown encouraging results.<sup>[252]</sup> In another study, Raiche et al. suggested an alternative approach for inducing osteogenesis based on the observation of temporal differences in the appearance of various members of the BMP family during fracture healing.<sup>[250]</sup> They found that sequential delivery of BMP-2 and insulin-like growth factor resulted in the most favorable cell behavior, while simultaneous or reversed sequential delivery had significantly lower efficacy in promoting bone healing.

Furthermore, the combined delivery of different agents has also been demonstrated to be promising for cancer treatment. Combination chemotherapy is emerging as a strategy to promote synergistic effects, overcoming multi-drug resistance and reducing side effects.<sup>[253]</sup> For example, the delivery of both vascular disrupting agents, which undermine the tumor microenvironment, and chemotherapeutic drugs have effectively inhibited tumor growth and metastasis.<sup>[254]</sup>

In light of the above considerations, it is evident that patch systems with dual drug delivery capabilities may be beneficial for a vast number of applications, holding great potential for increasing the therapeutic efficacy of current treatment modalities.<sup>[30]</sup> In this context, various strategies are being employed to tackle the challenge of designing systems capable of delivering multiple therapeutics in a controlled manner and with different release kinetics.<sup>[249]</sup> For example, passive sequential delivery of two different molecules has been achieved in a fibrous patch by loading a first agent in the sheath region of the fibers, which is rapidly released in an initial burst, and a second agent in the fiber core, which is released with a sustained profile over time.<sup>[254]</sup> A similar dual delivery profile was obtained by incorporating the first drug directly into a hydrogel and loading the second one in polymer microspheres embedded within it, providing them with a double encapsulation level to ensure slower release (**Figure 11a**).<sup>[252]</sup> Alternatively, Cao et al. developed a semi-passive system in which hydrophilic and hydrophobic molecules were loaded into a hydrogel through different links. These links can be cleaved by different endogenous stimuli, namely pH and high concentrations



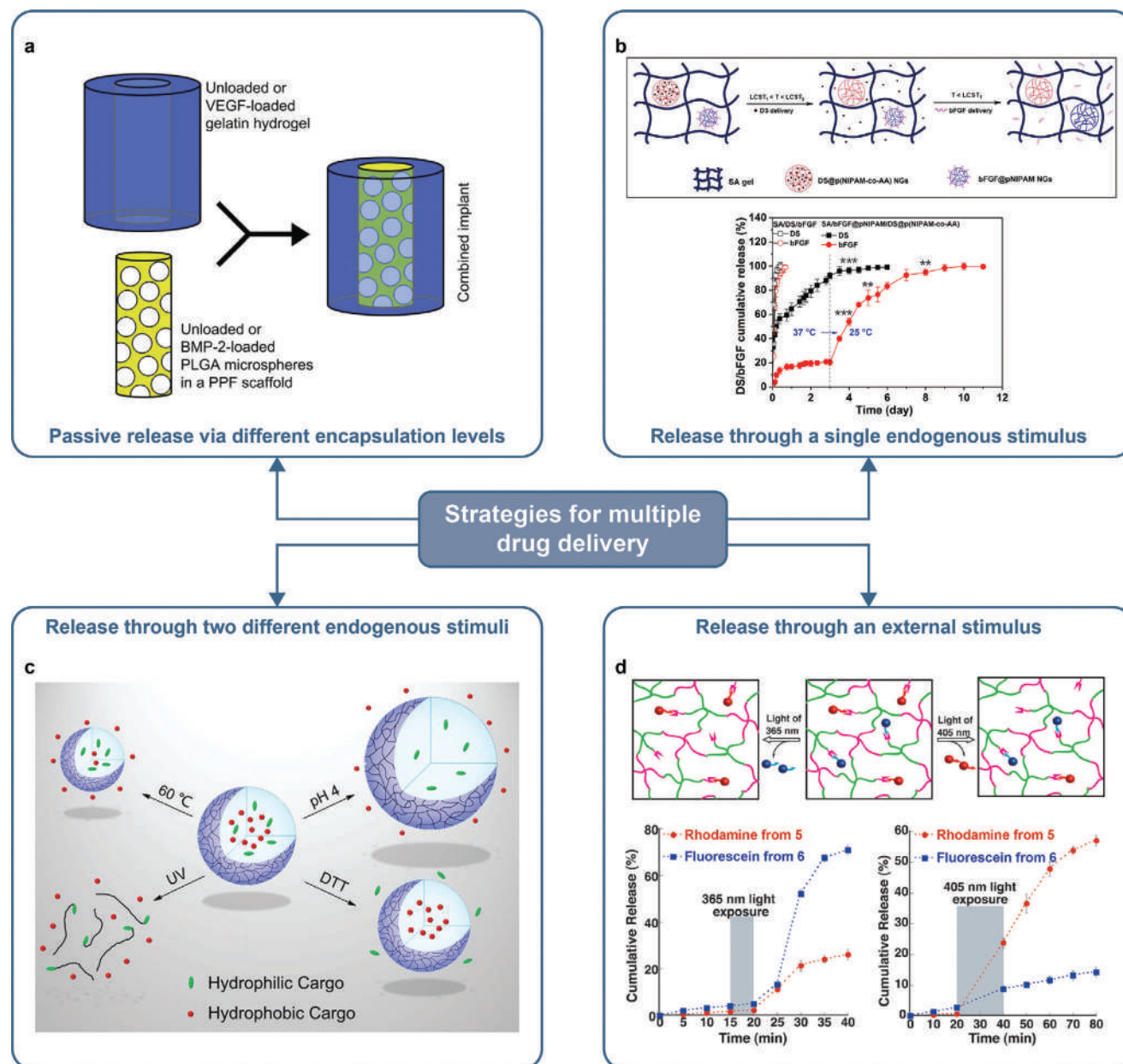


**Figure 11.** Some of the strategies employed for releasing multiple drugs from a single device. a) In a passive system, a drug was incorporated directly into the hydrogel to have a fast release, while a second drug was loaded in polymer microspheres embedded in the same matrix to ensure a slower release. Image reproduced with permission.<sup>[252]</sup> Copyright 2009, Elsevier. b) The independent release of two drugs has been achieved in a semi-passive system by loading them into a hydrogel matrix through two different links, which can be cleaved by different endogenous stimuli. Image reproduced with permission.<sup>[253]</sup> Copyright 2016, American Chemical Society. c) A scaffold composed of two thermo-responsive hydrogels with different critical temperatures, each encapsulating a different therapeutic, has been developed for their sequential release: in an early phase, characterized by higher endogenous temperatures, only the first agent was released, and only afterwards, when the temperature decreased, the second was delivered as well. Reproduced with permission.<sup>[255]</sup> Copyright 2020, Elsevier. d) In a photo-responsive system, two different proteins have been incorporated into a hydrogel through different photocleavable bonds, selectively triggerable, depending on the wavelength of the excitation light, allowing a controllable and independent delivery of the two molecules. Reproduced with permission.<sup>[256]</sup> Copyright 2013, Wiley-VCH.

of redox species. This allows the release of the two drugs at different times, corresponding to specific conditions of the target environment (Figure 11b).<sup>[253]</sup> In contrast, Lin et al. proposed a hybrid scaffold composed of two different thermo-responsive hydrogels with different critical temperatures, each encapsulating

a different therapeutic agent. In the early inflammatory phases, at higher endogenous temperatures, only the first agent was released, and only after overcoming the acute inflammatory phase, characterized by a lower temperature, the second drug was released (Figure 11c).<sup>[255]</sup> Furthermore, some studies attempted



to develop active systems with the ability to release two drugs with different profiles in a controlled and externally triggerable manner. For example, two different proteins have been incorporated into a single hydrogel through two different photocleavable bonds, so that the release of one over the other depended on the wavelength of the excitation light (Figure 11d).<sup>[256]</sup> In another study, two drugs were loaded into different thermo-responsive fibers, which could be selectively heated by an electronic control system, allowing an independent release of the two therapeutic agents.<sup>[89]</sup>

Some of the above-mentioned technologies have already been exploited to develop smart and innovative patch formulations, while to the best of our knowledge, others have only been employed in other types of therapeutic systems, such as 3D scaffolds or injectable hydrogels. However, they are all mostly compatible with the integration into a patch structure and could offer interesting possibilities to further advance efforts aimed at including multifunctionality features in patch systems. This, in turn, could contribute to improving their therapeutic efficacy for a broader range of clinical needs.

To achieve multifunctionality, an interesting prospect lies in the development of highly tunable stimuli-responsive materials. These materials can be functionalized in multiple ways to respond to various stimuli, including different types of stimulation within the same category. For example, metal-organic frameworks (MOFs) are garnering increasing attention in this context. They are porous hybrid solids composed of metal clusters connected by organic ligands. Recently, they have been intensely studied as promising drug carriers due to their high surface area and porosity, which guarantee a high drug-loading capability, high chemical stability, and relatively easy synthesis.<sup>[257]</sup> Additionally, MOFs are characterized by a very versatile composition, enabling the integration of a wide variety of metal ions and organic molecules with very different properties in their structure, which are transferred to the MOF. This functionalization versatility makes them extremely tunable, allowing them to change their properties upon exposure to specific stimuli.<sup>[258]</sup> To date, majority of the stimuli-responsive MOFs currently investigated for therapeutic applications are light-responsive, which include functional groups as azobenzenes and photosensitizers, such as porphyrin.<sup>[259]</sup> Recently, photo-responsive MOFs have been frequently employed in patch systems, especially for photodynamic therapy purposes.<sup>[260–262]</sup> Additionally, other types of responsive MOFs were already investigated, such as thermo-responsive ones, incorporating thermo-labile bonds, or possessing a crystal structure that undergoes a phase transition upon temperature increase.<sup>[259]</sup> There are also mechanically-responsive MOFs whose highly porous crystalline structure rearranges under the application of pressure, electrically responsive ones, usually incorporating redox-sensitive units, conductor atoms, or electrochromic groups,<sup>[263]</sup> and magnetically responsive ones, including magnetic atoms or NPs.<sup>[264]</sup> Recent study efforts have also focused on the development of multi-responsive MOFs. This can be achieved by functionalizing their structure with multiple types of functional ions and groups to be triggered by different stimuli.<sup>[263,264]</sup> Multi-functionalization of a single MOF platform is a field that is still in its early stage, but that may lead to great advancements in the next decades.

## 4. Conclusions

Medical patches have garnered increasing attention over the last few decades for a broad variety of therapeutic applications and clinical targets due to their versatility and relative simplicity of use. Particularly, externally triggerable smart patches appear nowadays to hold the most interesting potential, as their action can be carefully controlled through the application of biophysical energies. These devices enable the release of drugs or direct stimulation of tissues, either chemically or physically in a controlled and carefully temporized manner, maximizing the therapeutic efficacy of the treatment. This review analyzed the main triggering stimuli, namely light, electric, and magnetic fields and US, highlighting their strengths and weaknesses for different applications in terms of tissue penetration ability, tunability, safety, and control. Moreover, significant attention has been given to the interaction mechanisms between these stimuli and specific responsive materials, which are the key enabling features of the smart character of triggerable patches. Advances in material science, biochemistry, and fabrication technologies have improved their functionalities by employing increasingly performant materials, and ongoing studies continue to propose innovative combinations of smart materials to overcome the current limitations.

Apart from maximizing responsiveness to the triggering signal, several other aspects deserve consideration during the design of a patch. Ensuring total biocompatibility of these devices is crucial. In some cases, biodegradability is a desirable feature as well. Properly tuning the mechanical properties of a patch to favor its interaction with a target tissue, and endowing the patch's surface with adhesive properties to avoid the need for glues or stitches are also essential aspects to be considered. Additionally, other details, though less critical, can still improve patch performances and guide further development in this field. Modeling the interaction mechanisms between smart patches and triggering stimuli may facilitate a more rational design of new formulations, while carefully controlling the stimulation dose in vitro and in vivo improves the reliability and repeatability of the results. Integrating sensing and monitoring functions in the patch could also offer the possibility to “close the loop,” delivering the treatment based on the real-time needs. Furthermore, making the patches multifunctional, such as endowing them with the ability to release two different drugs in a controllable manner, would greatly benefit therapeutic efficacy for a wide range of pathologies. Finally, ensuring the portability of these devices and identifying minimally invasive delivery techniques, particularly for implantable patches, could significantly improve usability and patients' compliance.

Several recent efforts tried to address many of the above-mentioned issues, leading to important advancements in the field. However, some aspects remain challenging, and concurrently addressing multiple issues in the design of a single patch is currently quite ambitious. Furthermore, majority of existing triggerable patches are currently meant as wearable devices for external applications. Their potential as implantable devices to target internal organs is still largely underexplored, albeit significant. Thus, there is still considerable potential to uncover in triggerable patches, and collaborative efforts from different fields, such as material science, bioengineering, chemistry, electronics, and

pharmaceutics, are required to facilitate the translation of these devices to clinics and markets.

## Acknowledgements

This work received funding from the European Union's Horizon Europe research and innovation program, grant agreement No 101091852, project REBORN (Remodeling of the infarcted heart: piezoelectric multifunctional patch enabling the sequential release of therapeutic factors). This publication was also produced with the co-funding of European Union – Next Generation EU, in the context of the National Recovery and Resilience Plan, Investment 1.5 Ecosystems of Innovation, Project Tuscany Health Ecosystem (THE), ECS00000017, Spoke 3, CUP: B83C22003920001. The authors thank Andrea Aliperta for the production of artistic figures.

## Conflict of Interest

The authors declare no conflict of interest.

## Keywords

biophysical stimuli, drug delivery, smart medical patches, tissue regeneration, triggerable systems

Received: September 29, 2023

Revised: June 5, 2024

Published online: July 1, 2024

- [1] <https://dictionary.cambridge.org/dictionary/english/patch> (accessed: February 2023).
- [2] M. Farahani, A. Shafiee, *Adv. Healthcare Mater.* **2021**, *10*, e2100477.
- [3] Y. Wang, G. Chen, H. Zhang, C. Zhao, L. Sun, Y. Zhao, *ACS Nano* **2021**, *15*, 5977.
- [4] D. H. Kim, N. Lu, R. Ma, Y. S. Kim, R. H. Kim, S. Wang, J. Wu, S. M. Won, H. Tao, A. Islam, K. J. Yu, T. I. Kim, R. Chowdhury, M. Ying, L. Xu, M. Li, H. J. Chung, H. Keum, M. McCormick, P. Liu, Y. W. Zhang, F. G. Omenetto, Y. Huang, T. Coleman, J. A. Rogers, *Science* **2011**, *333*, 838.
- [5] X. Wang, M. Wang, H. Sheng, L. Zhu, J. Zhu, H. Zhang, Y. Liu, L. Zhan, X. Wang, J. Zhang, X. Wu, Z. Suo, W. Xi, H. Wang, *Biomaterials* **2022**, *287*, 121352.
- [6] M. Yuan, K. Liu, T. Jiang, S. Li, J. Chen, Z. Wu, W. Li, R. Tan, W. Wei, X. Yang, H. Dai, Z. Chen, *J. Nanobiotechnol.* **2022**, *20*, 147.
- [7] Q. Zhu, Y. Hong, Y. Huang, Y. Zhang, C. Xie, R. Liang, C. Li, T. Zhang, H. Wu, J. Ye, X. Zhang, S. Zhang, X. Zou, H. Ouyang, *Adv. Sci.* **2022**, *9*, 2106115.
- [8] J. Zhu, H. Zhou, E. M. Gerhard, S. Zhang, F. I. Parra Rodríguez, T. Pan, H. Yang, Y. Lin, J. Yang, H. Cheng, *Bioact. Mater.* **2023**, *19*, 360.
- [9] Z. Qiu, J. Zhao, F. Huang, L. Bao, Y. Chen, K. Yang, W. Cui, W. Jin, *NPJ Regen. Med.* **2021**, *6*, 44.
- [10] N. Z. Ezazi, R. Ajdary, A. Correia, E. Mä, J. Salonen, M. Kemell, J. Hirvonen, O. J. Rojas, H. J. Ruskoaho, H. A. Santos, *ACS Appl. Mater. Interfaces* **2020**, *12*, 6899.
- [11] M. Ghovvati, M. Kharazili, R. Ardehali, N. Annabi, *Adv. Healthcare Mater.* **2022**, *11*, 2200055.
- [12] Y. Song, M. Li, S. Lei, L. Hao, Q. Lv, M. Liu, G. Wang, Z. Wang, X. Fu, L. Wang, *Biomaterials* **2022**, *287*, 121630.
- [13] Y. Xie, F. Zhang, O. Akku, M. W. King, *J. Biomed. Mater. Res.* **2022**, *110*, 2624.
- [14] J. Wang, C. Feng, Y. Zhu, Z. Wang, X. Ren, X. Li, Y. Ying, Y. Tian, K. Yu, S. Liu, C. Liu, X. Zeng, *Mater. Des.* **2022**, *220*, 1108212.
- [15] Y. Zhu, S. Li, Y. Li, H. Tan, Y. Zhao, L. Sun, *Chem. Eng. J.* **2022**, *449*, 137786.
- [16] C. Cristallini, G. Vaccari, N. Barbani, E. Cibrario Rocchietti, R. Barberis, M. Falzone, K. Cabiale, G. Perona, E. Bellotti, R. Rastaldo, S. Pascale, P. Pagliaro, C. Giachino, *J. Tissue Eng. Regen. Med.* **2019**, *13*, 1253.
- [17] I. Hwang, H. Nam Kim, M. Seong, S. H. Lee, M. Kang, H. Yi, W. Gyu Bae, M. Kyu Kwak, H. Eui Jeong, *Adv. Healthcare Mater.* **2018**, *7*, 1800275.
- [18] Y. Chen, Q. An, K. Teng, Y. Zhang, Y. Zhao, *Eur. Polym. J.* **2022**, *170*, 111164.
- [19] F. Sabbagh, B. S. Kim, *J. Control Release* **2022**, *341*, 132.
- [20] S. S. Moon, M. Richter-Roche, T. K. Resch, Y. Wang, K. R. Foytich, H. Wang, B. A. Mainou, W. Pewin, J. Lee, S. Henry, D. v. McAllister, B. Jiang, *NPJ Vaccines* **2022**, *7*, 26.
- [21] J. Kim, M. Kudisch, S. Mudumba, H. Asada, E. Aya-Shibuya, R. B. Bhisitkul, T. A. Desai, *Invest. Ophthalmol. Vis. Sci.* **2016**, *57*, 4341.
- [22] L. Xu, H. Wang, Z. Chu, L. Cai, H. Shi, C. Zhu, D. Pan, J. Pan, X. Fei, Y. Lei, *ACS Appl. Polym. Mater.* **2020**, *2*, 741.
- [23] J. Lee, H. R. Cho, G. Doo Cha, H. Seo, S. Lee, C. K. Park, J. W. Kim, S. Qiao, L. Wang, D. Kang, T. Kang, T. Ichikawa, J. Kim, H. Lee, W. Lee, S. Kim, S. T. Lee, N. Lu, T. Hyeon, S. H. Choi, D. H. Kim, *Nat. Commun.* **2019**, *10*, 5205.
- [24] R. Dong, B. Guo, *Nano Today* **2021**, *40*, 101290.
- [25] M. Boffito, C. Gentile, S. M. Giannitelli, S. Cohen, A. Bar, *Front. Bioeng. Biotechnol.* **2020**, *8*, 126.
- [26] M. Amjadi, S. Sheykhansari, B. J. Nelson, M. Sitti, *Adv. Mater.* **2018**, *30*, 1704530.
- [27] R. Ajdary, N. Z. Ezazi, A. Correia, M. Kemell, S. Huan, H. J. Ruskoaho, J. Hirvonen, H. A. Santos, O. J. Rojas, *Adv. Funct. Mater.* **2020**, *30*, 2003440.
- [28] H. Derakhshandeh, S. S. Kashaf, F. Aghabaglou, I. O. Ghanavati, A. Tamayol, *Trends Biotechnol.* **2018**, *36*, 1259.
- [29] A. Ghofrani, L. Taghavi, B. Khalilivavdareh, A. Rohani Shirvan, A. Nouri, *Eur. Polym. J.* **2022**, *174*, 111332.
- [30] J. Leijten, J. Seo, K. Yue, G. Trujillo-de Santiago, A. Tamayol, G. U. Ruiz-Esparza, S. R. Shin, R. Sharifi, I. Noshadi, M. M. Álvarez, Y. S. Zhang, A. Khademhosseini, *Mater. Sci. Eng. R Rep.* **2017**, *119*, 1.
- [31] J. J. Rice, M. M. Martino, L. de Laporte, F. Tortelli, P. S. Briquez, J. A. Hubbell, *Adv. Healthcare Mater.* **2013**, *2*, 57.
- [32] R. L. C. Kwan, S. Lu, H. M. C. Choi, L. C. Kloth, G. L. Y. Cheing, *Int. J. Mol. Sci.* **2019**, *20*, 368.
- [33] S. M. Z. Uddin, D. E. Komatsu, T. Motyka, S. Petterson, *J. Clin. Med.* **2021**, *10*, 2698.
- [34] T. Saliev, Z. Mustapova, G. Kulsharova, D. Bulanin, S. Mikhailovsky, *Cell Prolif.* **2014**, *47*, 485.
- [35] M. Wei, Y. Gao, X. Li, M. J. Serpe, *Polym. Chem.* **2017**, *8*, 127.
- [36] E. Fleige, M. A. Quadir, R. Haag, *Adv. Drug Delivery Rev.* **2012**, *64*, 866.
- [37] P. Makvandi, R. Jamaledin, G. Chen, Z. Baghbantarghadari, E. N. Zare, C. Di Natale, V. Onesto, R. Vecchione, J. Lee, F. R. Tay, P. Netti, V. Mattoli, A. Jaklenec, Z. Gu, R. Langer, *Mater. Today* **2021**, *47*, 206.
- [38] D. H. Sliney, *Eye* **2016**, *30*, 222.
- [39] E. Hecht, *Optics*, Addison Wesley, San Francisco, CA **2002**.
- [40] D. B. Tata, R. W. Waynant, *Laser Photonics Rev.* **2011**, *5*, 1.
- [41] D. Zhi, T. Yang, J. O'Hagan, S. Zhang, R. F. Donnelly, *J. Control Release* **2020**, *325*, 52.
- [42] H. Y. Fan, Z. I. Zhu, W. I. Zhang, Y. J. Yin, Y. I. Tang, X. H. Liang, L. Zhang, *Eur. J. Med. Chem.* **2020**, *199*, 112394.
- [43] S. R. Tsai, M. R. Hamblin, *J. Photochem. Photobiol. B: Biol.* **2017**, *170*, 197.
- [44] C. Dompe, L. Moncrieff, J. Matys, K. Grzech-Leśniak, I. Kocherova, A. Bryja, M. Bruska, M. Dominiak, P. Mozdziak, T. H. I. Skiba, J. A. Shibli, A. A. Volponi, B. Kempisty, M. Dyszkiewicz-Konwińska, *J. Clin. Med.* **2020**, *9*, 1724.

- [45] E. R. Ruskowitz, C. A. Deforest, *Nat. Rev. Mater.* **2018**, *3*, 17087.
- [46] M. Karimi, A. Ghasemi, P. Sahandi Zangabad, R. Rahighi, S. M. M. Basri, H. Mirshekari, M. Amiri, Z. Shafaei Pishabad, A. Aslani, M. Bozorgomid, D. Ghosh, A. Beyzavi, A. Vaseghi, A. R. Aref, L. Haghani, S. Bahrami, M. R. Hamblin, *Chem. Soc. Rev.* **2016**, *45*, 1457.
- [47] R. Weissleder, *Nat. Biotechnol.* **2001**, *19*, 316.
- [48] E. Cheah, Z. Wu, S. S. Thakur, S. J. O'Carroll, D. Svirskis, *J. Control Release* **2021**, *332*, 74.
- [49] S. Stolik, J. A. Delgado, A. Pérez, L. Anasagasti, *J. Photochem. Photobiol. B: Biol.* **2000**, *57*, 90.
- [50] W. Zhao, Y. Li, X. Zhang, R. Zhang, Y. Hu, C. Boyer, F. J. Xu, *J. Control Release* **2020**, *323*, 24.
- [51] Y. Ren, Y. Yan, H. Qi, *Adv. Colloid Interface Sci.* **2022**, *308*, 102753.
- [52] J. Hu, Y. Chen, Y. Li, Z. Zhou, Y. Cheng, *Biomaterials* **2017**, *112*, 133.
- [53] F. Teodorescu, G. Quéniat, C. Foulon, M. Lecoœur, A. Barras, S. Boulahneche, M. S. Medjram, T. Hubert, A. Abderrahmani, R. Boukherroub, S. Szunerits, *J. Control Release* **2017**, *245*, 137.
- [54] S. S. Lucky, K. C. Soo, Y. Zhang, *Chem. Rev.* **2015**, *115*, 1990.
- [55] Y. Zhang, S. Wang, Y. Yang, S. Zhao, J. You, J. Wang, J. Cai, H. Wang, J. Wang, W. Zhang, J. Yu, C. Han, Y. Zhang, Z. Gu, *Nat. Commun.* **2023**, *14*, 3431.
- [56] S. Y. Lee, S. Jeon, Y. W. Kwon, M. Kwon, M. S. Kang, K. Y. Seong, T. E. Park, S. Y. Yang, D. W. Han, S. W. Hong, K. S. Kim, *Sci. Adv.* **2022**, *8*, 1646.
- [57] Y. Jeon, H. R. Choi, M. Lim, S. Choi, H. Kim, J. H. Kwon, K. C. Park, K. C. Choi, *Adv. Mater. Technol.* **2018**, *3*, 1700391.
- [58] C. Li, R. Ye, J. Bouckaert, A. Zurutuza, D. Drider, T. Dumych, S. Paryzhak, V. Vovk, R. O. Bilyy, S. Melinte, M. Li, R. Boukherroub, S. Szunerits, *ACS Appl. Mater. Interfaces* **2017**, *9*, 36665.
- [59] X. Yu, J. Zhao, D. Fan, *Chem. Eng. J.* **2022**, *437*, 135475.
- [60] Q. Pang, D. Lou, S. Li, G. Wang, B. Qiao, S. Dong, L. Ma, C. Gao, Z. Wu, *Adv. Sci.* **2020**, *7*, 1902673.
- [61] H. Kim, H. Lee, K. Y. Seong, E. Lee, S. Yun Yang, J. Yoon, *Adv. Healthcare Mater.* **2015**, *4*, 2071.
- [62] D. Wu, X. Shou, Y. Yu, X. Wang, G. Chen, Y. Zhao, L. Sun, *Adv. Funct. Mater.* **2022**, *32*, 2205847.
- [63] E. M. Purcell, D. J. Morin, *Electricity and Magnetism*, Cambridge University Press, Cambridge, UK **2013**.
- [64] J. D. Jackson, *Classical Electrodynamics*, John Wiley and Sons, Inc, Hoboken, NJ **1999**.
- [65] R. A. Serway, C. Vuille, *College Physics*, Brooks/Cole, Boston, MA **2012**.
- [66] G. Thakral, J. LaFontaine, B. Najafi, T. K. Talal, P. Kim, L. A. Lavery, *Diabet. Foot Ankle* **2013**, *4*, 22081.
- [67] J. Zhang, N. Jia, J. Yang, J. Liu, *Chin. J. Plast. Reconstr. Surg.* **2021**, *3*, 95.
- [68] H. Kim, I. Makin, J. Skiba, A. Ho, G. Housler, A. Stojadinovic, M. Izadjoo, *Open Microbiol. J.* **2014**, *8*, 15.
- [69] C. Wang, X. Jiang, H. J. Kim, S. Zhang, X. Zhou, Y. Chen, H. Ling, Y. Xue, Z. Chen, M. Qu, L. Ren, J. Zhu, A. Libanori, Y. Zhu, H. Kang, S. Ahadian, M. R. Dokmeci, P. Servati, X. He, Z. Gu, W. Sun, A. Khademhosseini, *Biomaterials* **2022**, *285*, 121479.
- [70] G. Zhao, H. Zhou, G. Jin, B. Jin, S. Geng, Z. Luo, Z. Ge, F. Xu, *Prog. Polym. Sci.* **2022**, *131*, 101573.
- [71] K. Ashtari, H. Nazari, H. Ko, P. Tebon, M. Akhshik, M. Akbari, S. N. Alhosseini, M. Mozafari, B. Mehravi, M. Soleimani, R. Ardehali, M. E. Warkiani, S. Ahadian, A. Khademhosseini, *Adv. Drug. Deliv. Rev.* **2019**, *144*, 162.
- [72] L. Li, J. Ge, L. Wang, B. Guo, P. X. Ma, *J. Mater. Chem. B* **2014**, *2*, 6119.
- [73] B. M. Doucet, A. Lam, L. Griffin, *Yale J. Biol. Med.* **2012**, *85*, 201.
- [74] K. Yang, C. Freeman, R. Torah, S. Beeby, J. Tudor, *Sens. Actuator A Phys.* **2014**, *213*, 108.
- [75] C. H. Moran, S. M. Wainerdi, T. K. Cherukuri, C. Kittrell, B. J. Wiley, N. W. Nicholas, S. A. Curley, J. S. Kanzius, P. Cherukuri, *Nano Res.* **2009**, *2*, 400.
- [76] Q. Wang, H. Sheng, Y. Lv, J. Liang, Y. Liu, N. Li, E. Xie, Q. Su, F. Ershad, W. Lan, J. Wang, C. Yu, *Adv. Funct. Mater.* **2022**, *32*, 2111228.
- [77] H. Priya James, R. John, A. Alex, K. R. Anoop, *Acta Pharm. Sin. B* **2014**, *4*, 120.
- [78] N. Jackson, F. Stam, *J. Appl. Polym. Sci.* **2015**, *132*, 41687.
- [79] S. S. Said, S. Campbell, T. Hoare, *Chem. Mater.* **2019**, *31*, 4971.
- [80] M. Jensen, B. Hansen, S. Murdan, S. Frokjaer, A. T. Florence, *Eur. J. Pharm. Sci.* **2002**, *15*, 139.
- [81] M. Bansal, A. Dravid, Z. Aqrave, J. Montgomery, Z. Wu, D. Svirskis, *J. Controlled Release* **2020**, *328*, 192.
- [82] M. L. Clingerman, J. A. King, K. H. Schulz, J. D. Meyers, *J. Appl. Polym. Sci.* **2002**, *83*, 1341.
- [83] Q. Yan, J. Yuan, Z. Cai, Y. Xin, Y. Kang, Y. Yin, *J. Am. Chem. Soc.* **2010**, *132*, 9268.
- [84] W. H. Lee, H. Ren, J. Wu, O. Novak, R. B. Brown, C. Xi, M. E. Meyerhoff, *ACS Biomater. Sci. Eng.* **2016**, *2*, 1432.
- [85] G. Xu, Y. Lu, C. Cheng, X. Li, J. Xu, Z. Liu, J. Liu, G. Liu, Z. Shi, Z. Chen, F. Zhang, Y. Jia, D. Xu, W. Yuan, Z. Cui, S. S. Low, Q. Liu, *Adv. Funct. Mater.* **2021**, *31*, 2100852.
- [86] H. W. Liu, S. H. Hu, Y. W. Chen, S. Y. Chen, *J. Mater. Chem.* **2012**, *22*, 17311.
- [87] S. H. Sung, Y. S. Kim, D. J. Joe, B. H. Mun, B. K. You, D. H. Keum, S. K. Hahn, M. Berggren, D. Kim, K. J. Lee, *Nano Energy* **2018**, *51*, 102.
- [88] A. Tamayol, A. Hassani Najafabadi, P. Mostafalu, A. K. Yetisen, M. Comotto, M. Aldahri, M. S. Abdel-Wahab, Z. I. Najafabadi, S. Latifi, M. Akbari, N. Annabi, S. H. Yun, A. Memic, M. R. Dokmeci, A. Khademhosseini, *Sci. Rep.* **2017**, *7*, 9220.
- [89] P. Mostafalu, G. Kiaee, G. Giatsidis, A. Khalilpour, M. Nabavinia, M. R. Dokmeci, S. Sonkusale, D. P. Orgill, A. Tamayol, A. Khademhosseini, *Adv. Funct. Mater.* **2017**, *27*, 1702399.
- [90] D. Son, J. Lee, S. Qiao, R. Ghaffari, J. Kim, J. E. Lee, C. Song, S. J. Kim, D. J. Lee, S. Woojoo Jun, S. Yang, M. Park, J. Shin, K. Do, M. Lee, K. Kang, C. S. Hwang, N. Lu, T. Hyeon, D. H. Kim, *Nat. Nanotechnol.* **2014**, *9*, 397.
- [91] M. S. Markov, *Electromagn. Biol. Med.* **2007**, *26*, 1.
- [92] O. Azie, Z. F. Greenberg, C. D. Batich, J. P. Dobson, *Int. J. Mol. Sci.* **2019**, *20*, 3190.
- [93] R. R. Shah, T. P. Davis, A. L. Glover, D. E. Nikles, C. S. Brazel, *J. Magn. Magn. Mater.* **2015**, *387*, 96.
- [94] S. T. Meikle, Y. Piñeiro, M. Bañobre López, J. Rivas, M. Santin, *Acta Biomater.* **2016**, *40*, 235.
- [95] H. Oliveira, E. Pérez-Andrés, J. Thevenot, O. Sandre, E. Berra, S. Lecommandoux, *J. Control Release* **2013**, *169*, 165.
- [96] K. J. Widder, A. E. Senyei, D. F. Ranney, *Cancer Res.* **1980**, *40*, 3512.
- [97] D. Luo, R. N. Poston, D. J. Gould, G. B. Sukhorukov, *Mater. Sci. Eng. C* **2019**, *94*, 647.
- [98] V. R. Jayaneththi, K. Aw, M. Sharma, J. Wen, D. Svirskis, A. J. McDaid, *Sens. Actuators, B* **2019**, *297*, 126708.
- [99] Y. Li, G. Huang, X. Zhang, B. Li, Y. Chen, T. Lu, T. J. Lu, F. Xu, *Adv. Funct. Mater.* **2013**, *23*, 660.
- [100] T. Hoare, B. P. Timko, J. Santamaria, G. F. Goya, S. Irusta, S. Lau, C. F. Stefanescu, D. Lin, R. Langer, D. S. Kohane, *Nano Lett.* **2011**, *11*, 1395.
- [101] H. Li, F. Gao, P. Wang, L. Yin, N. Ji, L. Zhang, L. Zhao, G. Hou, B. Lu, Y. Chen, Y. Ma, X. Feng, *ACS Appl. Mater. Interfaces* **2021**, *13*, 21067.
- [102] J. Lee, D. Kim, S. Bang, S. Park, *Adv. Intell. Syst.* **2022**, *4*, 2100203.
- [103] N. Andryšková, P. Sourivong, M. Babinčová, M. Šimaljaková, *Appl. Sci.* **2021**, *11*, 11022.
- [104] A. Gonçalves, F. V. Almeida, P. Borges, P. I. P. Soares, *Gels* **2021**, *7*, 28.



- [105] A. Cafarelli, A. Marino, L. Vannozi, J. Puigmartí-Luis, S. Pané, G. Ciofani, L. Ricotti, *ACS Nano* **2021**, *15*, 11066.
- [106] L. Mei, Z. Zhang, *Ultrasound Med. Biol.* **2021**, *47*, 2839.
- [107] W. Chen, J. Du, *Sci. Rep.* **2013**, *3*, 2162.
- [108] M. Postema, A. Van Wamel, C. T. Lancée, N. De Jong, *Ultrasound Med. Biol.* **2004**, *30*, 827.
- [109] O. Boerman, Z. Abedin, R. A. Dimaria-Ghalili, M. S. Weingarten, M. Neidrauer, P. A. Lewin, K. L. Spiller, *bioRxiv* **2022**, <https://doi.org/10.1101/2022.04.13.488030>.
- [110] F. Fontana, F. Iacoponi, F. Orlando, T. Pratellesi, A. Cafarelli, L. Ricotti, *J. Neural Eng.* **2023**, *20*, 026033.
- [111] X. Jiang, O. Savchenko, Y. Li, S. Qi, T. Yang, W. Zhang, J. Chen, *IEEE Trans. Biomed. Eng.* **2019**, *66*, 2704.
- [112] F. Iacoponi, A. Cafarelli, F. Fontana, T. Pratellesi, E. Dumont, I. Barravecchia, D. Angeloni, L. Ricotti, *APL Bioeng.* **2023**, *7*, 016114.
- [113] F. C. Kao, H. H. Ho, P. Y. Chiu, M. K. Hsieh, J. C. Liao, P. L. Lai, Y. F. Huang, M. Y. Dong, T. T. Tsai, Z. H. Lin, *Sci. Technol. Adv. Mater.* **2022**, *23*, 1.
- [114] C. Paci, F. Iberite, L. Arrico, L. Vannozi, P. Parlanti, M. Gemmi, L. Ricotti, *Biomater. Sci.* **2022**, *10*, 5265.
- [115] A. Ranjan, G. C. Jacobs, D. L. Woods, A. H. Negussie, A. Partanen, P. S. Yarmolenko, C. E. Gacchina, K. V. Sharma, V. Frenkel, B. J. Wood, M. R. Dreher, *J. Control Release* **2012**, *158*, 487.
- [116] H. Zhang, H. Xia, J. Wang, Y. Li, *J. Control Release* **2009**, *139*, 31.
- [117] A. Moncion, K. J. Arlotta, O. D. Kripfgans, J. B. Fowlkes, P. L. Carson, A. J. Putnam, R. T. Franceschi, M. L. Fabiilli, *Ultrasound Med. Biol.* **2016**, *42*, 257.
- [118] A. Moncion, M. Lin, E. G. O'Neill, R. T. Franceschi, O. D. Kripfgans, A. J. Putnam, M. L. Fabiilli, *Biomaterials* **2017**, *140*, 26.
- [119] C. H. Wu, M. K. Sun, J. Shieh, C. S. Chen, C. W. Huang, C. A. Dai, S. W. Chang, W. S. Chen, T. H. Young, *Ultrasonics* **2018**, *83*, 157.
- [120] J. Kost, K. Leongt, R. Langero, *Proc. Natl. Acad. Sci. USA* **1989**, *86*, 7663.
- [121] F. Soto, I. Jeerapan, C. Silva-López, M. A. Lopez-Ramirez, I. Chai, L. Xiaolong, J. Lv, J. F. Kurniawan, I. Martin, K. Chakravarthy, J. Wang, *Small* **2018**, *14*, 1803266.
- [122] D. Huang, M. Sun, Y. Bu, F. Luo, C. Lin, Z. Lin, Z. Weng, F. Yang, D. Wu, *J. Mater. Chem. B* **2019**, *7*, 2330.
- [123] L. Vannozi, L. Ricotti, C. Filippeschi, S. Sartini, V. Coviello, V. Piazza, P. Pingue, C. La Motta, P. Dario, A. Menciassi, *Int. J. Nanomed.* **2016**, *11*, 69.
- [124] L. Gazvoda, M. Perišić Nanut, M. Spreitzer, M. Vukomanović, *Biomater. Sci.* **2022**, *10*, 4933.
- [125] X. Shi, Y. Chen, Y. Zhao, M. Ye, S. Zhang, S. Gong, *Biomater. Sci.* **2022**, *10*, 692.
- [126] W. Lyu, Y. Ma, S. Chen, H. Li, P. Wang, Y. Chen, X. Feng, *Adv. Healthcare Mater.* **2021**, *10*, 2100785.
- [127] V. Van Tran, M. Chae, J. Y. Moon, Y. C. Lee, *Opt. Laser Technol.* **2021**, *135*, 106698.
- [128] J. Xu, M. Zeng, X. Xu, J. Liu, X. Huo, D. Han, Z. Wang, L. Tian, *Sensors* **2021**, *21*, 5133.
- [129] M. Rubart, *Circ. Res.* **2004**, *95*, 1154.
- [130] J. G. Troughton, Y. O. Ansong, N. Duobaite, C. M. Proctor, *APL Bioeng.* **2023**, *7*, 046109.
- [131] R. Liu, R. Ma, X. Liu, X. Zhou, X. Wang, T. Yin, Z. Liu, *IEEE Trans. Ultrason. Ferroelectr. Freq. Control* **2022**, *69*, 2474.
- [132] H. A. C. Wark, R. Sharma, K. S. Mathews, E. Fernandez, J. Yoo, B. Christensen, P. Tresco, L. Rieth, F. Solzbacher, R. A. Normann, P. Tathireddy, *J. Neural Eng.* **2013**, *10*, 045003.
- [133] N. Crook, L. Robinson, *Radiography* **2009**, *15*, 351.
- [134] A. E. Nieminen, J. O. Nieminen, M. Stenroos, P. Novikov, M. Nazarova, S. Vaalto, V. Nikulin, R. J. Ilmoniemi, *J. Neural Eng.* **2022**, *19*, 066037.
- [135] EN 60601-2-5:2015: Medical electrical equipment – Part 2–5: Particular requirements for the basic safety and essential performance of ultrasonic physiotherapy equipment, **2015**.
- [136] J. O. Jeong, Y. M. Lim, J. Y. Lee, J. S. Park, *Eur. Polym. J.* **2023**, *184*, 111726.
- [137] M. Malki, S. Fleischer, A. Shapira, T. Dvir, *Nano Lett.* **2018**, *18*, 4069.
- [138] G. Jia, A. Zheng, X. Wang, L. Zhang, L. Li, C. Li, Y. Zhang, L. Cao, *Sens. Actuators, B* **2021**, *346*, 130507.
- [139] E. Sciurti, R. Primavera, D. Di Mascolo, A. Rizzo, A. Balena, S. K. Padmanabhan, F. Rizzi, P. Decuzzi, M. De Vittorio, *Microelectron. Eng.* **2020**, *229*, 111360.
- [140] P. Cabras, A. Cafarelli, L. Ricotti, E. Dumont, *2022 IEEE International Ultrasonics Symposium (IUS)*, **2022**, pp. 1–4.
- [141] H. Lee, T. K. Choi, Y. B. Lee, H. R. Cho, R. Ghaffari, L. Wang, J. Choi, T. D. Chung, N. Lu, T. Hyeon, S. H. Choi, D. H. Kim, *Nat. Nanotechnol.* **2016**, *11*, 566.
- [142] D. G. Yu, M. Wang, R. Ge, *Wiley Interdiscip. Rev. Nanomed. Nanobiotechnol.* **2022**, *14*, e1772.
- [143] P. Mostafalu, A. Tamayol, R. Rahimi, M. Ochoa, A. Khalilpour, G. Kiaee, I. K. Yazdi, S. Bagherifard, M. R. Dokmeci, B. Ziaie, S. R. Sonkusale, A. Khademhosseini, *Small* **2018**, *14*, 1703509.
- [144] N. Ashammakhi, S. Ahadian, M. A. Darabi, M. El Tahchi, J. Lee, K. Suthiwanich, A. Sheikhi, M. R. Dokmeci, R. Oklu, A. Khademhosseini, *Adv. Mater.* **2019**, *31*, 1804041.
- [145] A. Talebi, S. Labbaf, F. Karimzadeh, E. Masaali, M. H. Nasr Esfahani, *ACS Biomater. Sci. Eng.* **2020**, *6*, 4214.
- [146] J. Li, D. J. Mooney, *Nat. Rev. Mater.* **2016**, *1*, 1.
- [147] P. Pushp, R. Bhaskar, S. Kelkar, N. Sharma, D. Pathak, M. Kumar Gupta, *Biotechnol. Bioeng.* **2021**, *118*, 2312.
- [148] S. Trombino, F. Curcio, R. Cassano, M. Curcio, G. Cirillo, F. Iemma, *Pharmaceutics* **2021**, *13*, 1038.
- [149] E. B. Dolan, C. E. Varela, K. Mendez, W. Whyte, R. E. Levey, S. T. Robinson, E. Maye, J. O'dwyer, R. Beatty, A. Rothman, Y. Fan, J. Hochstein, S. E. Rothenbucher, R. Wylie, J. R. Starr, M. Monaghan, P. Dockery, G. P. Duffy, E. T. Roche, *Sci. Robot.* **2019**, *4*, eaax7043.
- [150] D. Trel'ová, A. R. Salgarella, L. Ricotti, G. Giudetti, A. Cutrone, P. Šrámková, A. Zahoranová, D. Chorvát, D. Haško, C. Canale, S. Micera, J. Kronek, A. Menciassi, I. Lacić, *Langmuir* **2019**, *35*, 1085.
- [151] J. O. Abaricia, N. Farzad, T. J. Heath, J. Simmons, L. Morandini, R. Olivares-Navarrete, *Acta Biomater.* **2021**, *133*, 58.
- [152] J. Yekrang, N. Gholam Shahbazi, F. Rostami, M. Ramyar, *Int. J. Biol. Macromol.* **2023**, *230*, 123187.
- [153] F. Carotenuto, S. Politi, A. Ul Haq, F. De Matteis, E. Tamburri, M. L. Terranova, L. Teodori, A. Pasquo, P. Di Nardo, *Micromachines* **2022**, *13*, 780.
- [154] K. Wang, C. Wu, Z. Qian, C. Zhang, B. Wang, M. A. Vannan, *Addit. Manuf.* **2016**, *12*, 31.
- [155] L. B. Bezak, M. P. Cauchi, R. De Vita, J. R. Foerst, C. B. Williams, *J. Mech. Behav. Biomed. Mater.* **2020**, *110*, 103971.
- [156] M. Zhou, J. Hou, G. Zhang, C. Luo, Y. Zeng, S. Mou, P. Xiao, A. Zhong, Q. Yuan, J. Yang, Z. Wang, J. Sun, *Biofabrication* **2019**, *12*, 015023.
- [157] C. Cimmino, L. Rossano, P. A. Netti, M. Ventre, *Front. Bioeng. Biotechnol.* **2018**, *6*, 190.
- [158] M. Guvendiren, J. A. Burdick, *Nat. Commun.* **2012**, *3*, 792.
- [159] N. Lang, M. J. Pereira, Y. Lee, I. Friehs, N. V. Vasilyev, E. N. Feins, K. Ablasser, E. D. O'Ceirbhail, C. Xu, A. Fabozzo, R. Padera, S. Wasserman, F. Freudenthal, L. S. Ferreira, R. Langer, J. M. Karp, P. J. del Nido, *Sci. Transl. Med.* **2014**, *6*, 218.
- [160] M. P. Sousa, A. I. Neto, T. R. Correia, S. P. Miguel, M. Matsusaki, I. J. Correia, J. F. Mano, *Biomater. Sci.* **2018**, *6*, 1962.
- [161] C. E. Brubaker, H. Kissler, L. J. Wang, D. B. Kaufman, P. B. Messersmith, *Biomater* **2010**, *31*, 420.



- [162] S. Du, N. Zhou, Y. Gao, G. Xie, H. Du, H. Jiang, L. Zhang, J. Tao, J. Zhu, *Nano Res.* **2020**, *13*, 2525.
- [163] S. Baik, H. J. Lee, D. W. Kim, J. W. Kim, Y. Lee, C. Pang, *Adv. Mater.* **2019**, *31*, 1803309.
- [164] J. Li, A. D. Celiz, J. Yang, Q. Yang, I. Wamala, W. Whyte, B. R. Seo, N. V. Vasilyev, J. J. Vlassak, Z. Suo, D. J. Mooney, *Science* **2017**, *357*, 378.
- [165] M. K. Kwak, H. E. Jeong, K. Y. Suh, *Adv. Mater.* **2011**, *23*, 3949.
- [166] W. G. Bae, D. Kim, M. K. Kwak, L. Ha, S. M. Kang, K. Y. Suh, *Adv. Healthcare Mater.* **2013**, *2*, 109.
- [167] Y. C. Chen, H. Yang, *ACS Nano* **2017**, *11*, 5332.
- [168] M. K. Choi, O. K. Park, C. Choi, S. Qiao, R. Ghaffari, J. Kim, D. J. Lee, M. Kim, W. Hyun, S. J. Kim, H. J. Hwang, S. H. Kwon, T. Hyeon, N. Lu, D. H. Kim, *Adv. Healthcare Mater.* **2016**, *5*, 80.
- [169] Z. Zhu, J. Wang, X. Pei, J. Chen, X. Wei, Y. Liu, P. Xia, Q. Wan, Z. Gu, Y. He, *Sci. Adv.* **2023**, *9*, eadh2213.
- [170] L. Sun, X. Zhu, X. Zhang, G. Chen, F. Bian, J. Wang, Q. Zhou, D. Wang, Y. Zhao, *J. Chem. Eng.* **2021**, *414*, 128723.
- [171] S. Y. Yang, E. D. O’Cearbhaill, G. C. Sisk, K. M. Park, W. K. Cho, M. Villiger, B. E. Bouma, B. Pomahac, J. M. Karp, *Nat. Commun.* **2013**, *4*, 1702.
- [172] C. B. Dayan, D. Son, A. Aghakhani, Y. Wu, S. O. Demir, M. Sitti, *Small* **2024**, *20*, 2304437.
- [173] T. C. Tang, B. An, Y. Huang, S. Vasikaran, Y. Wang, X. Jiang, T. K. Lu, C. Zhong, *Nat. Rev. Mater.* **2021**, *6*, 332.
- [174] C. Zhong, T. Gurry, A. A. Cheng, J. Downey, Z. Deng, C. M. Stultz, T. K. Lu, *Nat. Nanotechnol.* **2014**, *9*, 858.
- [175] M. Cui, X. Wang, B. An, C. Zhang, X. Gui, K. Li, Y. Li, P. Ge, J. Zhang, C. Liu, C. Zhong, *Sci. Adv.* **2019**, *5*, eaax3155.
- [176] D. W. Y. Toong, H. W. Toh, J. C. K. Ng, P. E. H. Wong, H. L. Leo, S. Venkatraman, L. P. Tan, H. Y. Ang, Y. Huang, *Int. J. Mol. Sci.* **2020**, *21*, 3444.
- [177] A. K. Lynn, I. V. Yannas, W. Bonfield, *J. Biomed. Mater. Res. Part B* **2004**, *71*, 343.
- [178] X. Li, L. Wang, Y. Fan, Q. Feng, F. Z. Cui, *J. Nanomater.* **2012**, *2012*, 6.
- [179] D. B. Warheit, B. R. Laurence, K. L. Reed, D. H. Roach, G. A. M. Reynolds, T. R. Webb, *Toxicol. Sci.* **2004**, *77*, 117.
- [180] J. Wu, T. Chen, Y. Wang, J. Bai, C. Lao, M. Luo, M. Chen, W. Peng, W. Zhi, J. Weng, J. Wang, *Biomedicines* **2022**, *10*, 1165.
- [181] A. Pena-Francesch, Z. Zhang, L. Marks, P. Cabanach, K. Richardson, D. Sheehan, J. McCracken, H. Shahsavan, M. Sitti, *Matter* **2024**, <https://doi.org/10.1016/j.matt.2023.12.015>.
- [182] M. Temirel, C. Hawxhurst, S. Tasoglu, *Micromachines* **2021**, *12*, 195.
- [183] S. McMahan, A. Taylor, K. M. Copeland, Z. Pan, J. Liao, Y. Hong, *J. Biomed. Mater. Res., Part A* **2020**, *108*, 972.
- [184] S. Pok, I. V. Stupin, C. Tsao, R. G. Pautler, Y. Gao, R. M. Nieto, Z. W. Tao, C. D. Fraser Jr., A. V. Annapragada, J. G. Jacot, *Adv. Healthcare Mater.* **2017**, *6*, 1600549.
- [185] J. A. Johnson, M. G. Finn, J. T. Koberstein, N. J. Turro, *Macromolecules* **2007**, *40*, 3589.
- [186] T. Liu, Y. Wang, M. Hong, J. Venezuela, W. Shi, M. Dargusch, *Nano Today* **2023**, *52*, 101945.
- [187] W. Sha, Y. Guo, Q. Yuan, S. Tang, X. Zhang, S. Lu, X. Guo, Y. C. Cao, S. Cheng, *Adv. Intell. Syst.* **2020**, *2*, 1900143.
- [188] N. Nosengo, *Nature* **2016**, *533*, 22.
- [189] G. Frenning, *Int. J. Pharm.* **2011**, *418*, 88.
- [190] D. Y. Arifin, L. Y. Lee, C. H. Wang, *Adv. Drug Delivery Rev.* **2006**, *58*, 1274.
- [191] R. W. Korsmeyer, R. Gumy, E. Doelker, P. Buri, N. A. Peppas, *Int. J. Pharm.* **1983**, *15*, 25.
- [192] P. L. Ritger, N. A. Peppas, *J. Control Release* **1987**, *5*, 23.
- [193] T. Higuchi, *J. Pharm. Sci.* **1961**, *50*, 874.
- [194] J. Siepmann, N. A. Peppas, *Adv. Drug Delivery Rev.* **2012**, *64*, 163.
- [195] J. Siepmann, F. Siepmann, *J. Control Release* **2012**, *161*, 351.
- [196] Z. Chen, J. Huo, L. Hao, J. Zhou, *Curr. Opin. Chem. Eng.* **2019**, *23*, 21.
- [197] J. Choi, H. Chung, J. H. Yun, M. Cho, *Appl. Phys. Lett.* **2014**, *105*, 221906.
- [198] X. Zheng, D. Wang, Z. Shuai, *Nanoscale* **2013**, *5*, 3681.
- [199] M. Ghani, A. Heiskanen, J. Kajtez, B. Rezaei, N. B. Larsen, P. Thomsen, A. Kristensen, A. Zukauskas, M. Alm, J. Emneús, *ACS Appl. Mater. Interfaces* **2021**, *13*, 3591.
- [200] M. J. Bassetti, A. N. Chatterjee, N. R. Aluru, D. J. Beebe, *J. Microelectromech. Syst.* **2005**, *14*, 1198.
- [201] R. Luo, H. Li, E. Birgersson, K. Y. Lam, *J. Biomed. Mater. Res., Part A* **2007**, *85*, 248.
- [202] M. Boas, M. Burman, A. L. Yarin, E. Zussman, *Polymer* **2018**, *158*, 262.
- [203] A. Marino, S. Arai, Y. Hou, E. Sinibaldi, M. Pellegrino, Y. T. Chang, B. Mazzolai, V. Mattoli, M. Suzuki, G. Ciofani, *ACS Nano* **2015**, *9*, 7678.
- [204] D. Zhao, P. J. Feng, J. H. Liu, M. Dong, X. Q. Shen, Y. X. Chen, Q. D. Shen, *Adv. Mater.* **2020**, *32*, 2003800.
- [205] P. Zhu, Y. Chen, J. Shi, *Adv. Mater.* **2020**, *32*, 2001976.
- [206] T. Lacour, M. Guédrá, T. Valier-Brasier, F. Coulouvrat, *J. Acoust. Soc. Am.* **2018**, *143*, 23.
- [207] M. Ghasemi, A. C. H. Yu, S. Sivaloganathan, *Ultrason. Sonochem.* **2022**, *83*, 105948.
- [208] M. Aliabouzar, O. D. Kripfgans, W. Y. Wang, B. M. Baker, J. Brian Fowlkes, M. L. Fabiilli, *Ultrason. Sonochem.* **2021**, *72*, 105430.
- [209] H. Kim, C. Kim, *Int. J. Heat Mass Transf.* **2021**, *181*, 121991.
- [210] M. S. Plesset, A. Prosperetti, *Ann. Rev. Fluid Mech.* **1977**, *9*, 145.
- [211] P. V. Melenev, A. V. Ryzhkov, M. Balasoju, *Soft Mater.* **2022**, *20*, S50.
- [212] A. V. Ryzhkov, Y. L. Raikher, *J. Magn. Magn. Mater.* **2017**, *431*, 192.
- [213] R. Weeber, P. Kreissl, C. Holm, *Arch. Appl. Mech.* **2019**, *89*, 3.
- [214] C. S. Brazel, *Pharm. Res.* **2009**, *26*, 644.
- [215] P. Thorngkham, N. Paradee, S. Niamlang, A. Sirivat, *J. Pharm. Sci.* **2015**, *104*, 1795.
- [216] N. Paradee, A. Sirivat, S. Niamlang, W. Prissanaroon-Ouajai, *J. Mater. Sci. Mater. Med.* **2012**, *23*, 999.
- [217] K. R. Harris, S. M. Howard, A. M. Hurrell, P. A. Lewin, M. E. Schafer, G. A. Wear, V. Wilkenson, B. Zeqiri, *IEEE Trans. Ultrason. Ferroelectr. Freq. Control* **2023**, *70*, 85.
- [218] E. Breschi, Z. Grujic, A. Weis, *Appl. Phys. B* **2014**, *115*, 85.
- [219] F. Fontana, F. Iberite, A. Cafarelli, A. Aliperta, G. Baldi, E. Gabusi, P. Dolzani, S. Cristino, G. Lisignoli, T. Pratellesi, E. Dumont, L. Ricotti, *Ultrasonics* **2021**, *116*, 106495.
- [220] S. A. Prael, M. Keijzer, S. L. Jacques, A. J. Welch, *Dosimetry of Laser Radiation in Medicine and Biology* **1989**, *10305*, 105.
- [221] R. T. Zaman, A. Gopal, K. Starr, X. Zhang, S. Thomsen, J. W. Tunnell, A. J. Welch, H. G. Rylander III, *Lasers Surg. Med.* **2012**, *44*, 30.
- [222] T. Kundu, D. Placko, E. Kabiri Rahani, T. Yanagita, C. Minh Dao, *IEEE Trans. Ultrason. Ferroelectr. Freq. Control* **2010**, *57*, 2795.
- [223] B. E. Treeby, J. Jaros, A. P. Rendell, *J. Acoust. Soc. Am.* **2012**, *131*, 4324.
- [224] M. Colella, D. Z. Press, R. M. Laher, C. E. McIllduff, S. B. Rutkove, A. M. Cassarà, F. Apollonio, A. Pascual-Leone, M. Liberti, G. Bonmassar, *Med. Phys.* **2023**, *50*, 1779.
- [225] R. R. Sarreal, P. Bhatti, *Sensors* **2020**, *20*, 6087.
- [226] K. Dong, W. C. Liu, Y. Su, Y. Lyu, H. Huang, N. Zheng, J. A. Rogers, K. Nan, *BME Front.* **2023**, *4*, 0034.
- [227] H. Bai, Z. Hu, J. A. Rogers, *MRS Bull.* **2023**, *48*, 1125.
- [228] T. G. La, L. H. Le, *Adv. Mater. Technol.* **2022**, *7*, 2100798.
- [229] Y. Zhang, G. Lee, S. Li, Z. Hu, K. Zhao, J. A. Rogers, *Chem. Rev.* **2023**, *123*, 11722.
- [230] Z. Hu, H. Guo, D. An, M. Wu, A. Kaura, H. Oh, Y. Wang, M. Zhao, S. Li, Q. Yang, X. Ji, S. Li, B. Wang, D. Yoo, P. Tran, N. Ghoreishi-

- Haack, Y. Kozorovitskiy, Y. Huang, R. Li, J. A. Rogers, *Adv. Mater.* **2024**, 2309421.
- [231] S. Selvarajan, A. Kim, S. H. Song, *IEEE Access* **2020**, *8*, 68219.
- [232] M. Montgomery, S. Ahadian, L. Davenport Huyer, M. Lo Rito, R. A. Civitarese, R. D. Vanderlaan, J. Wu, L. A. Reis, A. Momen, S. Akbari, A. Pahnke, R. K. Li, C. A. Caldarone, M. Radisic, *Nat. Mater.* **2017**, *16*, 1038.
- [233] S. J. Wu, H. Yuk, J. Wu, C. S. Nabzdyk, X. Zhao, *Adv. Mater.* **2021**, *33*, 2007667.
- [234] Z. Fan, Y. Wei, Z. Yin, H. Huang, X. Liao, L. Sun, B. Liu, F. Liu, *ACS Appl. Mater. Interfaces* **2021**, *13*, 40278.
- [235] X. Mei, D. Zhu, J. Li, K. Huang, S. Hu, Z. Li, B. L. de Juan Abad, K. Cheng, *Med.* **2021**, *2*, 1253.
- [236] J. Lee, H. Lee, S. H. Kwon, S. Park, *Med. Eng. Phys.* **2020**, *85*, 87.
- [237] K. Luo, L. Wang, M. X. Wang, R. Du, L. Tang, K. K. Yang, Y. Z. Wang, *ACS Appl. Mater. Interfaces* **2023**, *15*, 44373.
- [238] E. S. Sani, C. Xu, C. Wang, Y. Song, J. Min, J. Tu, S. A. Solomon, J. Li, J. L. Banks, D. G. Armstrong, W. Gao, *Sci. Adv.* **2023**, *9*, 7388.
- [239] B. Mirani, E. Pagan, B. Currie, M. A. Siddiqui, R. Hosseinzadeh, P. Mostafalu, Y. S. Zhang, A. Ghahary, M. Akbari, *Adv. Healthcare Mater.* **2017**, *6*, 1700718.
- [240] B. Qiao, Q. Pang, P. Yuan, Y. Luo, L. Ma, *Biomater. Sci.* **2020**, *8*, 1649.
- [241] Z. Li, E. Roussakis, P. G. L. Koolen, A. M. S. Ibrahim, K. Kim, L. F. Rose, J. Wu, A. J. Nichols, Y. Baek, R. Birngruber, G. Apiou-Sbirlea, R. Matyal, T. Huang, R. Chan, S. J. Lin, C. L. Evans, *Biomed. Opt. Express* **2014**, *5*, 3748.
- [242] O. Pedreira, C. Papadacci, L. Augeul, J. Loufouat, M. Lo-Grasso, M. Tanter, R. Ferrera, M. Pernot, *EBioMedicine* **2022**, *83*, 104201.
- [243] J. A. Sebastian, E. M. Strohm, J. Baranger, O. Villemain, M. C. Kolios, C. A. Simmons, *Biomaterial* **2023**, *296*, 122054.
- [244] A. Kiourti, K. A. Psathas, K. S. Nikita, *Bioelectromagnetics* **2014**, *35*, 1.
- [245] S. R. Khan, S. K. Pavuluri, G. Cummins, M. P. Y. Desmulliez, *Sensors* **2020**, *20*, 3487.
- [246] J. Di, J. Yu, Q. Wang, S. Yao, D. Suo, Y. Ye, M. Pless, Y. Zhu, Y. Jing, Z. Gu, *Nano Res.* **2017**, *10*, 1393.
- [247] S. Ciancia, A. Cafarelli, A. Zahoranova, A. Menciaci, L. Ricotti, *Front. Bioeng. Biotechnol.* **2020**, *8*, 317.
- [248] L. Badimon, M. Borrell, *Curr. Pharm. Des.* **2018**, *24*, 2967.
- [249] F. Buket Basmanav, G. T. Kose, V. Hasirci, *Biomaterail* **2008**, *29*, 4195.
- [250] A. T. Raiche, D. A. Puleo, *Biomaterial* **2004**, *25*, 677.
- [251] R. R. Chen, E. A. Silva, W. W. Yuen, D. J. Mooney, *Pharm. Res.* **2007**, *24*, 258.
- [252] D. H. R. Kempen, L. Lu, A. Heijink, T. E. Hefferan, L. B. Creemers, A. Maran, M. J. Yaszemski, W. J. A. Dhert, *Biomaterial* **2009**, *30*, 2816.
- [253] Z. Cao, X. Zhou, G. Wang, *ACS Appl. Mater. Interfaces* **2016**, *8*, 28888.
- [254] X. Luo, H. Zhang, M. Chen, J. Wei, Y. Zhang, X. Li, *Int. J. Pharm.* **2014**, *475*, 438.
- [255] X. Lin, X. Guan, Y. Wu, S. Zhuang, Y. Wu, L. Du, J. Zhao, J. Rong, J. Zhao, M. Tu, *Mater. Sci. Eng. C* **2020**, *115*, 111123.
- [256] M. A. Azagarsamy, K. S. Anseth, *Angew. Chem., Int. Ed.* **2013**, *52*, 13803.
- [257] Y. Wang, J. Yan, N. Wen, H. Xiong, S. Cai, Q. He, Y. Hu, D. Peng, Z. Liu, Y. Liu, *Biomaterials* **2020**, *230*, 119619.
- [258] S. Karimzadeh, S. Javanbakht, B. Baradaran, M. A. Shahbazi, M. Hashemzaei, A. Mokhtarzadeh, H. A. Santos, *J. Chem. Eng.* **2021**, *408*, 127233.
- [259] Z. Liu, L. Zhang, D. Sun, *Chem. Commun.* **2020**, *56*, 9416.
- [260] S. Yao, Y. Wang, J. Chi, Y. Yu, Y. Zhao, Y. Luo, Y. Wang, *Adv. Sci.* **2022**, *9*, 2103449.
- [261] Y. Zeng, C. Wang, K. Lei, C. Xiao, X. Jiang, W. Zhang, L. Wu, J. Huang, W. Li, *Adv. Healthcare Mater.* **2023**, *12*, 2300250.
- [262] Y. Wang, X. Nie, Z. Lv, Y. Hao, Q. Wang, Q. Wei, *J. Colloid Interface Sci.* **2024**, *656*, 376.
- [263] M. Wei, Y. Wan, X. Zhang, *J. Compos. Sci.* **2021**, *5*, 101.
- [264] W. Cai, J. Wang, C. Chu, W. Chen, C. Wu, G. Liu, *Adv. Sci.* **2019**, *6*, 1801526.



**Sofia Sirolli** is a Ph.D. student at the Regenerative Technologies Lab, the BioRobotics Institute of Scuola Superiore Sant'Anna (Pisa, Italy). Her Ph.D. research project is focused on smart materials for drug delivery applications.



**Daniele Guarnera** is a Post-Doc research fellow at the Regenerative Technologies Lab, the BioRobotics Institute of Scuola Superiore Sant'Anna (Pisa, Italy). His research interests include analytical and numerical models applied to biomedical devices.



**Leonardo Ricotti** is an Associate Professor of bioengineering and PI of the Regenerative Technologies Lab, at the BioRobotics Institute of Scuola Superiore Sant'Anna (Pisa, Italy). His research interests include regenerative medicine, tissue engineering, biohybrid technologies, and implantable medical devices.



**Andrea Cafarelli** is an Assistant Professor of bioengineering at the Regenerative Technologies Lab, the BioRobotics Institute of Scuola Superiore Sant'Anna (Pisa, Italy). His main research interests focus on ultrasound technologies for regenerative medicine applications.